

NAVAL POSTGRADUATE SCHOOL

Monterey, California



THESIS

**FINITE ELEMENT MODELING OF THE RAH-66
COMANCHE HELICOPTER TAILCONE SECTION USING
PATRAN AND DYTRAN**

by

Mark S. Gorak
Jeffrey A. Libby

June 2001

Thesis Advisor:
Second Reader:

Donald A. Danielson
David Canright

Approved for public release, distribution is unlimited

Form SF298 Citation Data

| | | |
|---|---------------------------|--|
| Report Date ("DD MON YYYY") 15 Jun 2001 | Report Type N/A | Dates Covered (from... to) ("DD MON YYYY") |
| Title and Subtitle FINITE ELEMENT MODELING OF THE RAH-66 COMANCHE HELICOPTER TAILCONE SECTION USING PATRAN AND DYTRAN | | Contract or Grant Number |
| | | Program Element Number |
| Authors | | Project Number |
| | | Task Number |
| | | Work Unit Number |
| Performing Organization Name(s) and Address(es) Naval Postgraduate School Monterey, CA 93943-5138 | | Performing Organization Number(s) |
| Sponsoring/Monitoring Agency Name(s) and Address(es) | | Monitoring Agency Acronym |
| | | Monitoring Agency Report Number(s) |
| Distribution/Availability Statement Approved for public release, distribution unlimited | | |
| Supplementary Notes | | |
| Abstract | | |
| Subject Terms | | |
| Document Classification unclassified | | Classification of SF298 unclassified |
| Classification of Abstract unclassified | | Limitation of Abstract unlimited |
| Number of Pages 109 | | |

THIS PAGE INTENTIONALLY LEFT BLANK

**FINITE ELEMENT MODELING OF THE RAH-66 COMANCHE HELICOPTER
TAILCONE SECTION USING PATRAN AND DYTRAN**

Mark S. Gorak-Captain, United States Army

B.S., Marquette University, 1991

and

Jeffrey A. Libby-Captain, United States Army

B.S., United States Military Academy, 1991

Master of Science in Applied Mathematics—June 2001

Advisor: Donald A. Danielson, Department of Mathematics

The United States Army contracted Boeing-Sikorsky to develop the RAH-66 Comanche, a new, armed reconnaissance helicopter that features stealth technology designed to improve survivability when operating in hostile environments. Ballistic testing is required on any new technology, to include the Comanche, prior to fielding. Computer based simulations are being employed to reduce the requirements for expensive live fire testing. This thesis uses computer programs called PATRAN and DYTRAN from MSC Software Corporation to build the model and simulate the effects of an explosive round detonating in the Comanche tailcone section. This thesis describes in great detail the process of creating and modifying the model in PATRAN to most accurately depict the Comanche tailcone section and creating the input decks for DYTRAN to run the analysis. A test case involving an explosion with a high amount of explosive energy, or specific internal energy (SIE) was simulated. From this test, several results are shown to display the capabilities of DYTRAN. These results, when compared with live fire data, can be used to validate the computer-based simulation in order to reduce the requirements of expensive live fire testing.

DoD KEY TECHNOLOGY AREA: Air Vehicles, Computing and Software, Materials, Processes, and Structures, Modeling and Simulation

KEYWORDS: Comanche, Ballistic Modeling, PATRAN, DYTRAN, Tailcone

Public reporting burden for this collection of information is estimated to average 1 hour per response, including the time for reviewing instruction, searching existing data sources, gathering and maintaining the data needed, and completing and reviewing the collection of information. Send comments regarding this burden estimate or any other aspect of this collection of information, including suggestions for reducing this burden, to Washington headquarters Services, Directorate for Information Operations and Reports, 1215 Jefferson Davis Highway, Suite 1204, Arlington, VA 22202-4302, and to the Office of Management and Budget, Paperwork Reduction Project (0704-0188) Washington DC 20503.

| | | | |
|---|---|--|---|
| 1. AGENCY USE ONLY (Leave blank) | 2. REPORT DATE June 2001 | 3. REPORT TYPE AND DATES COVERED Master's Thesis | |
| 4. TITLE AND SUBTITLE: Title (Mix case letters) Finite Element Modeling of the RAH-66 Comanche Helicopter Tailcone Section Using MSC PATRAN and DYTRAN Software | | 5. FUNDING NUMBERS | |
| 6. AUTHOR(S) Mark S. Gorak and Jeffrey A. Libby | | 8. PERFORMING ORGANIZATION REPORT NUMBER | |
| 7. PERFORMING ORGANIZATION NAME(S) AND ADDRESS(ES) Naval Postgraduate School Monterey, CA 93943-5000 | | 10. SPONSORING / MONITORING AGENCY REPORT NUMBER | |
| 9. SPONSORING / MONITORING AGENCY NAME(S) AND ADDRESS(ES) N/A | | | |
| 11. SUPPLEMENTARY NOTES The views expressed in this thesis are those of the author and do not reflect the official policy or position of the Department of Defense or the U.S. Government. | | | |
| 12a. DISTRIBUTION / AVAILABILITY STATEMENT Approved for public release, distribution is unlimited | | 12b. DISTRIBUTION CODE | |
| 13. ABSTRACT (maximum 200 words) The United States Army contracted Boeing-Sikorsky to develop the RAH-66 Comanche, a new, armed reconnaissance helicopter that features stealth technology designed to improve survivability when operating in hostile environments. Ballistic testing is required on any new technology, including the Comanche, prior to fielding. This thesis uses computer programs called PATRAN and DYTRAN from MSC Software Corporation to build a model and simulate the effects of an explosive round detonating in the Comanche tailcone section. This thesis describes in great detail the process of creating and modifying the model in PATRAN to most accurately depict the Comanche tailcone section, and of creating the input decks for DYTRAN to run the analysis. A test case involving an explosion with a high amount of explosive energy, or specific internal energy (SIE) was simulated. From this test, several results are shown to display the capabilities of DYTRAN. These results, when compared with live fire data, can be used to validate the computer-based simulation in order to reduce the requirements of expensive live fire testing. | | | |
| 14. SUBJECT TERMS Comanche, Ballistic Modeling, PATRAN, DYTRAN, Tailcone | | | 15. NUMBER OF PAGES |
| | | | 16. PRICE CODE |
| 17. SECURITY CLASSIFICATION OF REPORT Unclassified | 18. SECURITY CLASSIFICATION OF THIS PAGE Unclassified | 19. SECURITY CLASSIFICATION OF ABSTRACT Unclassified | 20. LIMITATION OF ABSTRACT UL |

NSN 7540-01-280-5500

Standard Form 298 (Rev. 2-89)
Prescribed by ANSI Std. Z39-18

THIS PAGE INTENTIONALLY LEFT BLANK

Approved for public release, distribution is unlimited

**FINITE ELEMENT MODELING OF THE RAH-66 COMANCHE HELICOPTER
TAILCONE SECTION USING MACNEAL-SCHWENDLER CORPORATION
PATRAN AND DYTRAN SOFTWARE**

Mark S. Gorak
Captain, United States Army
B.S., Marquette University, 1991

Jeffrey A. Libby
Captain, United States Army
B.S., United States Military Academy, 1991

Submitted in partial fulfillment of the
requirements for the degree of

MASTER OF SCIENCE IN APPLIED MATHEMATICS

from the

**NAVAL POSTGRADUATE SCHOOL
June 2001**

Authors: _____
Mark S. Gorak

Jeffrey A. Libby

Approved by: _____
Donald A. Danielson, Thesis Advisor

David Canright, Second Reader

Mike Morgan, Chairman
Department of Mathematics

THIS PAGE INTENTIONALLY LEFT BLANK

ABSTRACT

The United States Army contracted Boeing-Sikorsky to develop the RAH-66 Comanche, a new, armed reconnaissance helicopter that features stealth technology designed to improve survivability when operating in hostile environments. Ballistic testing is required on any new technology, including the Comanche, prior to fielding. This thesis uses computer programs called PATRAN and DYTRAN from MSC Software Corporation to build a model and simulate the effects of an explosive round detonating in the Comanche tailcone section. This thesis describes in great detail the process of creating and modifying the model in PATRAN to most accurately depict the Comanche tailcone section, and of creating the input decks for DYTRAN to run the analysis. A test case involving an explosion with a high amount of explosive energy, or specific internal energy (SIE) was simulated. From this test, several results are shown to display the capabilities of DYTRAN. These results, when compared with live fire data, can be used to validate the computer-based simulation in order to reduce the requirements of expensive live fire testing.

THIS PAGE INTENTIONALLY LEFT BLANK

TABLE OF CONTENTS

| | | |
|------|---|----|
| I. | INTRODUCTION..... | 1 |
| | A. GENERAL | 1 |
| | B. SCOPE..... | 2 |
| | C. STATEMENT OF PURPOSE..... | 3 |
| II. | BACKGROUND..... | 5 |
| | A. FINITE ELEMENT METHOD..... | 5 |
| | B. COMPUTER SOFTWARE | 6 |
| | 1. UNIX..... | 6 |
| | 2. PATRAN | 7 |
| | 3. DYTRAN..... | 8 |
| | C. BLAST MECHANICS | 10 |
| | D. COMPOSITE MATERIALS | 11 |
| III. | MODEL DEVELOPMENT | 13 |
| | A. OVERVIEW | 13 |
| | B. CATIA TRANSLATION | 14 |
| | C. GEOMETRY CREATION, MODIFICATION AND MODELING | 16 |
| | D. MESHING..... | 29 |
| | E. ASSIGNMENT OF MATERIALS AND PROPERTIES | 36 |
| | F. FINAL MODEL CHECKS | 41 |
| | G. DYTRAN TRANSLATION | 43 |
| | H. PATRAN ANALYSIS..... | 54 |
| IV. | RESULTS..... | 55 |
| | A. ASSUMPTIONS USED IN ANALYSIS..... | 55 |
| | B. PRESSURE | 56 |
| | C. DISPLACEMENT..... | 57 |
| | D. STRESS AND STRAIN | 63 |
| | E. FAILURE | 82 |
| V. | CONCLUSIONS AND RECOMMENDATIONS..... | 85 |
| | A. CONCLUSIONS..... | 85 |
| | B. RECOMMENDATIONS | 86 |
| | LIST OF REFERENCES | 89 |
| | INITIAL DISTRIBUTION LIST | 91 |

THIS PAGE INTENTIONALLY LEFT BLANK

LIST OF FIGURES

| | |
|---|----|
| Figure 1: RAH-66 Comanche | 1 |
| Figure 2: Schematic View of Blast Analysis Area..... | 3 |
| Figure 3: CATIA Model of STA Tailcone..... | 15 |
| Figure 4: CATIA Back Frame..... | 16 |
| Figure 5: PATRAN Back Frame..... | 16 |
| Figure 6: Front Tailcone Group | 20 |
| Figure 7: Bottom Tailcone Group | 21 |
| Figure 8: Bottom-Side Panels Tailcone Group | 22 |
| Figure 9: Side and Longerons Tailcone Group | 23 |
| Figure 10: Topside Panels Tailcone Group..... | 24 |
| Figure 11: Top Tailcone Group..... | 25 |
| Figure 12: Top Panels Tailcone Group | 26 |
| Figure 13: Vents Tailcone Group..... | 27 |
| Figure 14: CATIA Drawing | 28 |
| Figure 15: Final Geometry of PATRAN Model | 28 |
| Figure 16: Mesh Using Paver..... | 31 |
| Figure 17: Manual Corrected Mesh | 31 |
| Figure 18: Meshed Vents on Back Group..... | 32 |
| Figure 19: View of Honeycomb Mesh..... | 33 |
| Figure 20: Meshed Back to Front View (Front Group Removed) | 34 |
| Figure 21: Meshed Front to Back View (Back Group Removed)..... | 34 |
| Figure 22: Meshed Left Side View | 35 |
| Figure 23: Meshed Top to Bottom View (Bottom Group Removed) | 35 |
| Figure 24: Engineering Drawing of Back Frame | 36 |
| Figure 25: Cross Section of Composite Ply Lay-up..... | 38 |
| Figure 26: Contact Surface for Front Group | 42 |
| Figure 27: Normals for Front Group | 42 |
| Figure 28: Fluid Region for the Model | 46 |
| Figure 29: Time-Pressure History Results | 57 |
| Figure 30: Displacement at Time 0.250 milliseconds..... | 58 |
| Figure 31: Displacement at Time 0.50 milliseconds..... | 58 |
| Figure 32: Displacement at Time 0.750 milliseconds..... | 59 |
| Figure 33: Displacement at Time 1 milliseconds..... | 59 |
| Figure 34: Displacement at Time 1.750 milliseconds..... | 60 |
| Figure 35: Displacement at Time 2.50 milliseconds..... | 60 |
| Figure 36: Displacement at Time 3.0 milliseconds..... | 61 |
| Figure 37: Displacement at Time 3.50 milliseconds..... | 61 |
| Figure 38: Displacement at Time 4.250 milliseconds..... | 62 |
| Figure 39: Displacement at Time 4.626 milliseconds..... | 62 |
| Figure 40: Solid Element Stress in XX Direction at Time = 0.25 milliseconds | 63 |
| Figure 41: Solid Element Stress in XX Direction at Time = 0.5 milliseconds | 64 |
| Figure 42: Solid Element Stress in XX Direction at Time = 1.0 milliseconds | 64 |

| | |
|---|----|
| Figure 43: Solid Element Stress in XX Direction at Time = 2.0 milliseconds | 65 |
| Figure 44: Solid Element Stress in XX Direction at Time = 3.0 milliseconds | 65 |
| Figure 45: Solid Element Stress in XX Direction at Time = 4.0 milliseconds | 66 |
| Figure 46: Solid Element Stress in YZ Direction at Time = 0.25 milliseconds..... | 66 |
| Figure 47: Solid Element Stress in YZ Direction at Time = 0.5 milliseconds..... | 67 |
| Figure 48: Solid Element Stress in YZ Direction at Time = 1.0 milliseconds..... | 67 |
| Figure 49: Solid Element Stress in YZ Direction at Time = 2.0 milliseconds..... | 68 |
| Figure 50: Solid Element Stress in YZ Direction at Time =3.0 milliseconds..... | 68 |
| Figure 51: Solid Element Stress in YZ Direction at Time = 4.0 milliseconds..... | 69 |
| Figure 52: Solid Element Stress in ZX Direction at Time = 0.25 milliseconds..... | 69 |
| Figure 53: Solid Element Stress in ZX Direction at Time = 0.5 milliseconds..... | 70 |
| Figure 54: Solid Element Stress in ZX Direction at Time = 1.0 milliseconds..... | 70 |
| Figure 55: Solid Element Stress in ZX Direction at Time = 2.0 milliseconds..... | 71 |
| Figure 56: Solid Element Stress in ZX Direction at Time = 3.0 milliseconds..... | 71 |
| Figure 57: Solid Element Stress in ZX Direction at Time = 4.0 milliseconds..... | 72 |
| Figure 58: Shell Element Strain in XX Direction at Time = 0.25 milliseconds | 73 |
| Figure 59: Shell Element Strain in XX Direction at Time = 0.5 milliseconds | 73 |
| Figure 60: Shell Element Strain in XX Direction at Time = 0.75 milliseconds | 74 |
| Figure 61: Shell Element Strain in XX Direction at Time = 1.0 milliseconds | 74 |
| Figure 62: Shell Element Strain in XX Direction at Time = 2.0 milliseconds | 75 |
| Figure 63: Shell Element Strain in XX Direction at Time = 3.0 milliseconds | 75 |
| Figure 64: Shell Element Strain in XX Direction at Time = 4.0 milliseconds | 76 |
| Figure 65: Shell Element Strain in XY Direction at Time = 0.25 milliseconds | 76 |
| Figure 66: Shell Element Strain in XY Direction at Time = 0.5 milliseconds | 77 |
| Figure 67: Shell Element Strain in XY Direction at Time = 1.0 milliseconds | 77 |
| Figure 68: Shell Element Strain in XY Direction at Time = 2.0 milliseconds | 78 |
| Figure 69: Shell Element Strain in XY Direction at Time = 3.0 milliseconds | 78 |
| Figure 70: Shell Element Strain in XY Direction at Time = 4.0 milliseconds | 79 |
| Figure 71: Shell Element Strain in YY Direction at Time = 0.25 milliseconds | 79 |
| Figure 72: Shell Element Strain in YY Direction at Time = 0.5 milliseconds | 80 |
| Figure 73: Shell Element Strain in YY Direction at Time = 1.0 milliseconds | 80 |
| Figure 74: Shell Element Strain in YY Direction at Time = 2.0 milliseconds | 81 |
| Figure 75: Shell Element Strain in YY Direction at Time = 3.0 milliseconds | 81 |
| Figure 76: Shell Element Strain in YY Direction at Time = 4.0 milliseconds | 82 |
| Figure 77: Failure of Shell Element Vents at Time = 0.25 milliseconds | 83 |
| Figure 78: Failure of Shell Element Vents at Time = 0.5 milliseconds | 83 |
| Figure 79: Failure of Front Shell Element at Time = 1.5 milliseconds..... | 84 |
| Figure 80: Failure of Shell Element Vents at Time = 4.25 milliseconds | 84 |

LIST OF TABLES

| | |
|--|----|
| Table 1: Comanche's Features | 2 |
| Table 2: Basic Unix Commands..... | 7 |
| Table 3: Partial Composite Ply Lay-up Table..... | 37 |
| Table 4: Isotropic Material Properties..... | 39 |
| Table 5: 2-D Orthotropic Material Properties | 39 |
| Table 6: Composite Material Layers for Longeron Middle Upper | 40 |
| Table 7: TAILCONE.dat File..... | 45 |
| Table 8: BULK.dat Partial File | 46 |
| Table 9: EULER.dat File..... | 48 |
| Table 10: PROPERTY.dat File | 51 |
| Table 11: SURFACE.dat Partial File | 52 |
| Table 12: Error Message Partial File..... | 53 |
| Table 13: DYTRAN Output Files | 54 |

THIS PAGE INTENTIONALLY LEFT BLANK

ACKNOWLEDGMENTS

We would like to acknowledge Don Danielson for his support, guidance and encouragement during this process. He always found time to answer our questions and provide advice in order to complete the project. We would also like to thank Mel Niederer and Jason Firko from the Boeing Corporation who took the time to answer questions and provide the data to incorporate into the project. This information allowed the project to proceed in a timely manner. We would like to thank Bob Wood for the time he spent in communicating with Boeing Corporation in order to ensure that we had all the information to complete the project. Finally, a special thanks goes to Kristin Gorak and Deanna Libby, our wives, for their love, understanding, patience and support during this entire process.

THIS PAGE INTENTIONALLY LEFT BLANK

I. INTRODUCTION

A. GENERAL

The Boeing-Sikorsky RAH-66 Comanche, shown in Figure 1, is the United States Army's first piece of equipment approved for use in the Army's new transformation.



Figure 1: RAH-66 Comanche

The Comanche has capabilities demanded of a smaller force structure, such as: improved mobility, increased survivability and dramatically reduced operation and

support costs. It is a twin-turbine, two-seat (tandem) armed reconnaissance helicopter with projected missions of armed reconnaissance, light attack and air combat. The Comanche's most significant systems and features include:

- Five-bladed bearingless main rotor
- FANTAIL anti-torque system
- Low-workload crew station
- Self-healing digital mission electronics
- Longbow fire-control radar
- Passive long-range, high-resolution sensors
- Triple redundant fly-by-wire flight control system
- Wide field-of-view (35 X 52 degrees) helmet-mounted display
- Low observables (radar, infrared, acoustic)
- Two 6- by 8-inch multifunctional displays
- Triple redundant electrical/hydraulic systems on-board diagnostic system
- Simple remove-and-replace maintenance
- Fully retractable missile armament system
- Stowable 20-mm Gatling gun

Table 1: Comanche's Features

The Army has contracted to purchase 1,213 Comanche helicopters with the first unit fielded in 2006. Currently, two technology demonstrators have been built and are undergoing testing. Design efforts are underway for 13 Engineering and Manufacturing Development (EMD) aircraft. The first four of these EMD aircraft are scheduled for delivery in 2005 with the remaining nine aircraft following in 2006.

B. SCOPE

Ballistic survivability is a major concern for all military vehicles. As a combat vehicle, Comanche is required to undergo ballistic testing prior to fielding. Ballistic testing can be extremely expensive because the static test article is usually destroyed. In

order to reduce program acquisition costs for military vehicles, the amount of ballistic testing is being reduced when possible, and new less expensive ballistic testing techniques are being employed. One of the most promising new testing techniques utilizes computer simulations instead of actual destructive testing. A major advantage of a computer simulation over actual testing is that the computer model does not get destroyed and can be reused as often as required. Additionally, modifying parameters in the computer model is easier and more precise than modifying physical models.

C. STATEMENT OF PURPOSE

This research is a study to validate structural integrity of the tailcone section of the Comanche helicopter to withstand an explosion of a certain Specific Internal Energy (SIE). The Comanche tailcone section for this report is shown in Figure 2.

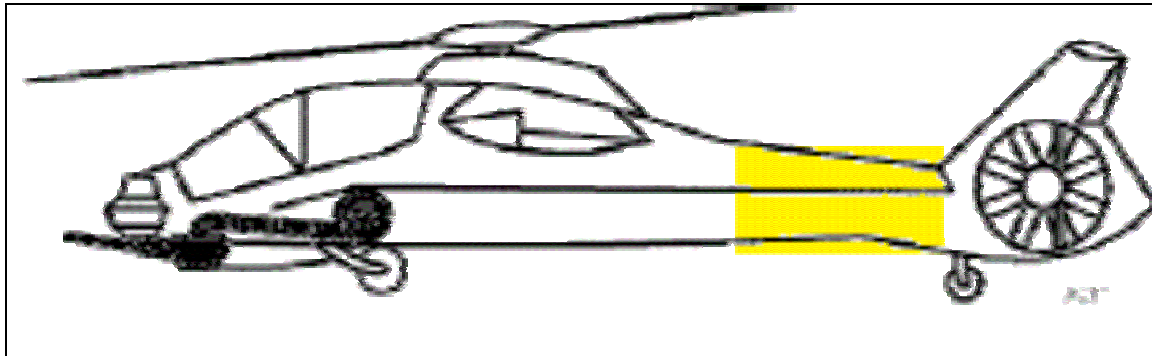


Figure 2: Schematic View of Blast Analysis Area

The explosion replicates the detonation of an explosive round at a specified location within the tailcone structure. The strength of the explosive round is measured in

terms of SIE. The higher the SIE of an explosive round, the more powerful the explosion.

The modelers developed a computer model to simulate the explosion of a round inside the tailcone section. The computer model replicates the blast and determines the blast effects including which portions of the structure fail. Evaluation of this data helps engineers determine structural failure information and aids in improving future designs.

II. BACKGROUND

A. FINITE ELEMENT METHOD

Modern aircraft, like Comanche, are complex assemblages of numerous structural elements. The response of each of these structural elements can usually be idealized by structural analysis methods such as beam bending theory, torsion theory, or shear flow methods. Complex structures, like those seen in Comanche, are very difficult to analyze with these simplified methods. To meet the need to analyze complex structures, the Finite Element Method (FEM) was developed in the late 1950's.

The FEM views complex structures as an assemblage of a finite number of discrete elements like beams, plates, and solids. The deformation response of each of these elements is relatively simple and easily solved when compared to the complete structure. The complete structure is broken down into elements, each element is analyzed separately for equilibrium, and the structure is tied back together by imposing compatibility requirements (on displacements) or equilibrium (on forces) at the joints or boundaries where the elements are connected. The FEM provides a mathematical model based on idealization of the complete structure into smaller, easier to manage elements.

The FEM does not provide an exact analytical solution of the original system. Some of the factors that effect accuracy of FEM are element size, element type, and shape of element used. When dealing with approximations involving the sums of smaller pieces, the accuracy of the results is directly proportional to the number of elements used

in the summation process. Small element size increases the number of summing pieces of the model and therefore improves the model's accuracy.

Elements can be one, two, or three-dimensional. For two-dimensional elements, three and four sided elements like triangles, squares and rectangles are used. Three-dimensional elements are made from the same shapes as the two-dimensional cases except they have a thickness giving them four sides for tetrahedral elements and six sides for the hexahedron or brick-shaped elements. Elements that are uniform in shape provide better results regardless of whether they are two-dimensional or three-dimensional. To get the most accurate results, triangular-shaped elements should be as close to equilateral triangles as possible while quadrilateral elements should be as close to squares as possible. Triangular elements are less accurate than quadrilaterals, so their use should be minimized.

B. COMPUTER SOFTWARE

1. UNIX

UNIX was developed and created by Bell Labs in the late 1960's. UNIX stands for "Multiplexed Information and Computing Service." UNIX operating systems all share two important characteristics: multitasking and multi-user timesharing systems. Multitasking means that a UNIX system can run more than one program at a time. Multi-user means that more than one user can utilize the UNIX system at the same time.

This research project was done on a Silicon Graphics IP30 (1CPU, 300MHz, MIPS R12000, 256 MB RAM) computer utilizing UNIX based software, IRIX 64 release 6.5. The following is a list of several basic commands needed to complete this project:

| UNIX Code | Meaning |
|-----------------|-------------------------|
| jot | Edit |
| ls | List |
| cd | Change directory |
| ps-ef | Show jobs running |
| rm | remove file |
| cp | copy file |
| kill -9 (job #) | stops current job |
| lp filename | print to file in PATRAN |
| patran& | run PATRAN |
| xdytran& | run DYTRAN |

Table 2: Basic Unix Commands

2. PATRAN

PATRAN version 2000 (r2) is an analysis software system produced and marketed by MSC Software, formally called MacNeal-Schwendler Corporation. The core of the system provides an integrated computer-aided engineering (CAE) environment for analysis. The PATRAN software provides both a pre-processor and post-processor usable with several finite element analysis codes, including DYTRAN. PATRAN is an open-architecture, general purpose, 3D Mechanical Computer Aided Engineering (MCAE) software package, with interactive graphics providing a complete CAE environment for linking engineering design, analysis and results evaluation functions. Pre-processing of the model was complete using PATRAN on a Unix based Silicon Graphics (SGI) computer. Post processing, or visualization of the simulated

results derived by DYTRAN, was done using PATRAN on a SGI and a Windows NT workstation PC.

PATRAN translates the numerical output from DYTRAN into a graphical representation. PATRAN can quickly and clearly display FEM analysis results in structural, thermal, fatigue, fluid, or magnetic terms. PATRAN displays time-dependent loads using multiple resultant color-coding on either deformed or undeformed geometry. Individual results can be sequenced in rapid succession to provide animation of the results. Additionally, PATRAN can be used to filter certain results and translate the results into other formats such as reports or graphs.

3. DYTRAN

DYTRAN is a three-dimensional analysis program for analyzing nonlinear behavior of structures and fluids. The program is designed to simulate and analyze extreme, short-duration events involving the interaction of fluids and structures, or problems involving the extreme deformation of structural materials. It has the capability to perform finite element structural analysis, material flow analysis, and coupled fluid-structure interaction with a single analysis package. Typical applications of DYTRAN include response of structures to explosive and blast loading and high-velocity penetration. Version 2000 (r2) of DYTRAN was used to determine the blast effects for this analysis.

To solve problems involving the flow of material, like those seen in an explosion, DYTRAN uses classic Eulerian and Lagrangian technology to enable modeling of both structures and fluids. The Eulerian solid elements remain fixed in space throughout the

analysis, while material flows from one element to the next based on a solution of the Euler equations. In addition to this classic Eulerian technology, DYTRAN also offers an Arbitrary Lagrange Euler (ALE) algorithm. In ALE, the Eulerian mesh does not necessarily remain fixed in space, but moves relative to the material that is flowing through it. Both the Eulerian and Lagrangian formulations in DYTRAN allow for the modeling of classic hydrodynamic materials like liquids and gases, as well as conventional structural materials such as steel. This latter capability provides a means of simulating structural response problems that are characterized by extreme deformation of material, such as projectile impact and penetration.

DYTRAN provides precise coupling of fluid-structure interaction. DYTRAN automatically and precisely calculates the physics of fluid-structure interaction by directly coupling the response of the finite element structural mesh and the Eulerian material flow mesh. In this approach, pressure forces from the Eulerian mesh automatically loads the structural finite element (FE) mesh at the boundaries between the Eulerian and FE meshes via an automatic coupling algorithm. As the structural FE mesh deforms under the action of the pressure forces from the Eulerian mesh, the resulting FE deformation then influences subsequent material flow and pressure forces in the Eulerian mesh, resulting in automatic and precise coupling of fluid-structure interaction. A typical DYTRAN application involving fluid-structure coupling is a structural response to an internal bomb blast.

DYTRAN's ability to model extreme, short-duration events where solid structure and fluids are coupled, make it an ideal choice for conducting computer based ballistic testing.

C. BLAST MECHANICS

Immediately after the explosive round detonates, the energy from the explosion expands in the form of a spherical pressure wave, which radiates from the blast location. As the pressure impacts on the surface of the tailcone, part of the energy transfers to the structure while the remaining portion reflects back into the blast area. The energy transferred to the structure causes the structure to deform and increase the strain. Additionally, the energy transferred to the structure excites responses in the structure causing it to resonate. The high frequency responses dampen out quickly as they translate through the structure, but the low frequency responses remain. The low frequency responses transfer energy to other portions of the structure and back into the blast area. The energy transferred back into the blast area joins the reflected blast energy and reflects around the structure to create additional deformation and strain changes in the structure. The reflecting energy forces the structure through a series of loading and unloading cycles. Over time the blast energy either dampens out or is removed from the system through the pressure vents of the model. As time progresses, the pressures and strains in the model become more uniform, eventually returning to their pre-blast condition provided they are not too badly damaged to return to their original condition.

D. COMPOSITE MATERIALS

Composite materials are predominantly used in aircraft construction because they are very lightweight, and yet, high strength. Additionally, by varying materials and material properties, composite materials allow the designer to tailor areas to withstand specific loads. Composites are a heat-treated combination of materials applied in thin layers, or plies, one on top of another, with a resin. The plies are added in various directions until the desired shape and strength is achieved. The ply layers are applied in different directions to give the structure greater strength in different directions. The resin holds the various materials together while heat is used to cure the resin and make it hard. Altering the type or amount of resin, or altering the time or temperature of the heating process, changes the properties of the composite material.

For example, suppose a composite has a yield strength of 10,000 psi in the normal directions, but no strength in the shear directions. If analysis indicates that the part needs to withstand 20,000 psi in both the shear and the normal directions, the part would need the combined strength of four plies to provide the required strength. Two of the plies must be aligned to provide strength in the normal direction and two plies must be aligned to provide strength in the shear direction. To ensure the plies are properly positioned, a reference direction, or 0° line, is selected. The reference direction is normally aligned with some feature or direction on the model. Rotating the plies designated to withstand loads in the shear direction at a 45° angle relative to the plies designated to withstand the normal loads will ensure the proper strength is achieved in all directions. Assuming the

0° line is parallel to the x-normal direction, the plies might be placed in order at 0° , 45° , 0° , and 45° to get the required strength in each direction .

The side components of the tailcone structure are made up of honeycomb material with a composite skin attached to each side of the honeycomb. Honeycomb is a lightweight series of small hexagonal structures that provides spacing between the composite skins. The honeycomb provides bending stiffness to the structure and most of the resistance to compressive forces that are applied in the direction normal to the skin surface. The composite skins provide the in-plane and shear strength in the tangential directions.

III. MODEL DEVELOPMENT

A. OVERVIEW

Following the live fire tests on the Comanche Static Test Article (STA) tailcone section, conducted in the summer of 2000, the Army requested further research to verify the structural integrity of the tailcone section after receiving a direct hit from a 23mm HE round. The Boeing Company requested this research to assist with the verification of DYTRAN as a suitable alternative for live fire testing. The Army requested verification of the Comanche tailcone model to help reduce or eliminate the high cost of continued live fire tests.

This research project began with an intense period of study, learning the mechanics of PATRAN and DYTRAN. Upon mastering the concepts of the software, additional information was required from Boeing to interpret engineering drawings, materials and properties of structures and tailcone geometry. To gather this information, a trip to the Boeing Company in Philadelphia, Pennsylvania was conducted to have face-to-face meetings with engineers and management. One meeting was a classified brief on the actual live fire test.

Extreme effort was taken to create an accurate model depicting the actual static test article (STA) tailcone used during the live fire test. Since the model is the most important portion of any analysis, construction of the model was the most time consuming, labor intensive portion of this project. To save time and frustration, daily back-ups are required to protect against input errors and computer file corruption. File

corruption is inherent in large PATRAN models. Model construction is completed in the following phases: 1) CATIA Translation, 2) Geometry Creation and Modification 3) Meshing, 4) Assignment of Materials and Properties, 5) Final Model Checks, 6) DYTRAN Translation and 7) PATRAN Analysis.

B. CATIA TRANSLATION

All of the technical drawings of the Comanche at Boeing are made and stored using a program called CATIA. CATIA is the world's leading computer aided design, manufacturing, and engineering software made by IBM and Dassault Systems. CATIA provides easy to use solutions tailored to the needs of small and medium sized enterprises as well as large industrial corporations in all industries. Its leading edge solutions and technologies for computer aided design, manufacturing and engineering including data management, lets the modeler achieve digital product definition and simulation goals. The modeler can easily implement all necessary changes on the digital model for a concurrent optimization of design and manufacturing. Therefore, the modeler minimizes the risk of late expensive modifications and reduces the number of iterations by designing the model right the first time.

For this project a CATIA bit-map picture was first imported into PATRAN. Due to the incompatibility between CATIA and PATRAN, numerous geometries were missing from the import and had to be recreated based upon the engineering computer-aided design (CAD) drawings. Furthermore, all geometries had to be rescaled from millimeters to inches to conform to a change in units. After translation, the PATRAN

parts had the same scaled dimensions, orientation and spatial location as the CATIA parts from which they were created. The following figure depicts the PATRAN bit-map of CATIA:

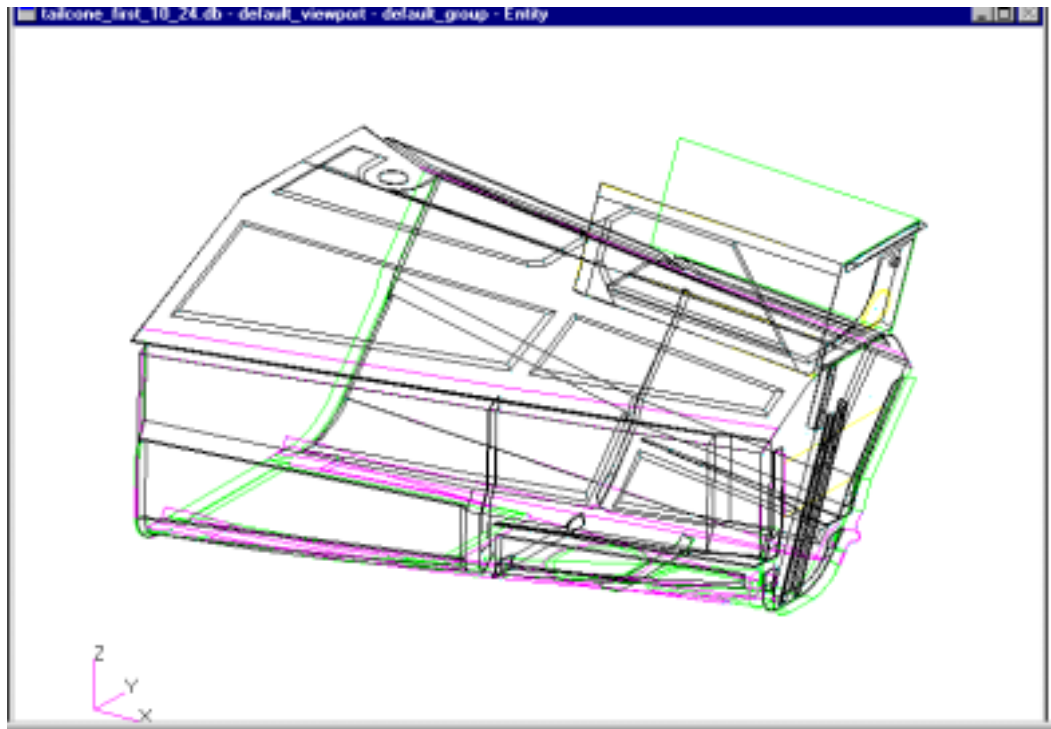


Figure 3: CATIA Model of STA Tailcone

The CATIA model contains all geometries needed to construct the tailcone at the factory. However, the irregular shapes, fine detail and numerous angle changes do not allow for accurate finite element results in PATRAN. This project consisted of taking this complex CATIA system and reducing it down to a workable model that produces the same results as the real world system. As a result, the PATRAN model required extensive geometry creation and modification.

C. GEOMETRY CREATION, MODIFICATION AND MODELING

CATIA is a drawing program that allows designers to design, edit, and store technical drawings. The CATIA drawings are used by designers to create, engineers to modify, and manufacturers to build the tailcone section. As a result, the CATIA drawings contain a fine detail of each sub-component used in assembling the tailcone. However, for this research, it was not necessary to analyze each individual sub-component but rather various groups of the tailcone section. For example, Figure 4 shows the CATIA drawings for the back frame of the tailcone section consisting of several different plates connected together to create the frame. Figure 5 shows the PATRAN model of the back frame modeled as one continuous plate.

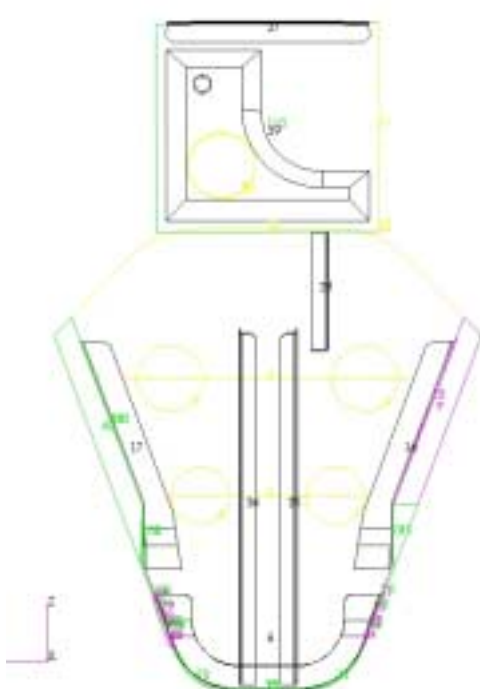


Figure 4: CATIA Back Frame

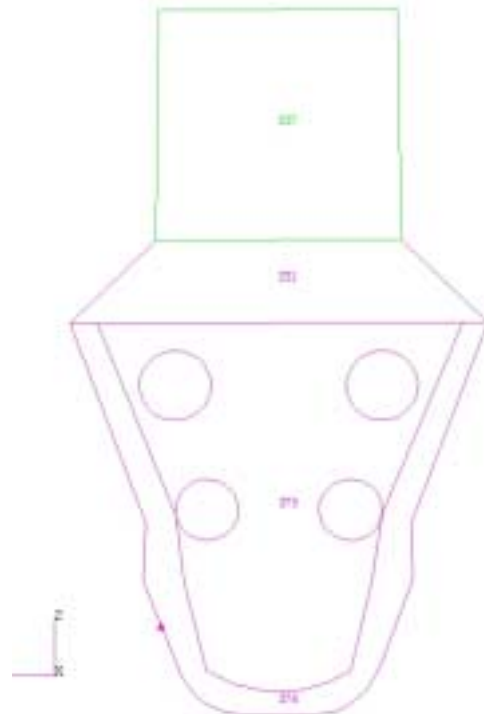


Figure 5: PATRAN Back Frame

The goal of simplifying the geometry from CATIA is to obtain a meshable structure. A lesson learned in this project was not to spend extensive amounts of time manipulating the geometry to have an exact replication of the CATIA drawings. The most important aspect is to have a mesh that accurately depicts the structure. The mesh elements are the only part of the model that is entered into the finite element code.

The first step in creating the meshable structure is to eliminate irregular geometries and modify the structure to eliminate gaps between sub-components. Irregular geometries are modified utilizing various commands under the geometry menu to include edit, create, and transform. One method to remove a “kinked” irregular geometry is extending existing lines together and deleting the original lines of the irregular shape. These new lines are formed into a curve using the PATRAN command: GEOMETRY/CREATE/CURVE/CHAIN. After creating two curves, a new surface is created using the command: GEOMETRY/CREATE/SURFACE/CURVE/2-CURVE. As a result of eliminating the “kink”, the surface in the PATRAN model is continuously smooth allowing for a simple mesh. After the creation of each surface, a quad-four mesh is created to determine the simplicity of the mesh using the command: ELEMENT/CREATE/MESH/SURFACE/QUAD-FOUR ISOMESH. Finally, the process for eliminating any gaps between sub-components is accomplished by creating curves between points on each side of the gap. Once the curves are created spanning the gap, the surface create method mentioned above is used to create the new surface.

For this project, the back frame had several solid sub-components in the CATIA drawings. In order to create the shell elements, these solid sub-components were changed into surfaces. One side of the solid sub-component was selected to create the

new surface, and the remaining geometries of the solid were deleted. After the creation and modification of all the surfaces of the back frame, one complete surface was created using the inner and outer curves of each surface. The new surface consisted of one entire component rather than all the sub-components in the CATIA drawing. The transformation from the CATIA drawing to the PATRAN model is easily seen in Figures 4 and 5.

The same method as described above for the back frame was used in eliminating irregularities and closing gaps in the remaining geometries of the CATIA drawings. An important lesson learned in this process is not to delete any geometry until the modeler is absolutely sure that it will not be needed in future creation or modification of geometries. An alternate method of removing geometries is to use the PLOT ERASE command: DISPLAY/PLOT-ERASE/SELECTED ENTITIES/ERASE. This command allows the modeler to erase any geometry or finite element in the PATRAN model. As a result, the modeler can remove specific geometries in order to allow a more visible work space for geometry creation or modification. After completing the specified work, the modeler can then use the PLOT ERASE command to redraw the erased geometries by utilizing the command: DISPLAY/PLOT-ERASE/SELECTED ENTITIES/PLOT ALL. This method is a strong tool as the erased geometries are not deleted and can be recalled at any time.

Several vents were created in the front, back, top and bottom groups of the tailcone section of the PATRAN model in order to replicate the STA tailcone section used in the live fire test. Most of these vents consisted of circular geometries. Since the vents and associated surfaces consisted of different materials, the GEOMETRY/EDIT/SURFACE/ADD_HOLE/INNER_LOOP command from the

geometry menu was utilized to create the vent holes, using the inner loop as the original surface of the vent. The front rectangular and irregular shaped bottom vents were created using various commands from the geometry menu.

After completing the necessary modification and creation of the geometries in the PATRAN model, the model was then separated into the following groups: back, bottom, bottom side panels, bottom vents, front, sides-longerons, top, top side panels, top panels, top panels-top surface, inner surface and vents (see following figures 6-13). The groups were created to allow for easier identification of the various subcomponents, assignment of materials and properties, meshing and to analyze results. Groups are created using the GROUP/CREATE/SELECTED ENTITIES command from the Group menu. This command allows the modeler to select specific geometries to be imported from the main model into the desired group. Once all the geometries are imported into the appropriate group, the next step is to create the finite element mesh for each group. The following figures show each PATRAN group and figures 14 and 15 show the transformation from CATIA to the PATRAN model.

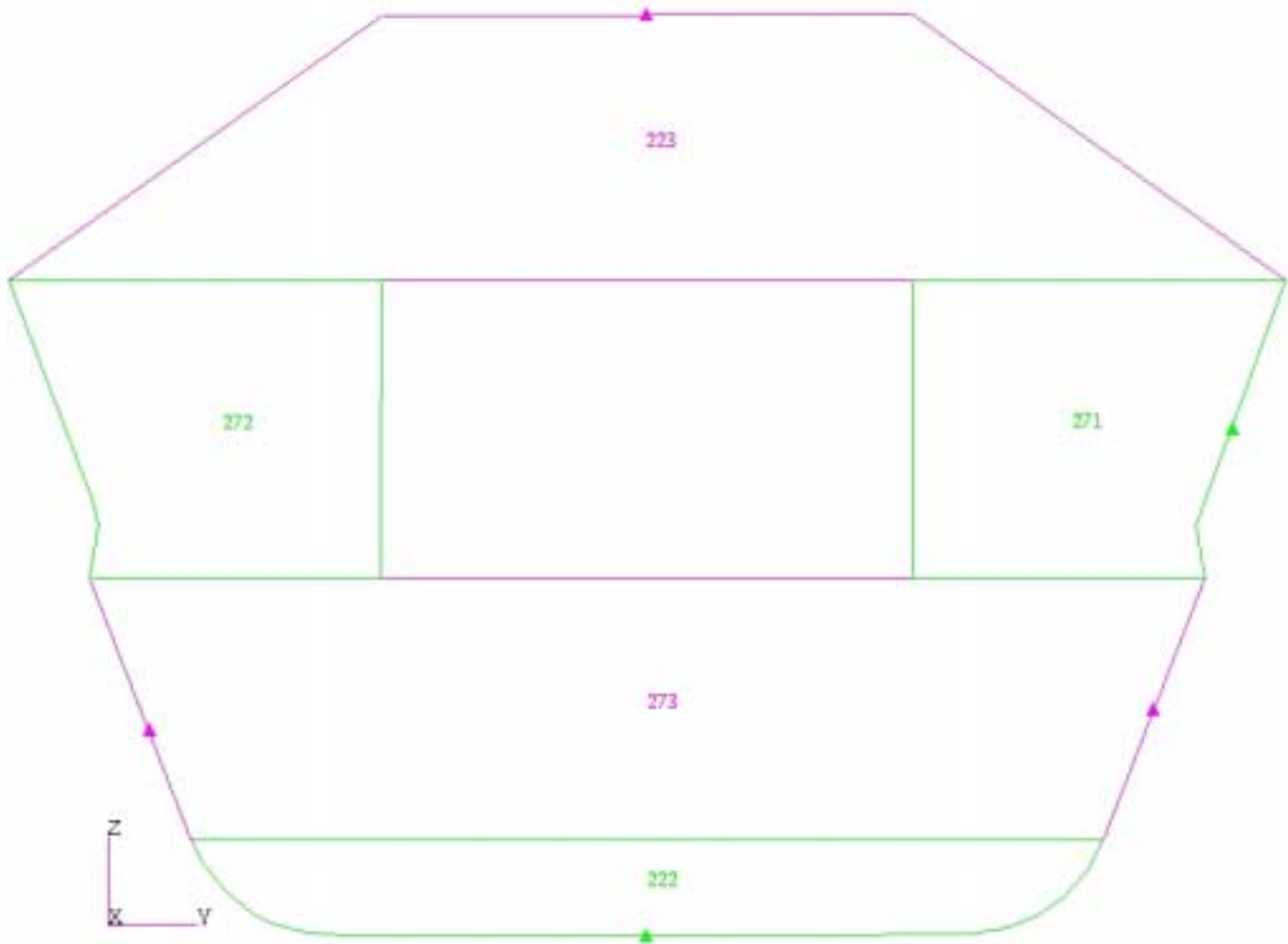


Figure 6: Front Tailcone Group

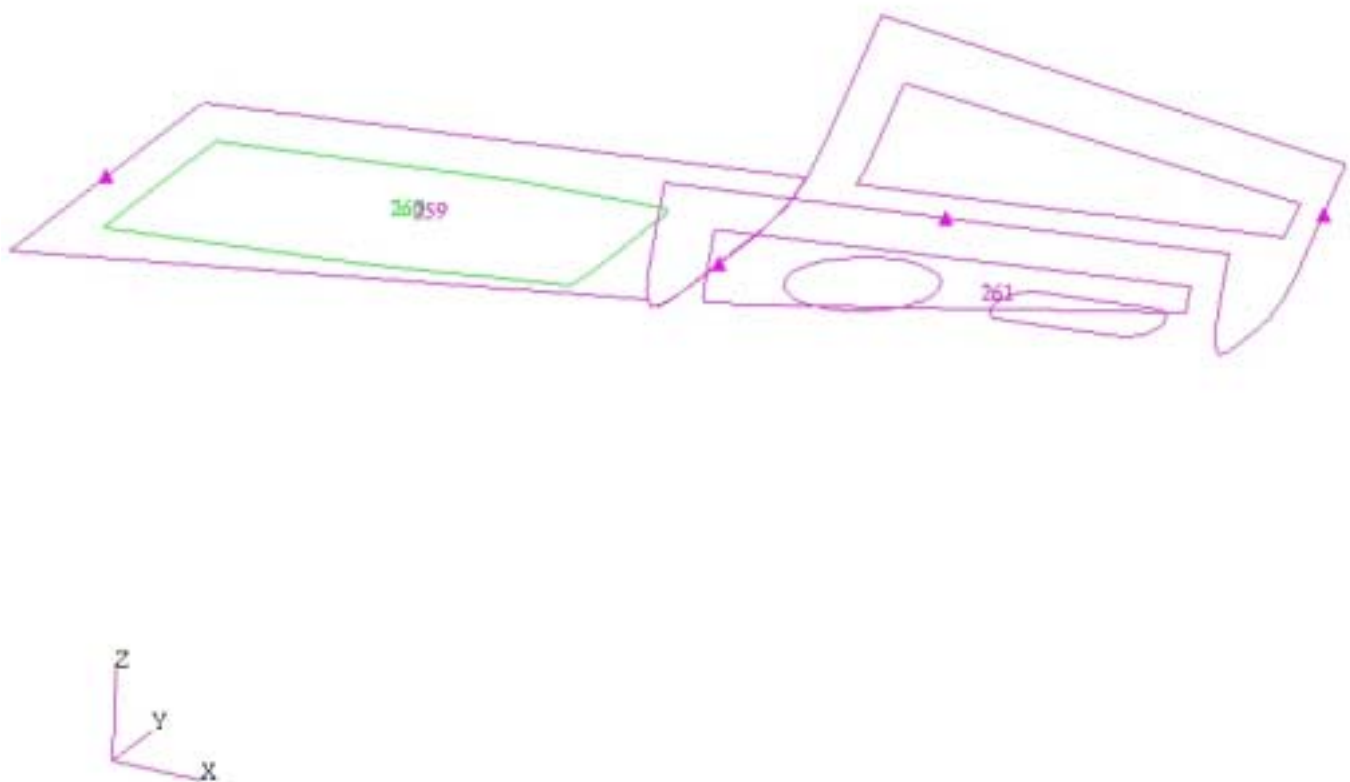


Figure 7: Bottom Tailcone Group

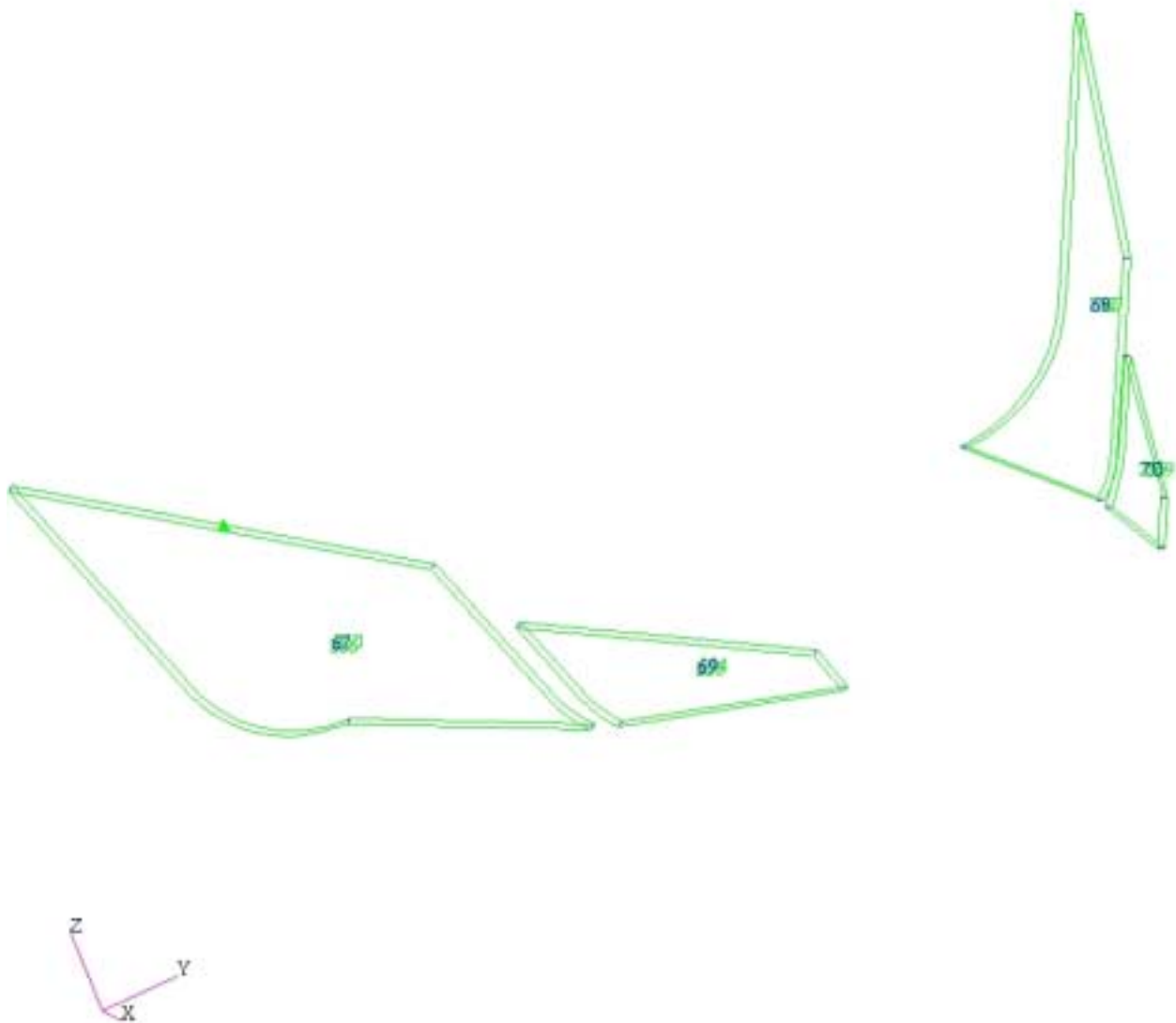


Figure 8: Bottom-Side Panels Tailcone Group

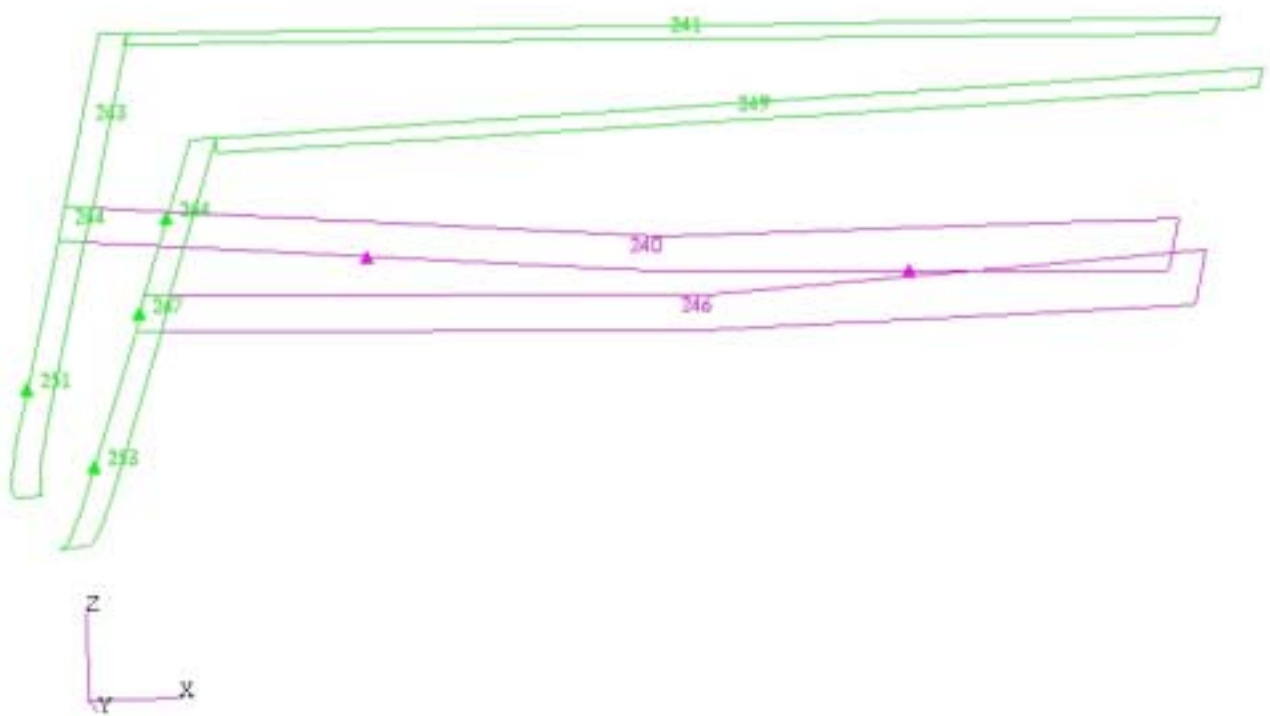


Figure 9: Side and Longerons Tailcone Group

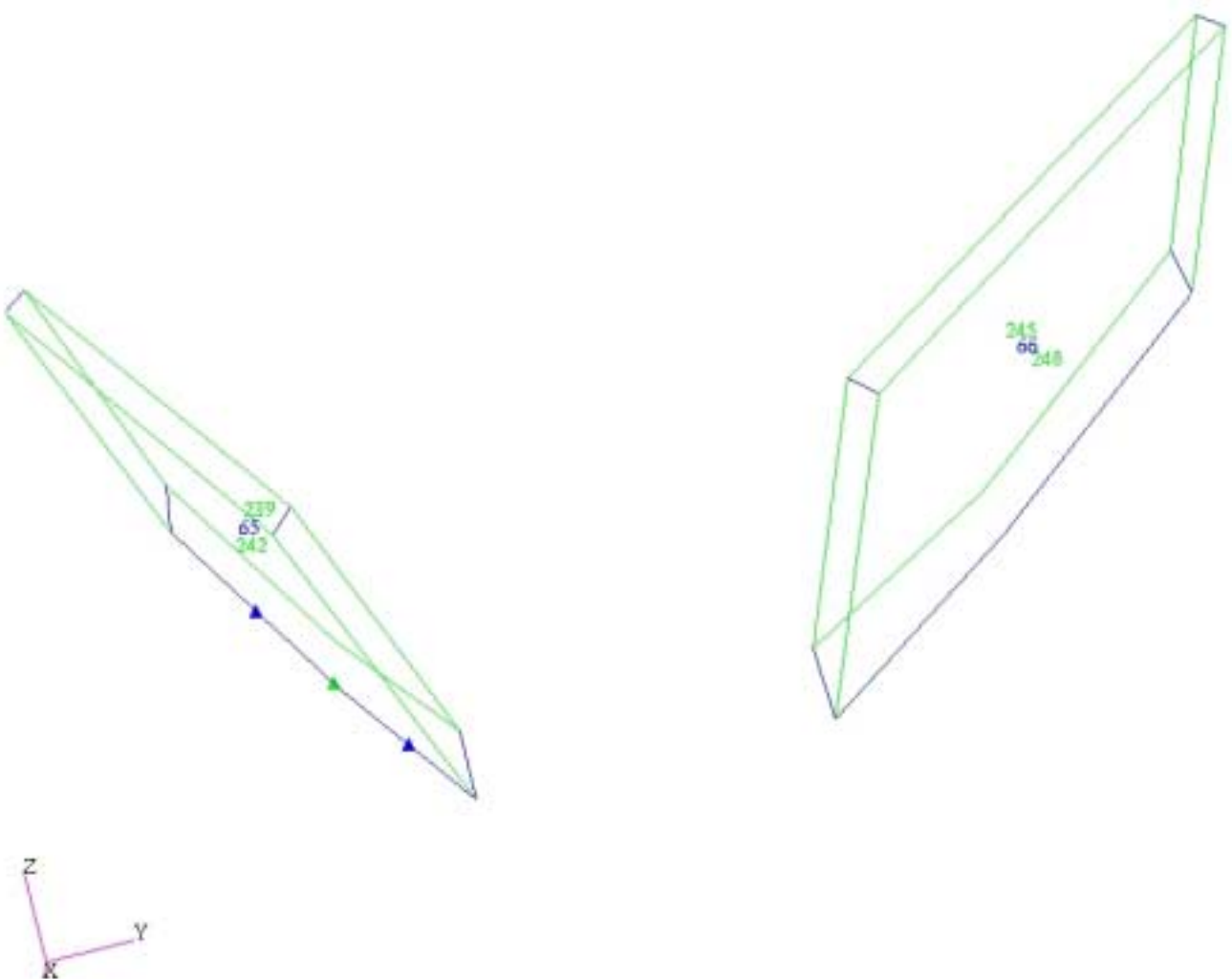


Figure 10: Topside Panels Tailcone Group

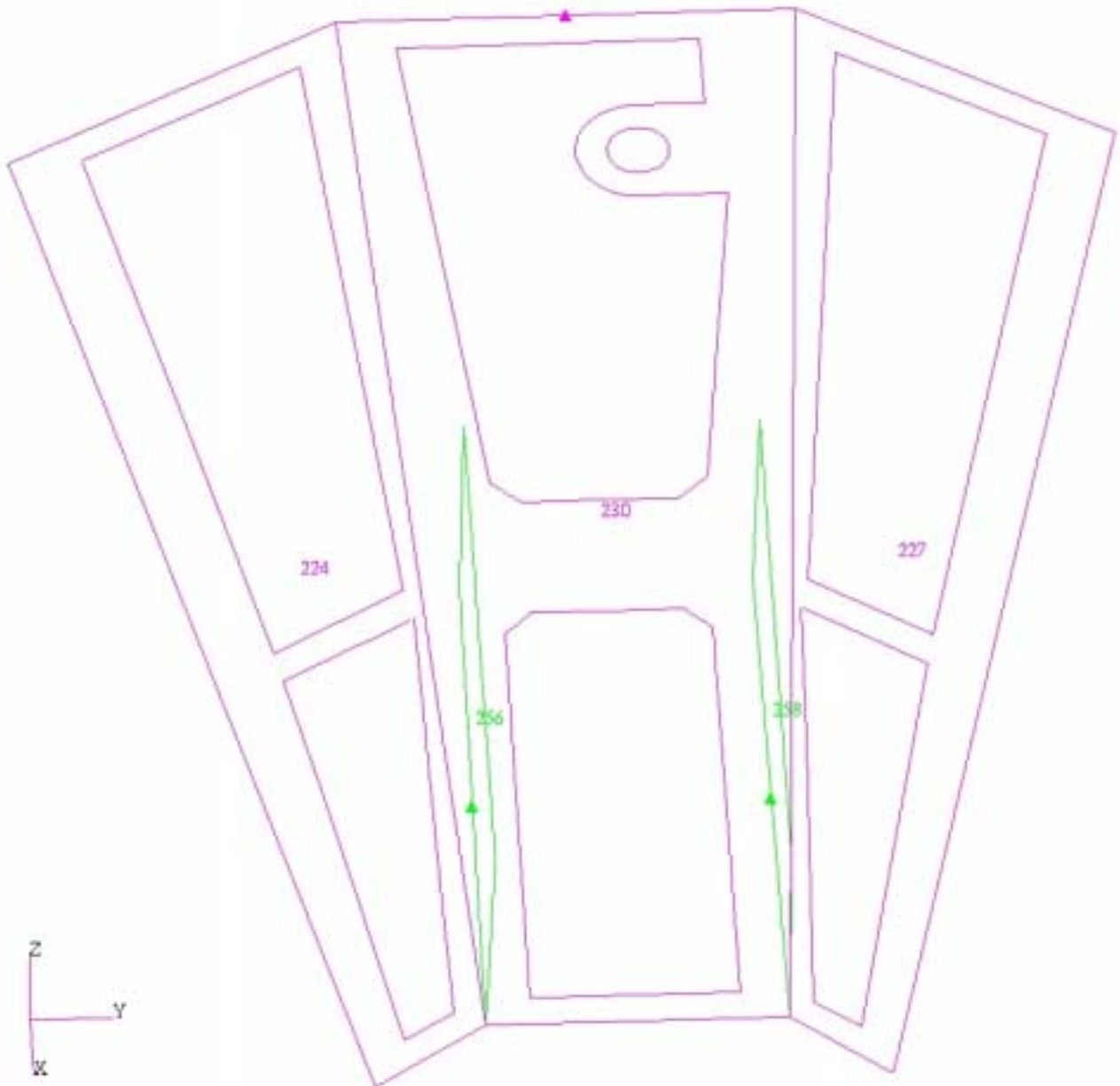


Figure 11: Top Tailcone Group

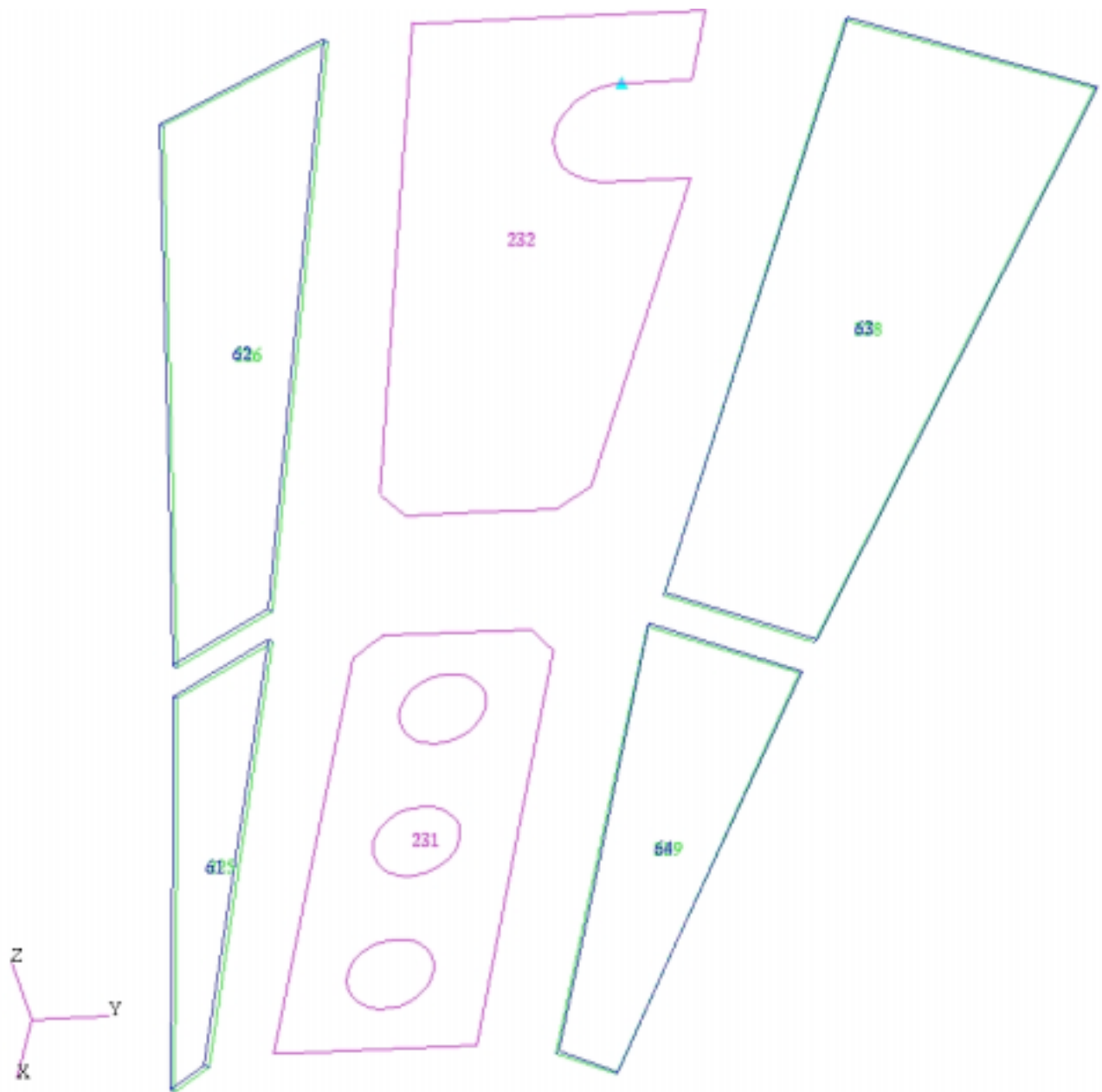


Figure 12: Top Panels Tailcone Group

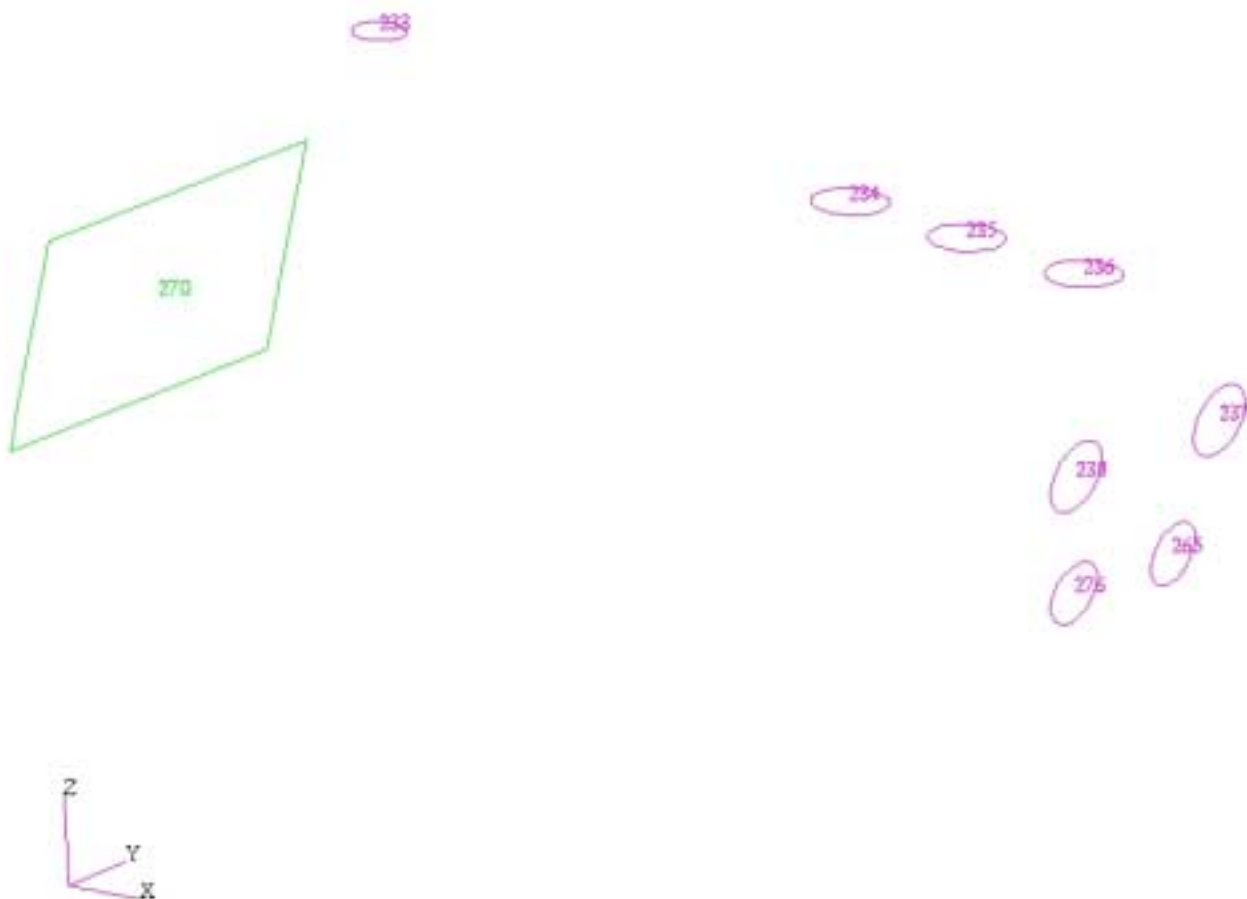


Figure 13: Vents Tailcone Group

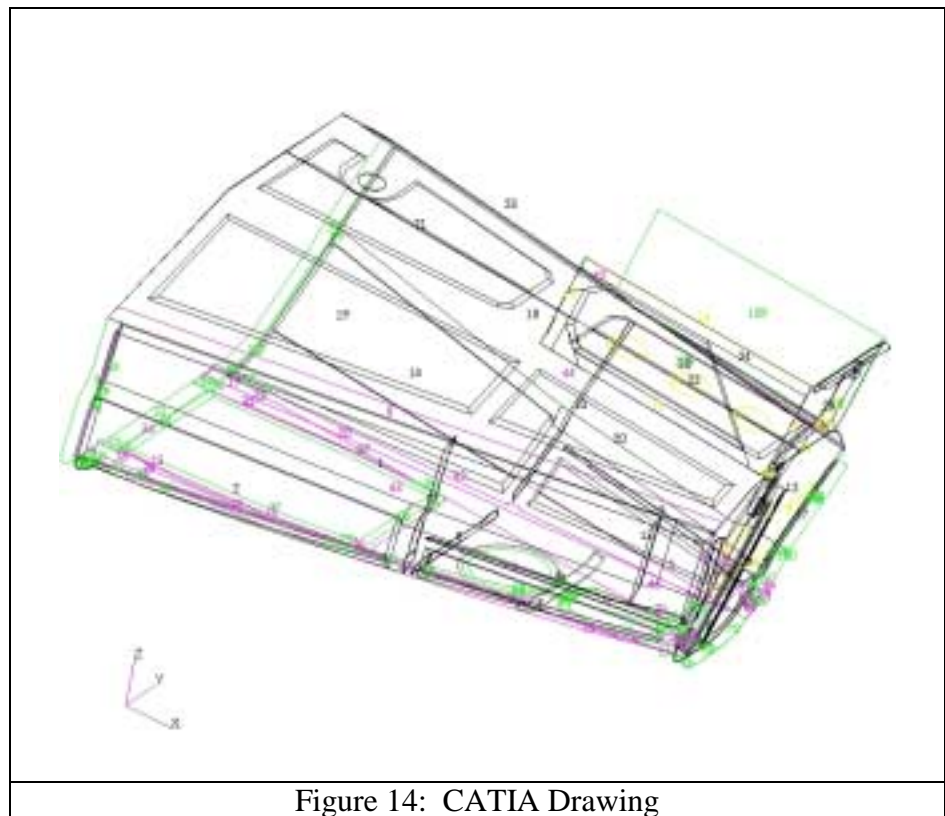


Figure 14: CATIA Drawing

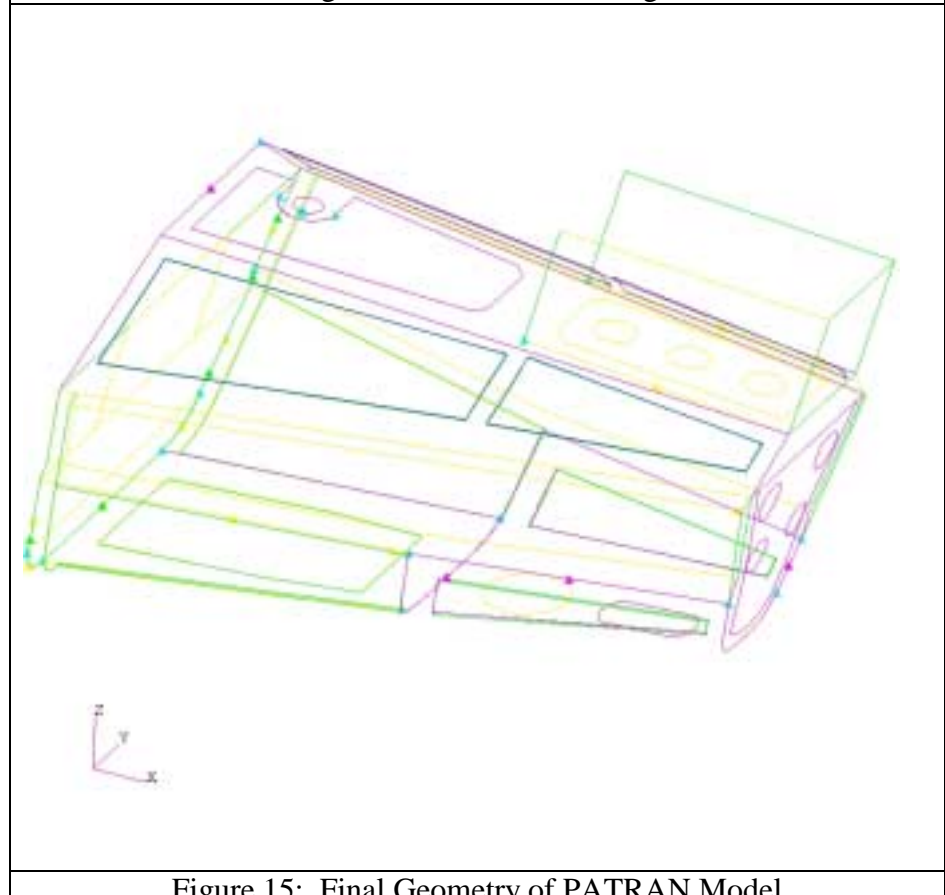


Figure 15: Final Geometry of PATRAN Model

D. MESHING

The extensive work in creating and modifying the geometry of the tailcone section, by eliminating irregular shapes, paid great dividends in the meshing process. The main advantage of removing the irregular shaped components is that meshing the model is now possible. With the model broken down into simple shapes and volumes, meshing is automatically done by PATRAN.

Groups are meshed using the command: ELEMENT/CREATE/MESH/SURFACE/QUAD-4/PAVER OR ISOMESH. The base size of the element mesh is assigned by the command: GLOBAL EDGE LENGTH. Smaller Global Edge Length creates more finite elements and provides greater accuracy and better results. Due to the large size of this model, the Global Edge Length was chosen to be one inch. The mesh command allows the modeler to choose between an Isomesh or Paver mesh. Isomesh creates equally spaced nodes along each edge in real space to include nonuniformly parameterized surfaces. Isomesh computes the number of elements and node spacing for every selected geometric edge before any individual region is meshed. This ensures that the mesh will match any existing mesh in neighboring regions. Isomesh requires the surfaces to be parameterized, green in color on PATRAN, and to have either three or four sides. If surfaces have more than four sides, the geometry must be modified to create smaller surfaces consisting of no more than four sides in order to utilize the Isomesh command.

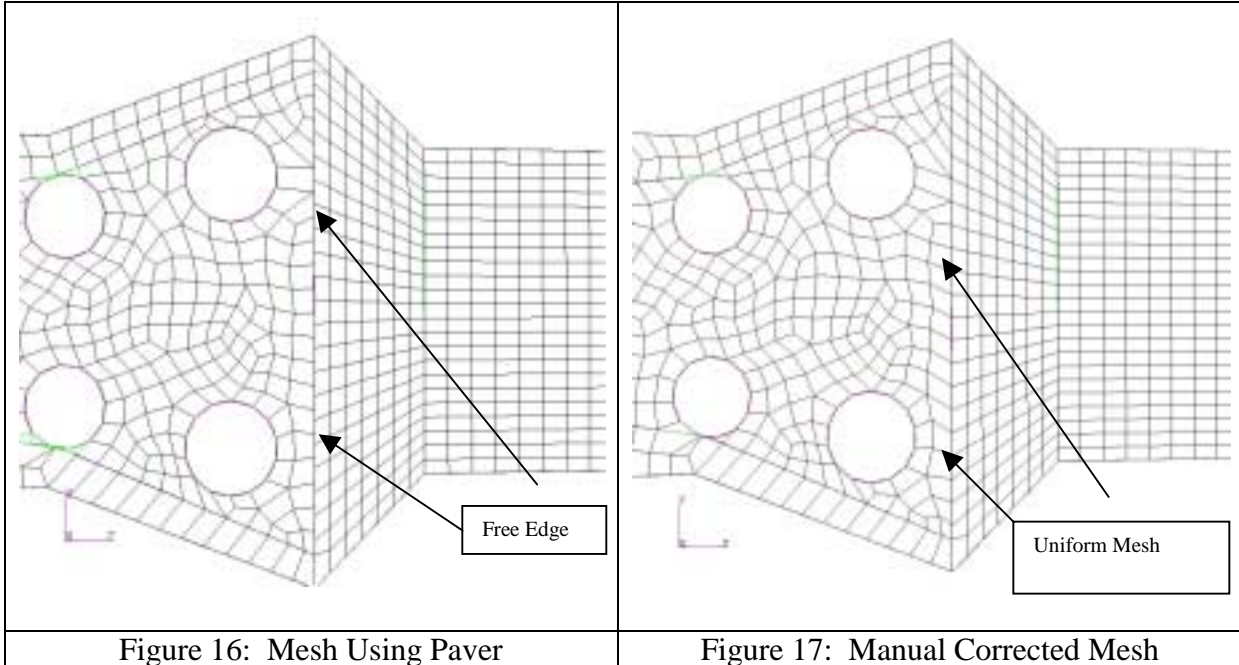
Instead of modifying the geometry, the modeler can use the Paver command. Paver is best suited for complex surfaces with more than four sides, such as surfaces with

holes or cut-outs. Paver is also well suited for surfaces requiring “deep” mesh transitions, such as going from four to twenty elements across a specified surface. Similar to Isomesh, Paver calculates the node locations in real space, but it does not require the surfaces to be parameterized. For a mesh consisting of all quadrilateral elements, Paver requires the total number of elements around the perimeter of each surface to be an even number, and will automatically adjust the number of elements on a free edge to ensure this condition is met.

During the meshing process, several groups may require the use of both Isomesh and Paver. This is a result of surfaces having a wide range of sides and having holes within particular surfaces. After each surface in a particular group is meshed, all nodes within the group are equivalenced in order to combine nodes within a one inch parameter of each other into a single node, using the command: ELEMENT/EQUIVALENCE/ALL.

After all nodes are equivalenced check each group to determine if any free edges exist using the command: ELEMENT/VERIFY/ELEMENT/BOUNDARIES/FREE EDGES. A free edge is any edge along which element node boundaries are not shared. Free edges develop on boundaries that require surfaces to be meshed with different methods. One method of eliminating free edges is to create mesh seeds along the surface edges prior to creating the mesh using the command: ELEMENT/CREATE/MESH SEED. This command creates nodes at the specified seed locations. The modeler then creates a mesh using these nodes for the two adjacent surfaces, resulting in a uniform meshing on the edge. The uniform meshing results from the adjacent surfaces sharing the same nodes and eliminates the free edge. In small cases, it is easier to manually

manipulate the nodes and elements in order to eliminate the free edges. The modeler deletes the specified elements along the free edge and then creates new elements to ensure adjacent elements share the same edges. The following figure shows the manual manipulation of elements to eliminate the free edges that occurred when meshing the back group:



In the figures above, the mesh of the vents is not present. The meshing of the vents is a more complex task. The vents can not contain any nodes internal to the surfaces. When nodes are present within the surface of the vents, the deformation of the nodes becomes too large during the DYTRAN analysis due to the material properties of the vents. As a result, the execution of the analysis terminates due to the excessive deformation of the vent's surface. In order to continue the analysis in DYTRAN, the nodes are removed from the internal surface of the vents. The mesh of the vents is created manually utilizing the nodes from the mesh of adjacent surfaces. Using this

method, the mesh of the vents had larger and regular shaped elements. The following figure shows the mesh of the vents associated with the back group:

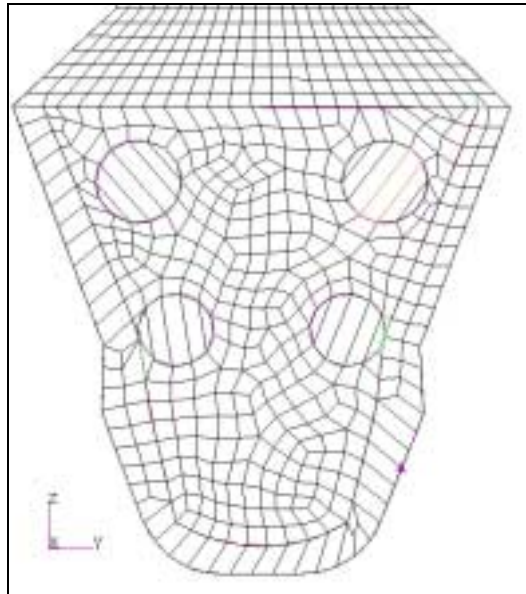


Figure 18: Meshed Vents on Back Group

The PATRAN model consists of shell and solid elements. Shell elements are 2-D elements used to replicate the skins attached to the honeycomb, surfaces of the tailcone, composite materials, and flat plates like the longerons and frames. The preceding figures of the back group illustrate examples of both triangular and quad4 shell elements. Solid elements are 3-D elements having a length, width and thickness. The solid elements are used to replicate the honeycomb material in the model. Solid elements are created using the command: ELEMENTS/SWEEP/ELEMENT/EXTRUDE. This command translates the existing shell element mesh on the inner surface of the honeycomb panel a specified distance and direction. The result is a solid geometry containing hex8 and wedge 3-D finite elements with a shell element mesh on the inner and outer surface of the honeycomb panels.

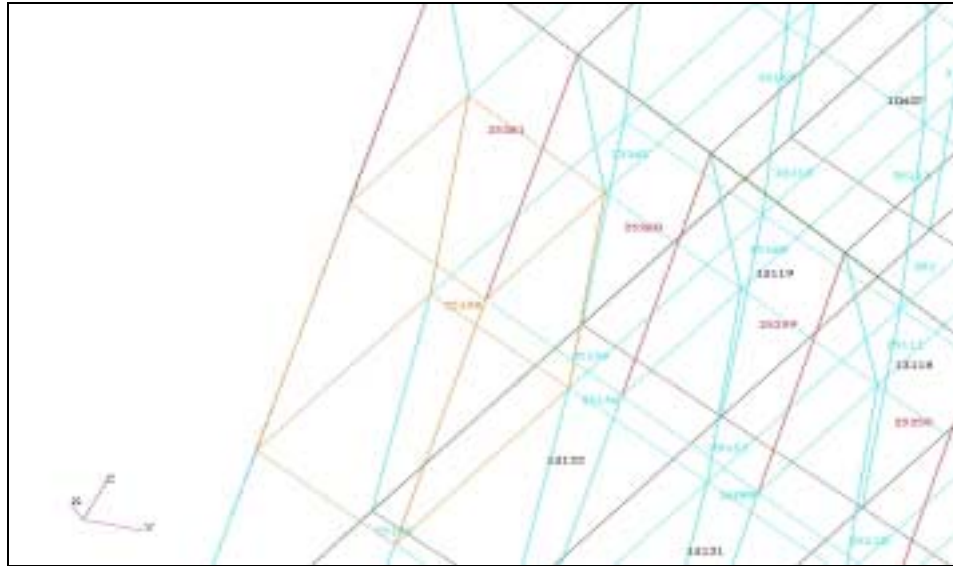
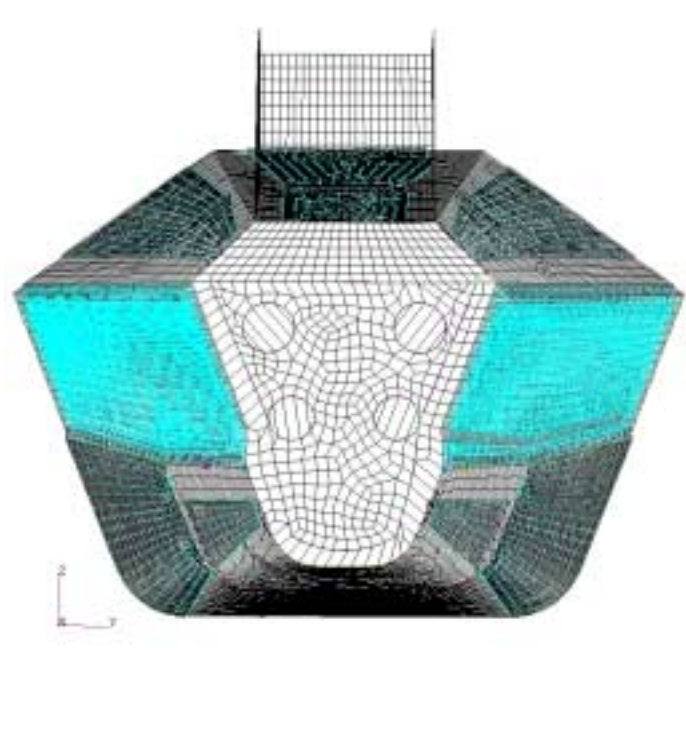
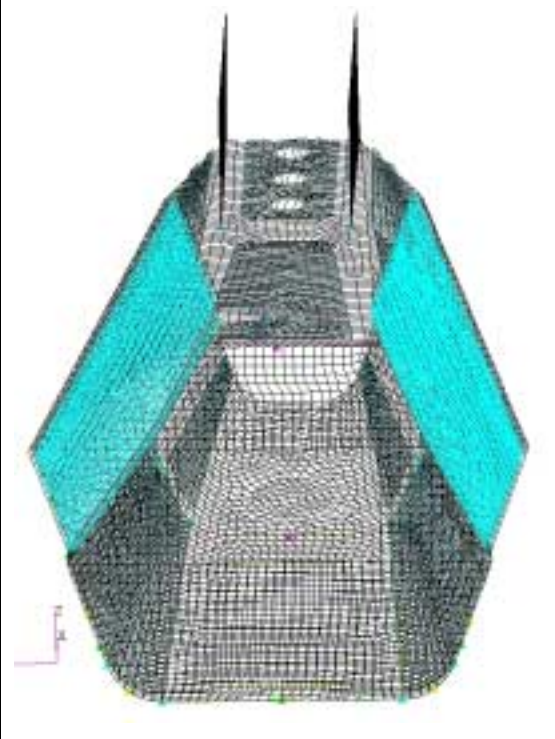


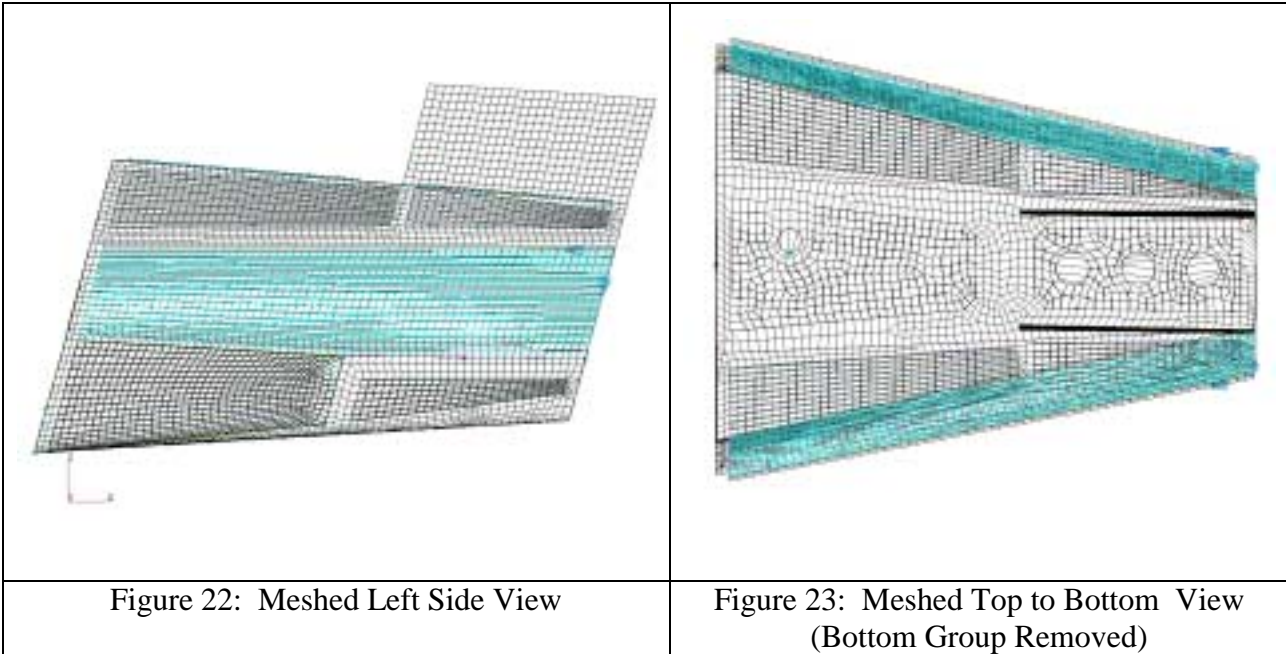
Figure 19: View of Honeycomb Mesh

The previous figure shows the end result of creating the solid elements for the honeycomb panels. The elements labeled in black are the shell element mesh for the inner and outer surfaces of the honeycomb panel. The solid 3-D elements are depicted in blue (hex8) and red (wedge). The orange element is shown to highlight one of the hex8 elements.

A combination of solid and shell elements provides the most accurate results. The best results are obtained using hex8 3-D and quad4 2-D elements. However, due to the non-uniform shape of the components, a few filler elements such as the 3-D wedge and 2-D triangular elements are used to complete the coverage of the structure with elements.

After completing the mesh for each of the individual groups, the meshes are imported into the main model group. This is accomplished using the command: TOOLS/LIST/CREATE/MODEL:FEM/OBJECT:ELEMENT/METHOD:ASSOCIATION/SURFACE which creates a list of all elements associated with the selected surface. This allows the modeler to copy the associated elements into a specified group. The following figures show different views of the entire meshed model:

| | |
|--|--|
|  A 3D perspective view of a meshed model. The model is a complex, multi-faceted shape, possibly a ship's hull or a similar structure. The front portion of the model is shown with a coarser, larger element size, while the rear portion is shown with a finer, smaller element size. A small coordinate system is visible in the bottom left corner. |  A 3D perspective view of the same meshed model, but from a different angle. In this view, the rear portion of the model is shown with a coarser, larger element size, while the front portion is shown with a finer, smaller element size. A small coordinate system is visible in the bottom left corner. |
| Figure 20: Meshed Back to Front View (Front Group Removed) | Figure 21: Meshed Front to Back View (Back Group Removed) |



A useful tool to verify the association of elements with a particular surface or solid is the **HIGHLIGHT** command from the list menu. This visually shows the elements in the list on the screen. The process of creating the main model is done to ensure the model has no free edges, ghost elements, duplicate elements or missing elements. At this point, the modeler should conduct a test run using generic materials and properties to ensure the main model will correctly run in DYTRAN and provide results. Following a successful run, the next step in the project is to assign the actual materials and properties to the components of the model.

E. ASSIGNMENT OF MATERIALS AND PROPERTIES

The assignment of materials and properties for all the components begins by interpreting the engineering drawings. The following diagram shows the complexity and detail of the engineering drawings.

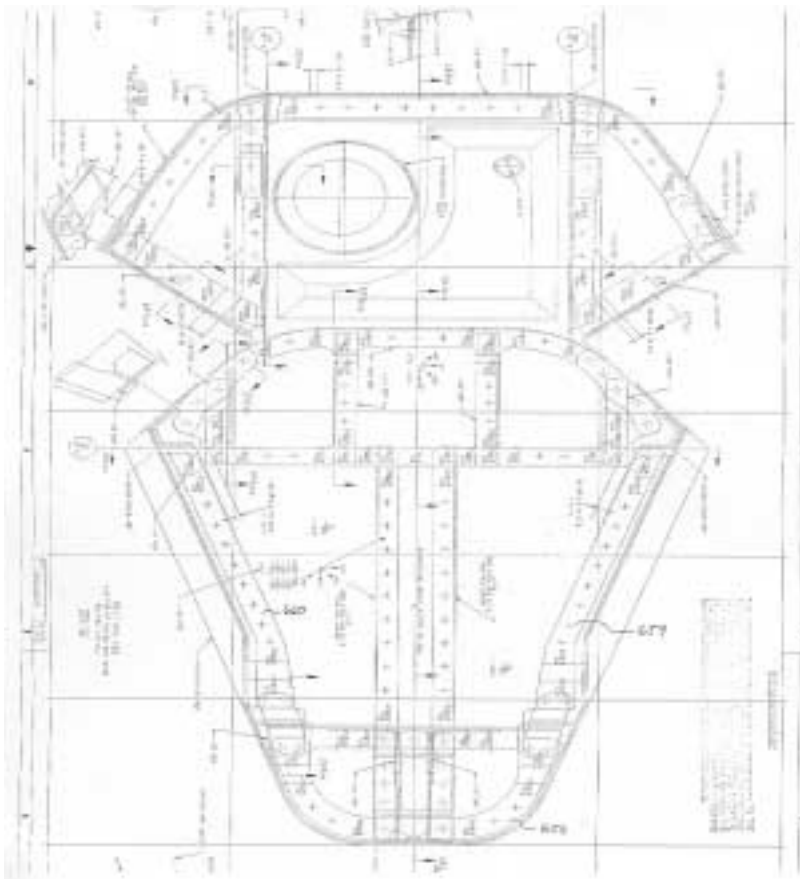


Figure 24: Engineering Drawing of Back Frame

The engineering drawings provide details for each of the components within the PATRAN model. The interpretation of the drawings provides the modeler with verification of component geometry, type of composite material identified by material

code, number of plies of each material for each component, and orientation of each ply for each component.

The “dash number” for each component allows the modeler to refer to the appropriate entry in the legend to obtain the needed material data. The following table shows a partial ply table from the engineering drawings:

| Dash Number | Ply Number | Orientation Degrees | Material Code |
|--------------------|--|----------------------------|----------------------|
| -111 | P1, P10 | NA | 6310 |
| -111 | P2, P3, P5, P6, P8, P9, P11, P12, P14, P15, P17, P18, P19, P20, P22, P23, P25, P26 | +/- 45 | 6250 |
| -111 | P7, P16, P21 | 0/90 | 6250 |
| -111 | P4, P13, P24 | 0 | 6100 |

Table 3: Partial Composite Ply Lay-up Table

The determination of the number of plies is the most difficult. Cross sectional areas of the desired component are located on the engineering drawing in order to count the number of plies for a particular component. Due to the complexity of the plies, an approximation of the number of plies is made for several of the components. The number of plies on a particular component range from 16 plies at the ends of the component to only 10 plies in the middle of the same component. This is due to the fact that certain areas of the tailcone need more structural support. The variation of the number of plies along a particular component made it difficult to assign the material properties to the model. The modeler would have to individually select the elements associated with the particular component to assign the varying ply make-up. To overcome this problem, an average number of plies is utilized in assigning the material properties to a particular component. This allows the same assignment of material properties to all elements

associated with a particular component. The figure below shows a component with 14 plies on the ends and 10 plies in the middle. The assignment of material properties is created using a 12 ply make-up. During this process, the modeler must ensure the orientation of the plies is still accurately depicted.

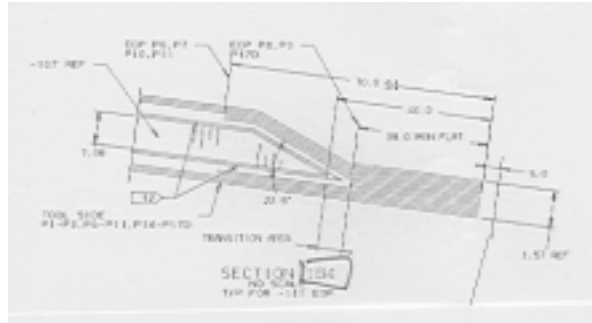


Figure 25: Cross Section of Composite Ply Lay-up

Following interpretation of the engineering drawings, the modeler assigns the material properties to the elements associated with each component. The first step is to input all the properties of the materials. The materials of the tailcone consist of Isotropic and 2-D Orthotropic properties. To input the properties use the command: MATERIAL/CREATE/ISOTROPIC OR 2-D ORTHOTROPIC/MANUAL INPUT/MATERIAL NAME. The modeler then selects Homogeneous for the Isotropic materials and Laminate for the 2D Orthotropic materials. The properties are entered using the INPUT PROPERTIES command in the same window, which assigns all data of a particular material a specific material name. The INPUT DATA window allows the modeler to identify the constitutive model, which is linear elastic for this project. The following data is also entered for the components: Elastic Modulus, Poisson Ratio, Shear Modulus and density. Boeing Corporation provided all the material and property data for

this project. This process results in the creation of the database for all material properties. This project's materials and properties are shown below:

| Material Name | Density | Elastic Modulus | Poisson ratio | Yield Stress | Maximum Strain | Plastic | Thickness (inches) |
|---------------|-----------|-----------------|---------------|--------------|----------------|---------|--------------------|
| Aluminum 7075 | 2.614 E-4 | 1.03 E+7 | 0.33 | NA | NA | | 0.1 |
| Air | 1.0 E-8 | 10 | .3 | 1.0 E-5 | 1.0 E-8 | | 0.001 |

Table 4: Isotropic Material Properties

| Material Name | Elastic Modulus E11 | Elastic Modulus E22 | Poisson Ratio | Shear Modulus G12 | Shear Modulus G2,z | Shear Modulus G1,z | Density | Thickness (inches) |
|-----------------------------------|---------------------|---------------------|---------------|-------------------|--------------------|--------------------|-----------|--------------------|
| 6100 Graphite Tape Unidirectional | 2.205 E+7 | 1.75 E+6 | 0.025 | 7.5 E+5 | 7.5 E+5 | 7.5 E+5 | 1.482 E-4 | 0.006 |
| 6250 Graphite Fabric | 11.2 E+6 | 11.2 E+6 | 0.05 | 7.5 E+5 | 7.5 E+5 | 7.5 E+5 | 1.475 E-4 | 0.0075 |
| 6270 Graphite Tape | 2.205 E+7 | 1.75 E+6 | .31 | 7.5 E+5 | 7.5 E+5 | 7.5 E+5 | 1.483 E-4 | 0.005 |
| 6350 Kevlar Fabric | 4.04 E+6 | 4.04 E+6 | .1 | 3.8 E+5 | 3.8 E+5 | 3.8 E+5 | 1.281 E-4 | 0.0075 |
| 6370 E-Glass style 120 | 3 E+6 | 3 E+6 | 0.13 | 4.8 E+5 | 4.8 E+5 | 4.8 E+5 | 1.563 E-4 | 0.0045 |

Table 5: 2-D Orthotropic Material Properties

The next step is to build the laminated composites. The laminated composites are developed for the groups that contain various ply make-ups. The only group that does not contain laminated composites is the vent group as this consists of only one layer of aluminum or weak material. The laminated composites are created using the command: MATERIALS/CREATE/COMPOSITE/LAMINATE. The modeler inputs the new material name for the laminated composite and then proceeds to develop the “stacking sequence” of the ply make-up. The stacking sequence identifies the type of material, thickness and orientation of each ply within the composite. This data is determined through the process of interpreting the engineering drawings for each component. The following table shows a composite material ply layer breakdown for the middle upper longeron.

| Composite Layer | Material | Thickness | Orientation |
|-----------------|-----------------------------------|-----------|-------------|
| 1 | 6250 Graphite Fabric | 7.5 E-3 | +45 |
| 2 | 6250 Graphite Fabric | 7.5 E-3 | -45 |
| 3 | 6100 Graphite Tape Unidirectional | 6.0 E-3 | 0 |
| 4 | 6100 Graphite Tape Unidirectional | 6.0 E-3 | 90 |
| 5 | 6250 Graphite Fabric | 7.5 E-3 | 45 |
| 6 | 6100 Graphite Tape Unidirectional | 6.0 E-3 | 0 |
| 7 | 6100 Graphite Tape Unidirectional | 6.0 E-3 | 90 |
| 8 | 6100 Graphite Tape Unidirectional | 6.0 E-3 | 0 |
| 9 | 6250 Graphite Fabric | 7.5 E-3 | 45 |

Table 6: Composite Material Layers for Longeron Middle Upper

After entering all the material properties and building the composite laminates, the elements and nodes in each of the groups that make up the main model are renumbered. The elements are renumbered in order to ensure a consecutive numbering scheme for each group and provides that no element numbers are skipped, as skipped numbers will create problems in DYTRAN. Additionally, renumbering makes identifying where the element is located on the model much easier, allows for an easier process of ensuring the appropriate material property is assigned to the components, and is necessary for entering into the DYTRAN code. The command to renumber the elements is ELEMENTS/RENUMBER/ELEMENT/SELECT ALL.

With the elements renumbered, the properties are assigned to the elements of each group. The creation of the different groups makes this process easy. Each group consists of components containing the same material and property make-up. As a result, all elements in the group are assigned the same properties. The command to assign the properties is PROPERTIES/CREATE/2D/SHELL for all components except for the honeycomb panels. The command to create the honeycomb panels is PROPERTIES/CREATE/3D/LAGRANGIAN SOLID.

The command window allows the modeler to select between a homogeneous and laminate material. The homogeneous material was selected for the vent groups and laminate material was selected for all remaining groups. The INPUT PROPERTIES command is selected from the same window in order to select the MATERIAL PROPERTY SET NAME to apply to the specified group. After selecting the appropriate material property set name, the elements of the group are selected in order to associate the properties with all the elements of a particular group. Once this process is completed for all groups, final checks are conducted prior to executing a run in DYTRAN.

F. FINAL MODEL CHECKS

To complete the model and make it suitable for running on DYTRAN, several checks must be completed. The first and most important is the free edge check of the entire model. The free edge check is completed earlier for each individual group and is now completed again with the main model to ensure that all of the elements of the main model do not have any gaps. Although the meshed model may look correct, tiny gaps, too small to see, may exist. Unwanted gaps in the model create a hole in the model and provide faulty results. This usually happens when the modeler puts two groups together that have different element mesh nodes on the edges. To fix these problems, PATRAN identifies those element edges that are not aligned with adjacent element edges. With the free edges identified, the modeler can fix any gaps that exist by manually manipulating the elements to ensure adjacent elements align with each other, as stated in the meshing section.

Each shell element has a front and a back. It is important that the fronts and backs of all elements in a section are pointing in the same direction. The direction pointing towards the outside of the model is the normal direction. In order to verify the normals, the modeler creates a contact surface. The command to create the contact surface is

Once the contact surface is created, the command ELEMENTS/VERIFY/ELEMENT/NORMALS in the Element menu verifies all normals point towards the outside of the model. The command to correct normals in the wrong direction is ELEMENTS/VERIFY/ELEMENT/NORMALS/TEST CONTROL: REVERSE option, and a select guiding element, an element pointing in the right direction. The following figures depict the contact surface and normals for the front group:

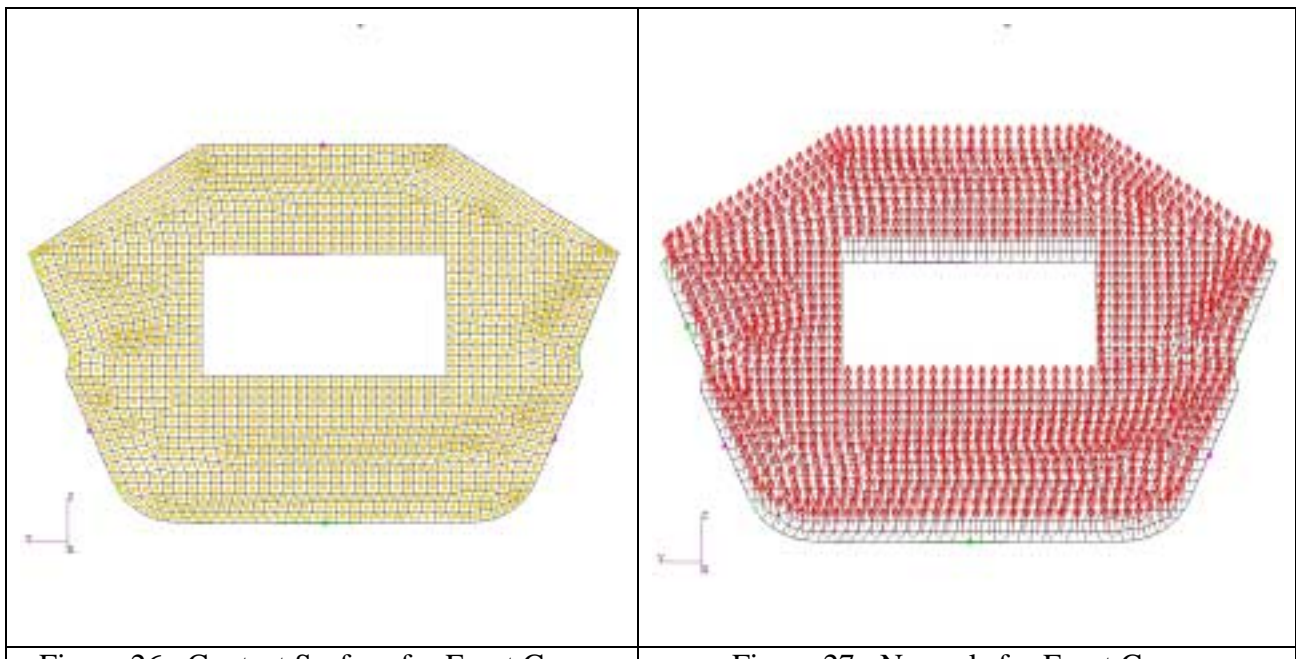


Figure 26: Contact Surface for Front Group

Figure 27: Normals for Front Group

All of the composite materials need a reference direction in order to put the plies of material in the proper direction. The 0° reference angle is normal to a curve that runs from the front to the back of the model. Plies of material are laid in directions relative to the 0° reference angle in such a way to provide the required strength in all directions.

After completing the final checks, the modeler uses PATRAN analyze tool to create the input files for DYTRAN. The command to create input files is ANALYZE/INPUT DECK/TRANSLATE/CODE:MSC.DYTRAN. The modeler then enters the JOB NAME and selects parameters for the output requests. This process creates a large text file, JOB NAME.dat, with all information needed to run an analysis in DYTRAN.

G. DYTRAN TRANSLATION

The “dat” file from PATRAN contains most of the needed information to run the analysis in DYTRAN. From the original “dat” file, five files are created: TAILCONE.dat, BULK.dat, EULER.dat, PROPERTY.dat and SURFACE.dat. The main file used to run the analysis in DYTRAN is TAILCONE.dat, which contains the basic executable specifications and output requests. Any requests for output that are not entered in the analysis menu of PATRAN are entered manually into this file. This file is created manually to ensure accuracy and assist in trouble-shooting. The file, TAILCONE.dat, allows the modeler to specify the time steps, execution time frame, specific requests for output from DYTRAN and data files to be read by DYTRAN.

Depending upon the purpose of the project, the modeler can request many different types of output.

The only measurement obtained from the live fire test was the time-history pressure results; thus, for the validation of the live fire test, the modeler requested a pressure output. To get the pressure output, the modeler chose Eulerian element number 37220 which is near the location of the actual pressure gauge from the live fire test.

Several other outputs, such as displacement, stress and strain, were requested in order to display the capabilities of DYTRAN. The users manual for DYTRAN provides numerous examples and explanations for each line of code. The file TAILCONE.dat and an explanation of specific lines of the code is shown below:

| TAILCONE.dat | Explanation of Code |
|---|--|
| <pre> START TIME=5555 CEND ENDTIME=.0005 ENDSTEP=99999 CHECK=NO TITLE= Jobname is: tailcone_3_20 TLOAD=1 TIC=1 SPC=1 \$ Output result for request: displacement TYPE (displacement) = ARCHIVE GRIDS (displacement) = 1 SET 1 = 1 THRU 16665 GPOUT (displacement) = XDIS YDIS ZDIS TIMES (displacement) = 0 thru end by .0001 SAVE (displacement) = 10000 \$ Output result for request: strain TYPE (strain) = ARCHIVE ELEMENTS (strain) = 2 SET 2 = 1 THRU 16665 ELOUT (strain) = EPSXX EPSYY EPSXY FAIL TIMES (strain) = 0 thru end by .0001 SAVE (strain) = 10000 \$ Output result for request: stress TYPE (stress) = ARCHIVE ELEMENTS (stress) = 3 SET 3 = 16666 THRU 25261 ELOUT (stress) = TXX TYY TZZ TXY TYZ TZX TIMES (stress) = 0 thru end by .0001 SAVE (stress) = 10000 \$ Output result for request: pressure TYPE (pressure) = ARCHIVE ELEMENTS (pressure) = 4 SET 4 = 25262 THRU 47374 ELOUT (pressure) = PRESSURE TIMES (pressure) = 0 thru end by .0001 </pre> | <p>ENDTIME: Termination time of analysis ENDSTEP: Termination time of analysis (maximum time)</p> <p>TIC: Transient Initial Condition Selection SPC: Single Point Constraint Set Selection</p> <p>SET1: Number of Shell Elements GPOUT: Output Displacement TIMES: Time at which data is written to output file</p> <p>SET2: Number of Shell Elements ELOUT: Output Strain</p> <p>SET3: Member of Solid Elements ELOUT: Output Stress</p> <p>SET4: Member of Eulerian Elements ELOUT: Output Pressure</p> |

| | |
|--|--|
| <pre> SAVE (pressure) = 10000 \$----- Parameter Section ----- PARAM,INISTEP,.5E-7 PARAM,MINSTEP,1.E-11 \$----- BULK DATA SECTION ----- BEGIN BULK INCLUDE bulk.dat INCLUDE euler.dat INCLUDE property.dat INCLUDE surface.dat \$ ENDDATA </pre> | INISTEP: Value of first time step MINSTEP: Minimum time step Files to read into DYTRAN |
|--|--|

Table 7: TAILCONE.dat File

The final lines of code in the TAILCONE.dat file allow DYTRAN to read the four other files. The file, BULK.dat, contains all the data to fully describe the analysis model, including the geometry, topology, constraints, and loading. The file BULK.dat contains all of the Lagrangian elements and nodes. The data for the file BULK.dat is imported from the file “Job Name.bdf.”

| BULK.dat File | Explanation of Code |
|--|---|
| <pre> \$ --- Define 20781 grid points --- \$ GRID 1 589.492-6.78704 130.037 GRID 2 589.317-7.47643 129.384 GRID 3 589.142-8.16582 128.731 GRID 4 588.967-8.85522 128.077 GRID 5 588.792-9.54461 127.424 GRID 6 588.617-10.2340 126.771 GRID 7 588.442-10.9234 126.118 GRID 8 588.267-11.6128 125.464 GRID 9 589.492-6.19409 130.036 GRID 10 589.317-6.82404 129.382 ... GRID 20772 587.888 1.71134 130.394 GRID 20773 587.887 .711399 130.396 GRID 20774 528.781-7.69439 135.483 GRID* 20775 585.482 -.363743*A000282 *A000282 130.368 GRID 20776 574.105 .768667 131.347 GRID 20777 567.958 1.95751 131.876 GRID* 20778 585.502 -.363437*A000283 *A000283 130.604 GRID 20779 574.126 .768973 131.583 GRID 20780 567.978 1.95782 132.112 GRID 20781 569.891 7.36171 104.645 \$ \$ --- Define 25261 elements \$ \$ ----- property set aluminum_vents ----- CQUAD4 5643 4 9820 9880 9879 9821 CQUAD4 5644 4 9819 9881 9880 9820 CQUAD4 5645 4 9818 9882 9881 9819 CQUAD4 5646 4 9880 9881 9901 9879 CQUAD4 5647 4 9821 9879 9878 9822 CQUAD4 5648 4 9817 9883 9882 9818 ... CQUAD4 16619 5 14694 14715 14713 14695 CQUAD4 16620 5 14695 14713 14711 14696 CQUAD4 16621 5 14696 14711 14709 14697 CQUAD4 16622 5 14697 14709 14707 14698 CQUAD4 16623 5 14698 14707 14705 14699 CQUAD4 16624 5 14699 14705 14703 14700 CTRIA3 16625 5 14700 14703 14701 </pre> | Grid-point location, coordinate system selection |
| | CQUAD4: Connection definition for a quadrilateral shell element with four grid points |

| | |
|--|--|
| CQUAD4 16626 5 8785 8780 8779 8777 CQUAD4 16627 5 8785 8784 8781 8780 CQUAD4 16628 5 8784 8783 8782 8781 CQUAD4 16629 5 19894 19889 19890 9423 CQUAD4 16634 5 19880 19877 19878 19879 CQUAD4 16635 5 19877 19880 19881 19876 CQUAD4 16636 5 19876 19881 19868 19875 CQUAD4 16637 5 19875 19868 19869 19874 ... CHEXA 22591 21 12470 12600 12665 12581 12471 12601+A008769 +A008769 12666 12582 CHEXA 22592 21 2117 2182 12600 12470 2118 2183+A008770 +A008770 12601 12471 CHEXA 22593 21 12665 12795 3546 3481 12666 12796+A008771 +A008771 3547 3482 CHEXA 22595 21 12663 12793 3544 3479 12664 12794+A008773 +A008773 3545 3480 CHEXA 22597 21 12925 2507 2571 3611 12926 2508+A008775 +A008775 2572 3612 CHEXA 22598 21 12600 12730 12795 12665 12601 12731+A008776 +A008776 12796 12666 CHEXA 22599 21 2182 2247 12730 12600 2183 2248+A008777 | CTRIA3: Connection definition for a triangular shell or membrane with three grid points CHEXA: Connection definition for brick element with eight grid points |
|--|--|

Table 8: BULK.dat Partial File

The file EULER.dat contains the entire fluids portion of the model. The entire tailcone structure is enclosed in a rectangular box, which is used to model the fluid. The fluid region is meshed with 22,113 3-D solid Eulerian elements of edge length 2 inches. The box for the fluid region is depicted in the following figure:

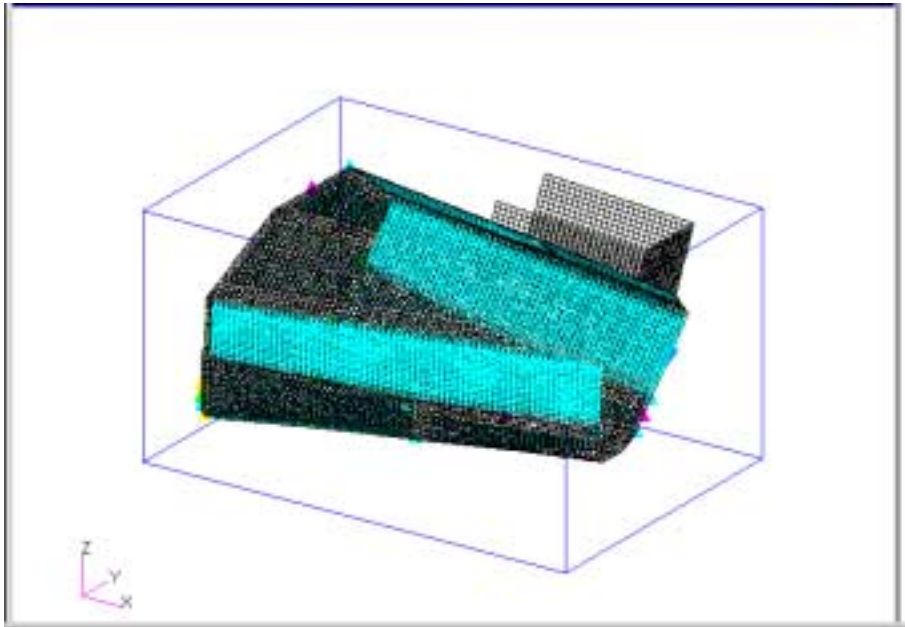


Figure 28: Fluid Region for the Model

The EULER.dat file also contains the specifications for the simulated explosion. A spherical geometry was created in the code of this file in order to specify the location and initial SIE conditions for the explosion. In addition to the initial energy of the explosion, the code includes the initial energy and density of the surrounding air. The EULER.dat file also specifies the type of time integration scheme to use in conducting the analysis. For this project, a three stage Runge-Kutta integration scheme is used. The final lines of code in the file stipulate the coupling surface and type of boundary flow that is allowed in the analysis. The coupling command defines the coupling surface that acts as the interface between the Eulerian and Lagrangian mesh. In the table below, the OUTSIDE command listed under the coupling heading in the following table of the EULER.dat file, allows DYTRAN to understand the processing strategy for the Eulerian elements. With this command, DYTRAN will not process the Eulerian elements outside the closed volume of the coupling surface. The flow boundary allows both an inflow and outflow of the material adjacent to the boundary.

| EULER.dat File | Explanation of Code |
|---|---|
| <pre> \$ Select ROE solver \$ PARAM, LIMITER, ROE PARAM, RKSHEME, 3 \$ \$ Use fast coupling \$ PARAM, FASTCOUP,,FAIL \$ \$ Mesh card for Euler element generation \$ MESH,1,BOX,,.,.,+1 +1,514,-27,96,78,54,42,,,+2 +2,39,27,21,,20782,25262,EULER,100 \$ PEULER1,100,,HYDRO,101 \$ TICEUL,101,,.,.,,+3 +3,SPHERE,400,50,54,2.0,,.,+4 +4,ELEM,500,50,55,1.0 \$ \$ Sphere containing the blast wave \$ SPHERE,400,,566.,-7.,118.,2. TICVAL,54,,DENSITY,5.5E- 7,SIE,8.E+9,YVEL,555 </pre> | <p>PARAM: Defines the type and the spatial accuracy of scheme used in the Euler solver</p> <p>RKSHEME: Defines the type of time-integration scheme used in ROE solver, 3 defines number of Runge-Kutta stages</p> <p>FASTCOUP: Defines the fast coupling algorithm, and specifies that the failure of the coupling surface will be taken into consideration</p> <p>MESH1: Creates the fluid region box with a rectangular mesh aligned with the basic coordinate system, filled with HEXA elements</p> <p>TICEUL: Defines the geometry of sphere which will contain the blast</p> <p>SPHERE: Defines center and radius of sphere</p> <p>TICVAL: Specification for Explosion</p> |

| | |
|--|---|
| <pre> \$ Set1 containing all the Euler elements \$ SET1,500,25262,THRU,47374 \$ Air \$ DMAT,50,1.147E-7,202,,,,,+5 +5,,1.01 EOSGAM,202,1.4,444851. TICVAL,55,,DENSITY,1.147E-7,SIE,217998. \$ Define the coupling \$ COUPLE1,1,1,OUTSIDE,,,,,+6 +6,,1 \$ FLOWDEF,1,,HYDRO,,,,,+7 +7,FLOW,BOTH </pre> | <p>SET1: All Euler elements of entire model</p> <p>DMAT: Material properties of air fluid surrounding the sphere</p> <p>EOSGAM: Defines the properties of a Gamma Law equation of state</p> <p>COUPLE: Defines a coupling surface that acts as the interface between an Eulerian and a Lagrangian mesh</p> <p>FLOWDEF: Defines the default Eulerian flow boundary condition. BOTH allows for an in- or outflow boundary</p> |
|--|---|

Table 9: EULER.dat File

The following table contains the file PROPERTY.dat which contains all of the material properties. These properties were discussed in the properties section in TABLE 3 and TABLE 4. In addition to the material properties, PROPERTY.dat contains failure and yield stresses for each material. For this project, Boeing provided all input values including: failure, yield stress, Poisson's ratio, density, Shear Modulus, Bulk Modulus, Young's Modulus and thickness.

| PROPERTY.dat File | Explanation of Code |
|--|--|
| <pre> \$ ===== PROPERTY SETS ===== \$ * aluminum_vents * \$ PSHELL 4 3 .1 \$ * air_vents * \$ PSHELL 5 4 .001 \$ * top_skin_6270 * \$ PCOMP 6 +A000001 +A000001 7 .005 0 7 .005 -45 +A000002 +A000002 7 .005 45 7 .005 45 +A000003 +A000003 7 .005 -45 7 .005 0 +A000004 +A000004 7 .005 0 7 .005 -45 +A000005 +A000005 7 .005 45 7 .005 45 +A000006 +A000006 7 .005 -45 7 .005 0 \$ * bottom_skin_6250 * \$ PCOMP 7 +A000007 +A000007 5 .0075 45 5 .0075 0 +A000008 +A000008 5 .0075 45 5 .0075 45 +A000009 </pre> | <p>PSHELL: Defines the properties of shell elements Thickness is last entry in the PSHELL line of code</p> <p>PCOMP: Defines the properties of a multi-ply laminate composite material; includes material number, thickness and orientation of plies</p> |

```

+A000009  5 .0075  45      5 .0075  0    +A00010
+A00010  5 .0075  45      5 .0075  45   +A00011
+A00011  5 .0075  45      5 .0075  0    +A00012
+A00012  5 .0075  45
$
$      * front_skin_6250 *
$
PCOMP    8                               +A00013
+A00013  5 .0075  0      5 .0075  45   +A00014
+A00014  5 .0075  0      5 .0075  45   +A00015
+A00015  5 .0075  45      5 .0075  0    +A00016
+A00016  5 .0075  45      5 .0075  0
$
$      * longerons_mid_uppr *
$
PCOMP    9                               +A00017
+A00017  5 .0075  45      5 .0075  -45  +A00018
+A00018  9 .006   0      9 .006   0    +A00019
+A00019  5 .0075  45      9 .006   0    +A00020
+A00020  9 .006   0      9 .006   0    +A00021
+A00021  5 .0075  45
$
$      * back_frame *
$
PCOMP    10                             +A00022
+A00022  5 .0075  45      5 .0075  -45  +A00023
+A00023  9 .006   0      9 .006   0    +A00024
+A00024  5 .0075  45      9 .006   0    +A00025
+A00025  9 .006   0      9 .006   0    +A00026
+A00026  5 .0075  45
$
$      * back_skin_6250 *
$
PCOMP    11                             +A00027
+A00027  5 .0075  0      5 .0075  45   +A00028
+A00028  5 .0075  0      5 .0075  45   +A00029
+A00029  5 .0075  45      5 .0075  0    +A00030
+A00030  5 .0075  45      5 .0075  0
$
$      * bottom_panels_honeycmb *
$
PSOLID   12   14
$
$      * bottom_large_panel_inout *
$
PCOMP    13                             +A00031
+A00031  5 .0075  0      5 .0075  45
$
$      * bottom_small_panels_inout *
$
PCOMP    14                             +A00032
+A00032  5 .0075  0      5 .0075  45   +A00033
+A00033  5 .0075  0
$
$      * top_panels_outer_srfs_6270 *
$
PCOMP    15                             +A00034
+A00034  7 .005   0      7 .005   45   +A00035
+A00035  7 .005   -45    7 .005   90
$
$      * top_inner_surf_6270 *
$
PCOMP    16                             +A00036
+A00036  7 .005   0      7 .005   45   +A00037
+A00037  7 .005   -45    7 .005   90
$
$      * top_panel_honeycmb *
$
PSOLID   17   14
$
```

PSOLID: Defines the properties of Lagrangian solid elements; includes unique property number and material number

| | |
|---|--|
| <pre> \$ * top_side_panel_outer_kevlar * \$ PCOMP 18 +A000038 +A000038 8 .0075 45 8 .0075 0 \$ * top_side_panel_inner_fabric * \$ PCOMP 19 +A000039 +A000039 5 .0075 0 5 .0075 45 \$ * top_side_honeycmb_248 * \$ PSOLID 20 20 \$ * top_side_honeycmb_242 * \$ PSOLID 21 21 \$ \$ ===== MATERIAL DEFINITIONS ===== \$ \$ \$ ----- Material aluminum_7075 id =3 \$ DMATEP* 3 0.0002614 1.03e+07 0.33*A000040 *A000040 \$ \$ ----- Material vents_air id =4 \$ DMATEP 4 1e-08 10 .3 4 4 \$ YLDVM 4 1e-05 \$ FAILMPS 4 1e-08 \$ \$ ----- Material 6250_graphite_fabric_IM7_8552 id =5 \$ MAT8* 5 1.12e+07 1.12e+07 0.05*A000041 *A000041 750000 750000 750000 0.0001475 \$ MAT8A 5 STRSS 18100. 0. ELEM + + 155000. 123000. 138000. 123000. + + + + + + 1111 1111 1111 1111 0001 \$ \$ ----- Material 6370_E_glass_style120 id =6 \$ MAT8* 6 3e+06 3e+06 0.13*A000042 *A000042 480000 480000 480000 0.0001563 \$ MAT8A 6 STRSS 13300. 0. ELEM + + 40000. 44400. 40000. 44400. + + + + + + 1111 1111 1111 1111 0001 \$ \$ ----- Material 6270_graphite_tape_IM7_8552 id =7 \$ MAT8* 7 2.205e+07 1.75e+06 0.31*A000043 *A000043 750000 750000 750000 0.0001483 \$ MAT8A 7 STRSS 17400. 0. ELEM + + 376000. 250000. 16800. 44400. + + + + + + 1111 1111 1111 1111 0001 \$ \$ ----- Material 6350_kevlar_fabric_K49_8552 id =8 \$ MAT8* 8 4.04e+06 4.04e+06 0.1*A000044 *A000044 380000 380000 380000 0.0001281 \$ MAT8A 8 STRSS 5400. 0. ELEM + + 72720. 36360. 72720. 36360. + + + + + + 1111 1111 1111 1111 0001 \$ \$ ----- Material 6100_graphite_tape_unidir id =9 \$ MAT8* 9 2.205e+07 1.75e+06 0.025*A000045 *A000045 750000 750000 750000 0.0001483 </pre> | <p>DMATEP: Defines the properties of an Isotropic-Elastoplastic material for shell and beam elements, includes density, Young's Modulus, Poisson's Ratio, Shear Modulus, Bulk Modulus, Yield and Failure for the material</p> <p>YLDVM: Defines a bilinear or piecewise linear yield model with Isotropic hardening using the Von Mises Yield Criterion, includes Yield Stress</p> <p>FAILMPS: Defines the properties of a failure model where failure occurs when the equivalent plastic strain exceeds the specified value, maximum plastic strain</p> <p>MAT8: Defines the properties for an Orthotropic material for shell elements, includes Modulus of Elasticity in longitudinal and lateral directions, Poisson's Ratio, In-plane Shear Modulus, Transverse Shear Modulus in 1Z and 2Z and mass density</p> <p>MAT8A: Defines the properties for an Orthotropic material for shell elements, includes Element layer fail theory: "maximum stress", failure stress for in-plane shear, transverse shear failure if element fails, tensile compressive failure stress</p> <p>1111: Property degradation due to fiber-tension failure</p> <p>0001: Property degradation due to in-plane shear failure</p> |
|---|--|

| | |
|---|--|
| <pre> \$----- Material honeycomb_Z_norm id =14 DMATOR* 14 4.793e-06 ELEM *A000046 *A000046 +A000047 10 10 27000 .3 .01 .01 +A000048 +A000048 10 13300 13300 +A000049 +A000049 \$----- Material honeycomb_2_vector_248 id =20 DMATOR* 20 4.793e-06 VECT *A000050 *A000050 +A000051 10 10 27000 .3 .01 .01 +A000052 +A000052 10 13300 13300 +A000053 +A000053-62.1882 12.8036-7.62939-3.44012-5.11019 -13.295 +A000054 +A000054 \$----- Material honeycomb_2_vector_242 id =21 DMATOR* 21 4.793e-06 VECT *A000055 *A000055 +A000056 10 10 27000 .3 .01 .01 +A000057 +A000057 10 13300 13300 +A000058 +A000058-62.1882-12.8036-7.62939-3.40125 5.19462-13.1502 +A000059 +A000059 </pre> | <p>DMATOR: Defines Orthotropic Elastic material for Lagrangian solid elements, includes density, globally orthotropic material definition, Young's Moduli, Poisson's Ratio, Shear Moduli</p> |
|---|--|

Table 10: PROPERTY.dat File

The following table contains the partial file SURFACE.dat which contains all of the contact elements. The code defines a multifaceted surface for contact and coupling interfaces.

| SURFACE.dat File | | Explanation of Code |
|--|--|--|
| <pre> Surface.dat \$----- Self Contact Surface for contact \$----- SURFACE: 1 SEG 1 SURFACE 1 SEG 1 CFACE 1 1 300 4 CFACE 2 1 301 4 CFACE 3 1 302 4 CFACE 4 1 303 4 CFACE 5 1 304 4 CFACE 6 1 305 4 CFACE 7 1 306 4 CFACE 8 1 307 4 CFACE 9 1 308 4 CFACE 10 1 309 4 CFACE 11 1 310 4 ... CFACE 10159 1 11189 4 CFACE 10160 1 11190 4 CFACE 10161 1 11191 4 CFACE 10162 1 11192 4 CFACE 10163 1 11193 4 CFACE 10164 1 11194 4 </pre> | | <p>SURFACE: Defines a multifaceted surface for contact and coupling interfaces</p> <p>CFACE: Defines a face on an Eulerian or a Lagrangian element</p> |

| | | | | | |
|-------|-------|---|-------|---|--|
| CFACE | 10165 | 1 | 11195 | 4 | |
| CFACE | 10166 | 1 | 11196 | 4 | |
| CFACE | 10167 | 1 | 11197 | 4 | |
| CFACE | 10168 | 1 | 11198 | 4 | |
| CFACE | 10169 | 1 | 11199 | 4 | |
| CFACE | 10170 | 1 | 11200 | 4 | |
| CFACE | 10171 | 1 | 11201 | 4 | |
| CFACE | 10172 | 1 | 11202 | 4 | |
| CFACE | 10173 | 1 | 11203 | 4 | |
| CFACE | 10174 | 1 | 11204 | 4 | |
| | \$ | | | | |

Table 11: SURFACE.dat Partial File

After creating and modifying the above five files needed for the analysis, the modeler is now ready to run DYTRAN. The command to execute DYTRAN from the UNIX window is: “dytran jid=tailcone size=large.” The “jid” is the job identification which is the name of the input file. “Size equals large” enables the greatest amount of allocated memory to execute DYTRAN. An alternate method to execute DYTRAN from the UNIX window is to use the command: “xdytran&.” However, this command does not allow the modeler to select a large allocated memory. As a result, the analysis process might be interrupted due to the lack of memory space depending upon the size of the model and output requested. The inadequacies of this command were determined from the error messages obtained on the first run of DYTRAN. In addition to the memory error, there were several other error messages. When errors occur the message provides three types of comments: information (I), warnings (W) and fatal errors (E). The modeler needs to only correct the fatal errors in order for DYTRAN to run completely. However, the modeler must understand the information and warning errors to ensure that their impact is negligible to the final analysis. The table shown below shows some of the error messages for the final run of this project.

Tailcone_4_12_error_summary.msg File

DATE :12-04-01 TIME :12:53:20

```
%W-P2082603-P2_CHECK_DMATEP_FAILURE...
  Shell elements with elastic material 3 do not have the
  strains and effective stress available as extended output.
  Only shell elements with elasto-plastic materials do have
  access to the additional data for output purposes.

%W-P2092103-P2_WRITE_COUPLE_INFO...
  The scaling factor for the time step is greater than the blending
  factor. For stability reasons use a PARAM STEPFC less than PARAM
  FBLEND.

%I-P3002405-P3_CHECK_POLYH_SURF_VOL...
  Volume covered by SURFACE SURFACE1 is 0.56611E+05

%I-P3002404-P3_CHECK_POLYH_SURF_VOL...
  Area of surface SURFACE1 is 0.90653E+04

%I-P3033302-P3_COMPOSITE_INT_POINTS...
  Defining integration and weight factors.
  Number of (composite) layers: 8.

NO MORE MESSAGES OF THIS KIND WILL BE WRITTEN

JOBNAME IS: TAILCONE_4_13
-----
MSC/DYTRAN MSC.DYTRAN 2000 Single-CPU Windows
SUMMARY OF MESSAGES (INCLUDING NON-PRINTED MESSAGES)
INFORMATIVE      :  20
WARNINGS        :  17
NO ERRORS
```

Table 12: Error Message Partial File

Correcting the fatal errors is a long and tedious process. The modeler must decipher the error message to determine whether corrections need to be made in PATRAN, the five input deck files or both. The error messages do not usually provide the modeler a good direction of where the error occurs. The best source for help is to contact the MSC DYTRAN help line. This source will look at your code and provide guidance and possible solutions to correct the errors.

After correcting all fatal errors, DYTRAN creates the following files upon the completion of the analysis:

| Type of File | File Extension Name |
|--------------------------|---------------------|
| Neutral File | .NIF |
| Output Archive Files | .ARC |
| Output Time History File | .THS |
| Restart Output File | .RST |
| Log File | .LOG |
| Error Message File | .MSG |
| File Summary File | .MSG |

Table 13: DYTRAN Output Files

Most of these files are informational files except the Output Archive and Time History Files, which are read into PATRAN for analysis.

H. PATRAN ANALYSIS

With the successful execution of DYTRAN, the modeler opens a new file in PATRAN. The command to import the results from DYTRAN is ANALYSIS/ACTION: READ ARCHIVE FILE/MODEL/TRANSLATE and then select the “.ARC” file that DYTRAN creates. In order to display the results on the original model, the modeler must also read in the model. The same process is used to import the time history file by changing ACTION: READ ARCHIVE FILE to ACTION: READ HISTORY FILE. Once these files are imported, the modeler can view the results by using the command: ANALYSIS/ANALYZE.

IV. RESULTS

A. ASSUMPTIONS USED IN ANALYSIS

The first assumption is that DYTRAN accurately models the characteristics of the explosion. Extensive testing of DYTRAN explosion analysis against real life explosions needs to be conducted in order to validate the DYTRAN output. To date, this comprehensive testing and comparison has not occurred. Boeing has begun an initial validation of this technique by attempting to correlate data from live-fire testing that was done on the static test article with computer simulations from DYTRAN. Additionally, Boeing is planning on conducting a live-fire test involving an explosion inside an instrumented test-box and comparing the results to the predicted results from the DYTRAN simulation.

The second assumption is that a complete, undamaged structure is present when the blast wave from the explosion impacts the structure. This assumption negates fragmentation damage, which is very difficult to predict. Fragments from the explosive round normally destroy or damage portions of the structure. If the structure is damaged or partially destroyed by fragmentation, it would most likely fail at lower stress and strain levels.

The third assumption is that detonating a stationary, spherical charge at the center of the explosion area provides results similar to those achieved if an explosive round were in motion and exploded at any other point inside the box. With a relatively small explosion area, the pressure wave created by the explosion will not have an opportunity

to dissipate before impacting the structure, so the same pressure will be seen regardless of where the round detonates in the blast area.

The final assumption is that the averaging of composite ply layers over the entire length and thickness of a component does not significantly change the material properties of the component.

B. PRESSURE

The time-pressure history analysis is the most important result for this project as this was the only data recorded during the live fire test. As the following figure shows, a sharp rise in the pressure, 134.49 pounds per square inch (psi), occurs at approximately 0.035 milliseconds. This data corresponds to the expected results of an explosion inside a structure. Following the sharp rise, the pressure wave continues to propagate and diminishes greatly in strength over a small time period.

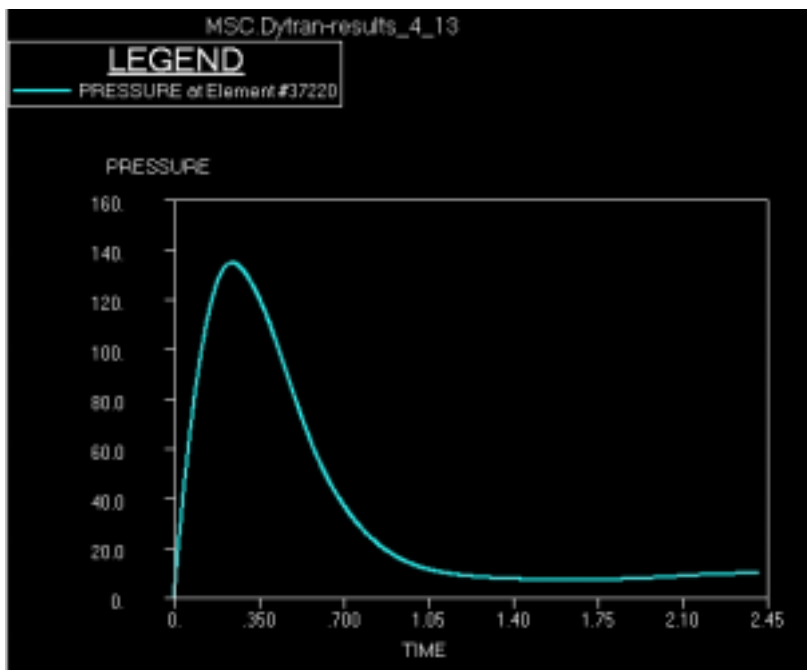


Figure 29: Time-Pressure History Results

These results can be easily compared with the actual live fire data to validate the accuracy of the model.

C. DISPLACEMENT

The displacement of the structure is shown in the following figures. The color codes indicate displacement in inches normalized to a default color “white” equaling zero displacement. Each figure indicates the actual display time, date, cycle time, and cycle number.

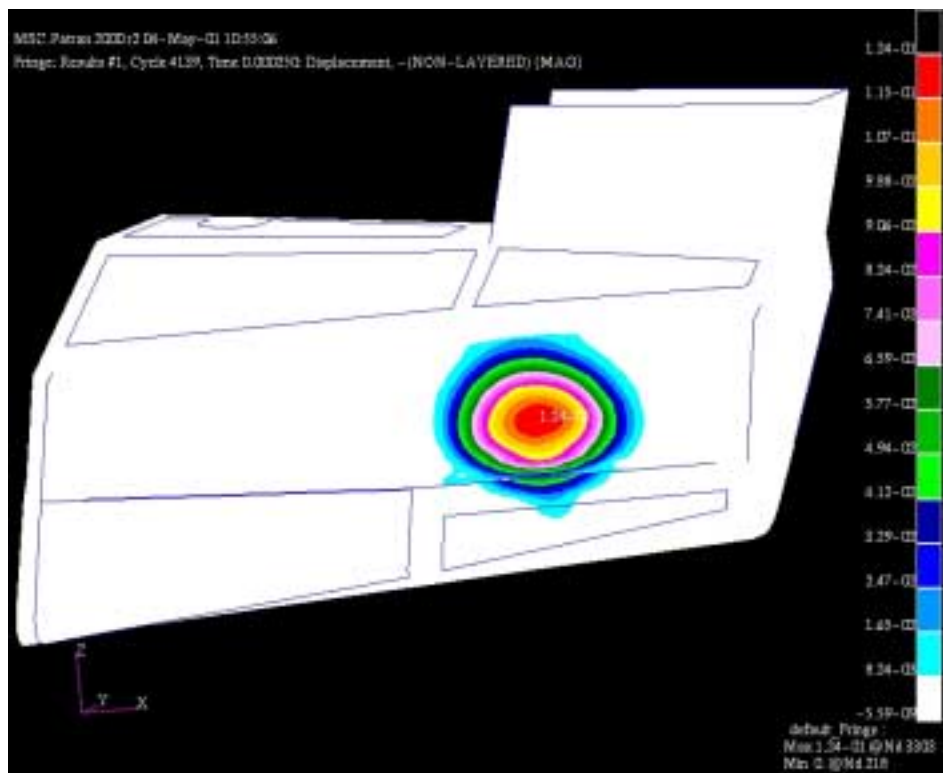


Figure 30: Displacement at Time 0.250 milliseconds

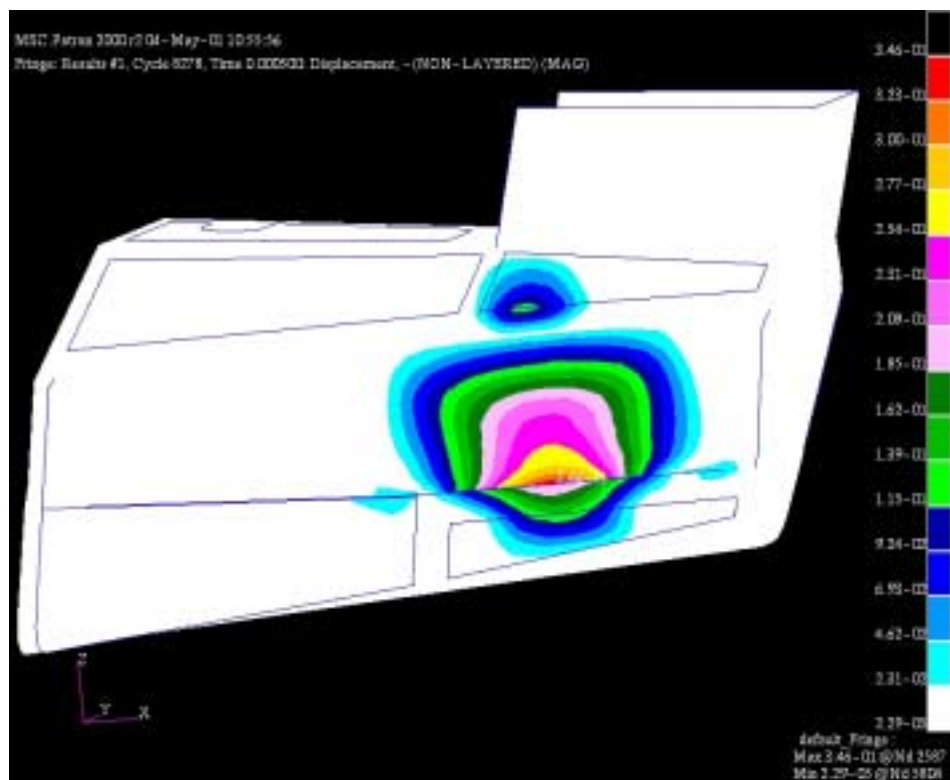


Figure 31: Displacement at Time 0.50 milliseconds

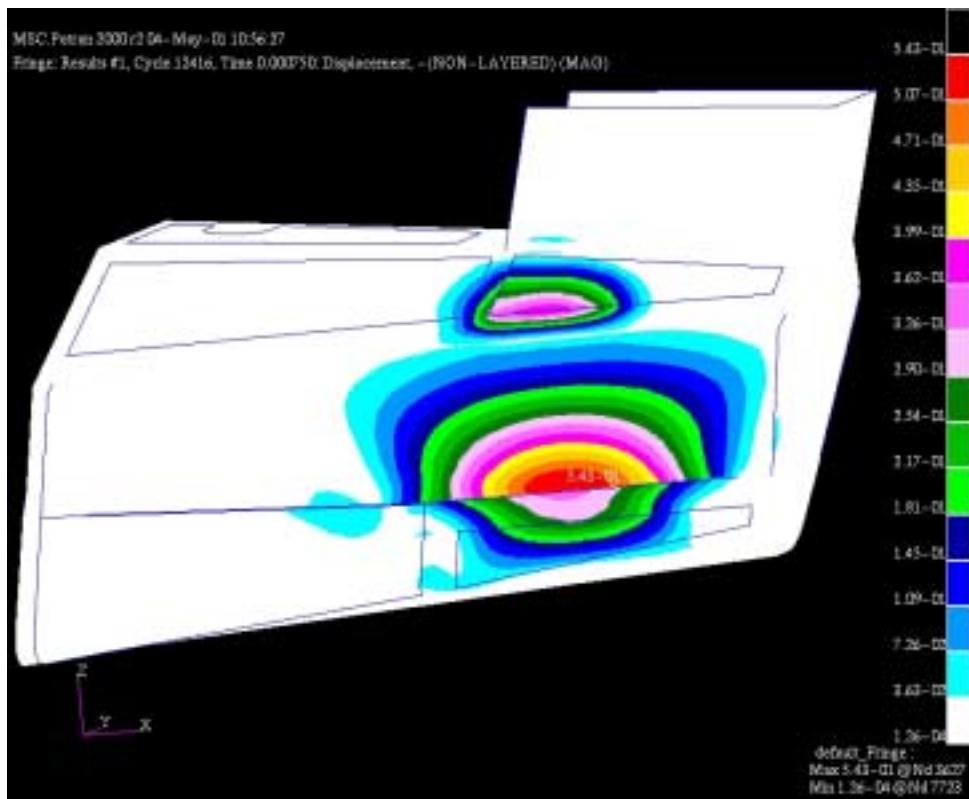


Figure 32: Displacement at Time 0.750 milliseconds

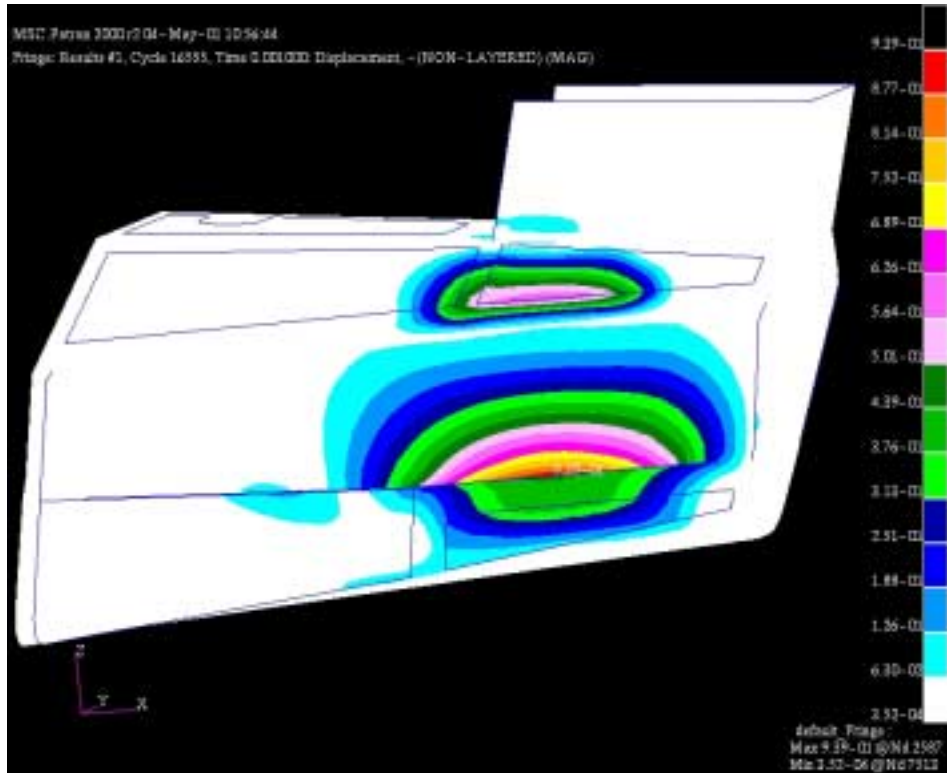


Figure 33: Displacement at Time 1 milliseconds

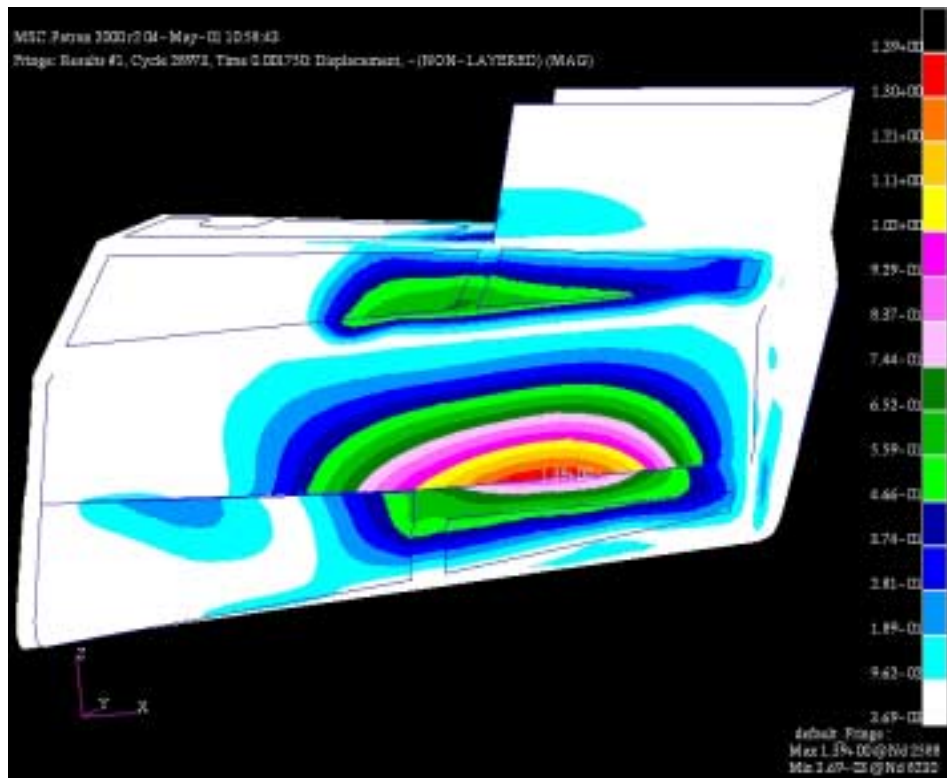


Figure 34: Displacement at Time 1.750 milliseconds

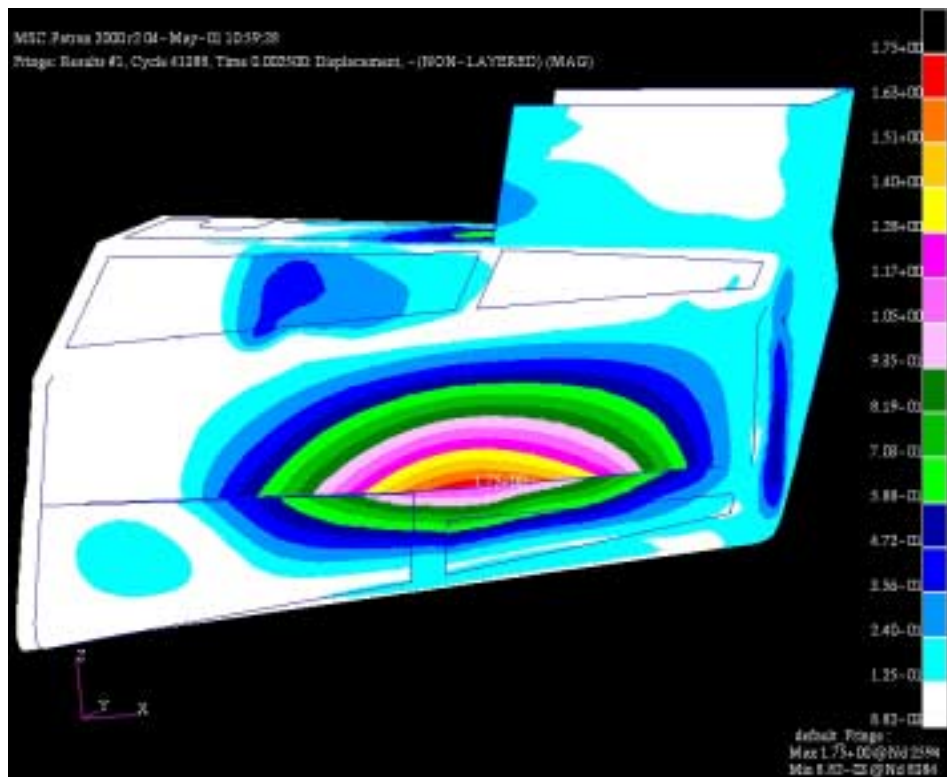


Figure 35: Displacement at Time 2.50 milliseconds

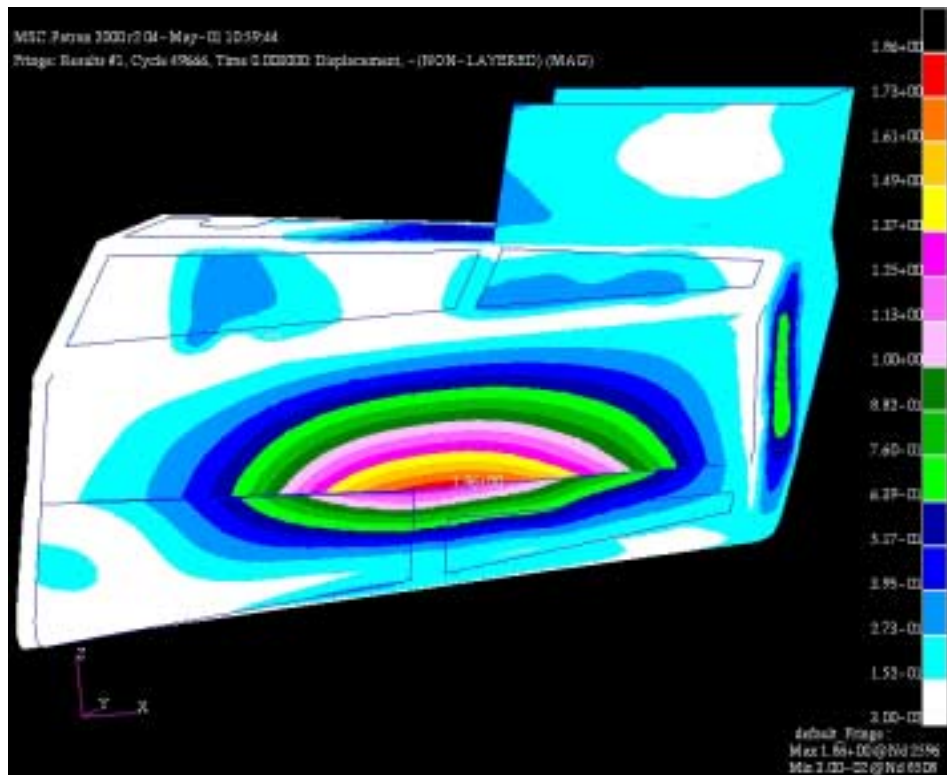


Figure 36: Displacement at Time 3.0 milliseconds

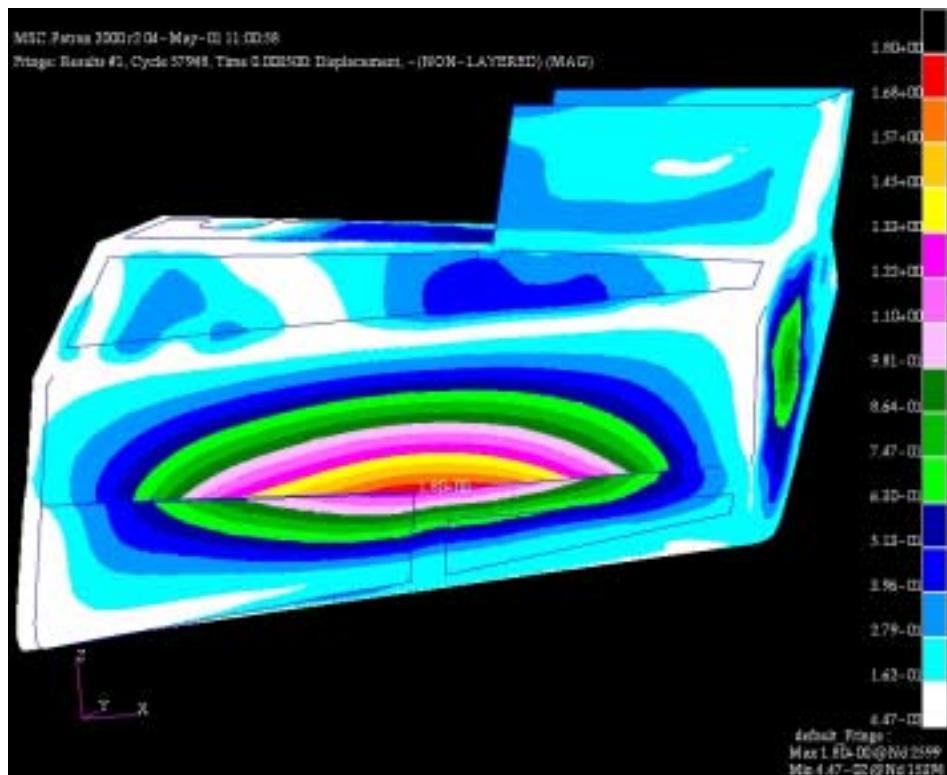


Figure 37: Displacement at Time 3.50 milliseconds

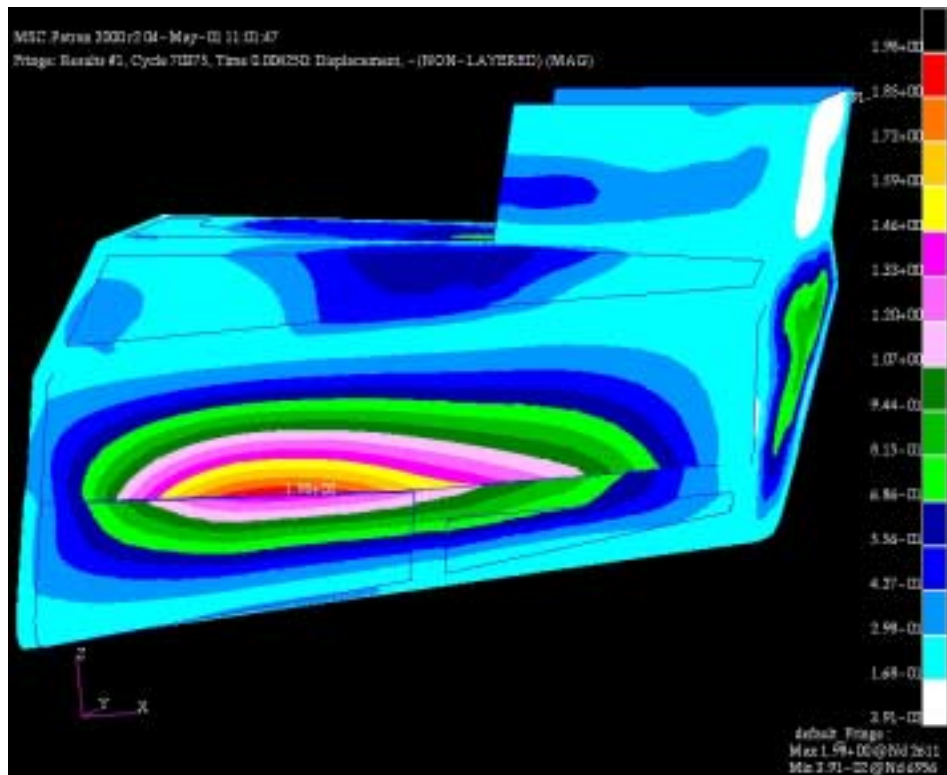


Figure 38: Displacement at Time 4.250 milliseconds

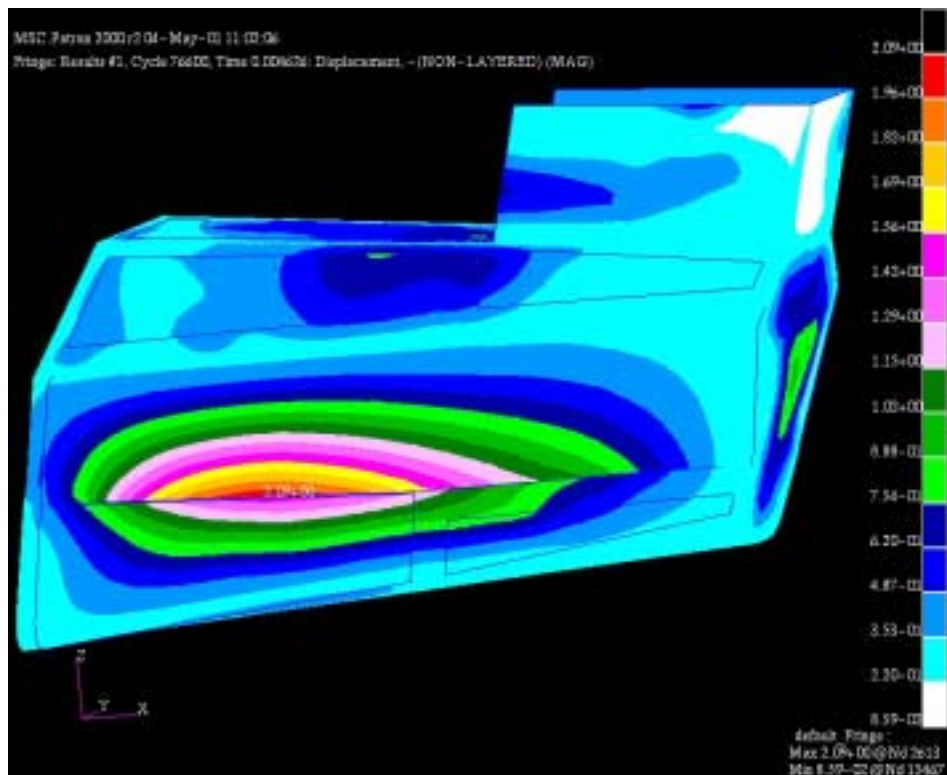


Figure 39: Displacement at Time 4.626 milliseconds

D. STRESS AND STRAIN

The tailcone model is initially in equilibrium but the explosive round creates a force that tends to stretch, shear, or compress the shape of the tailcone. If the tailcone returns to its original shape after the explosion, it survives and is said to be elastic. Most objects are elastic for forces up to a certain limit called the elastic limit. If this limit is exceeded, the component is either permanently deformed or fails.

Stress is defined as the ratio of the force to the cross sectional area. Strain is defined as the fractional change in the length of the material divided by its original length. As requested in the DYTRAN input deck file, TAILCONE.dat, the following figures show some sample output of the results for stress (psi) and strain in the XX, YZ, and ZX directions, with local coordinate axis system, for varying times:

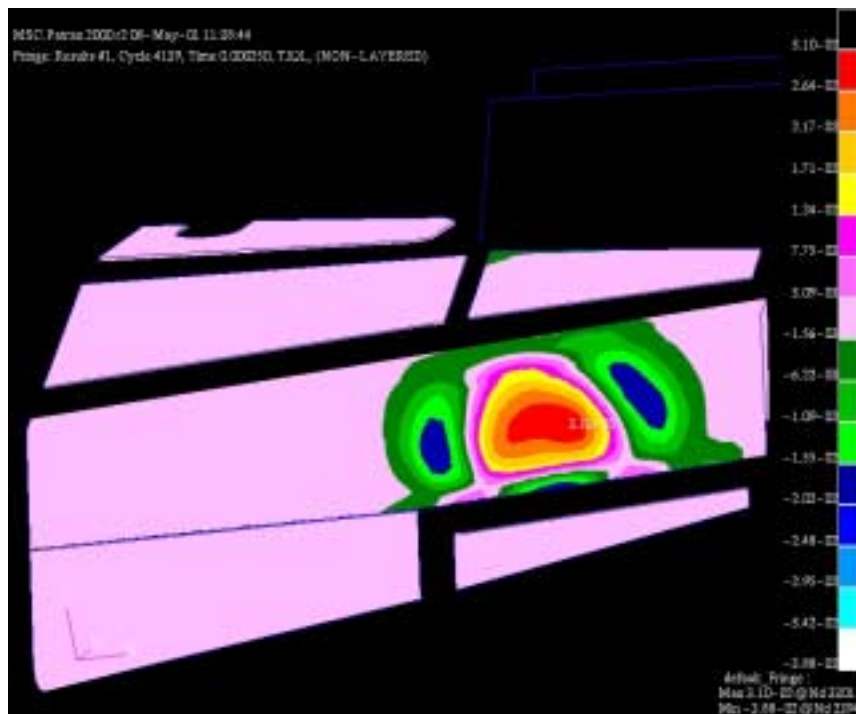


Figure 40: Solid Element Stress in XX Direction at Time = 0.25 milliseconds

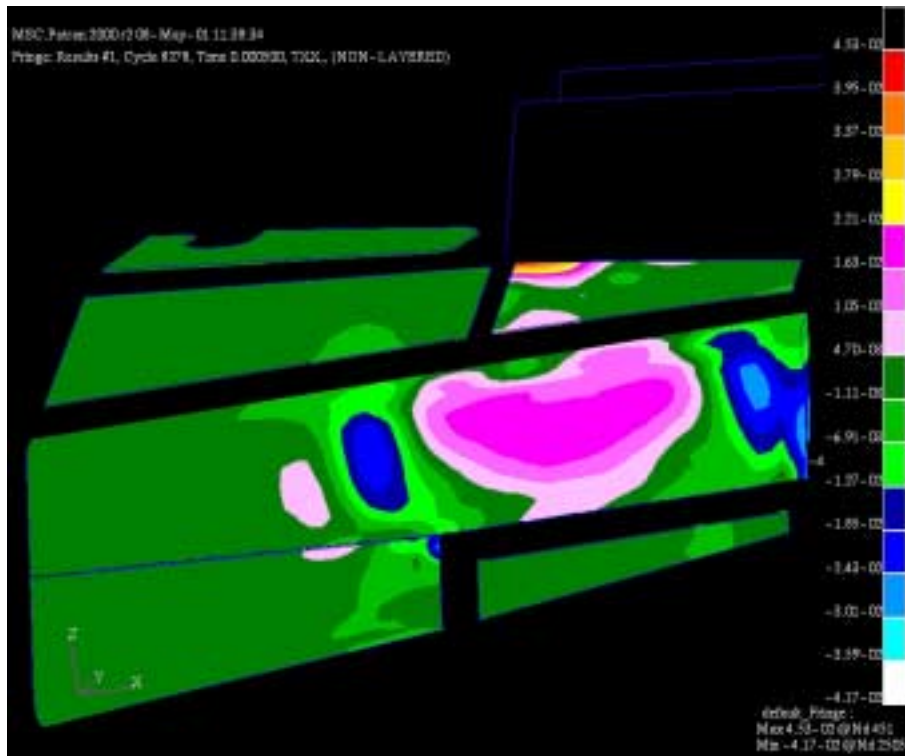


Figure 41: Solid Element Stress in XX Direction at Time = 0.5 milliseconds

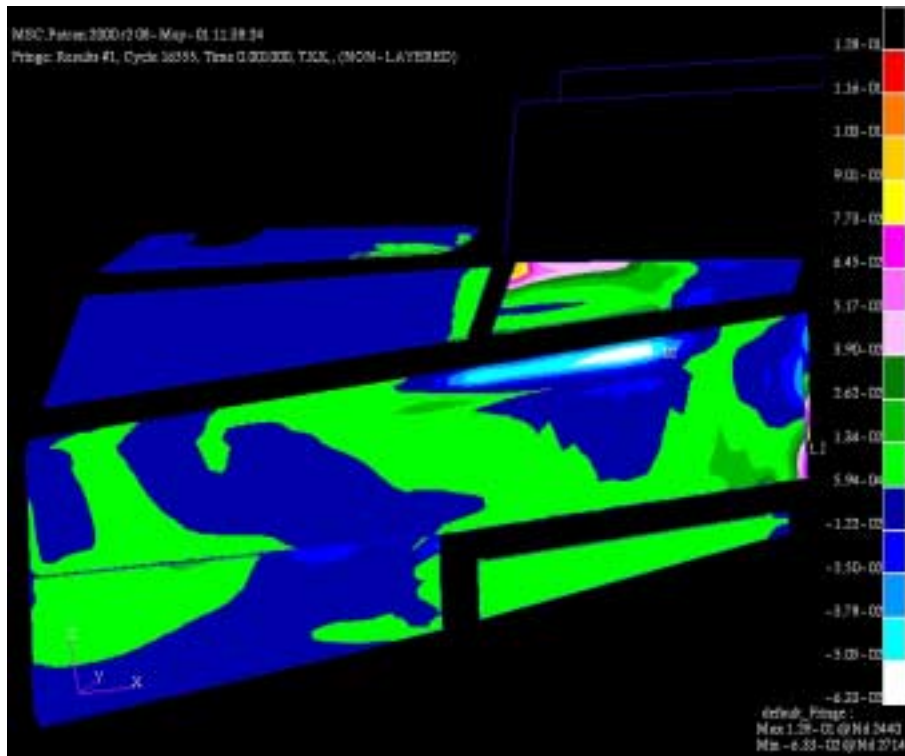


Figure 42: Solid Element Stress in XX Direction at Time = 1.0 milliseconds

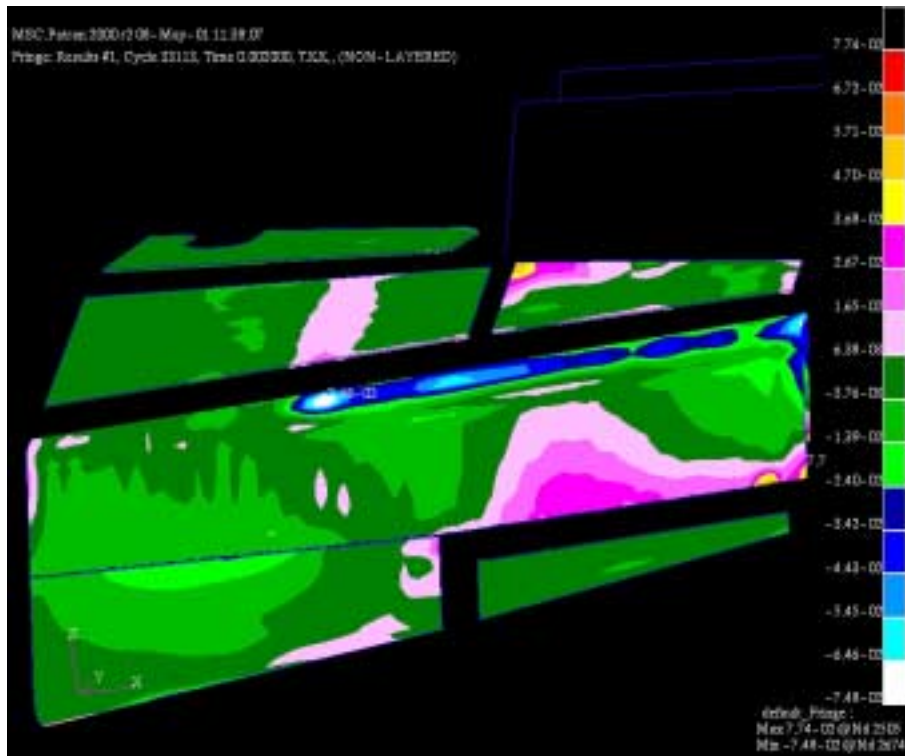


Figure 43: Solid Element Stress in XX Direction at Time = 2.0 milliseconds

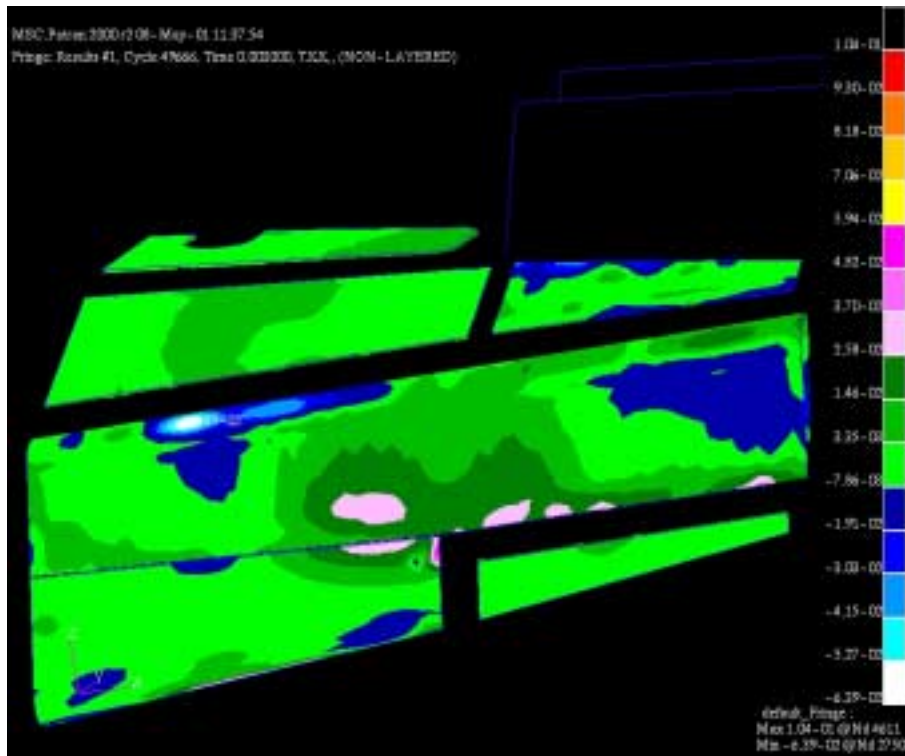


Figure 44: Solid Element Stress in XX Direction at Time = 3.0 milliseconds

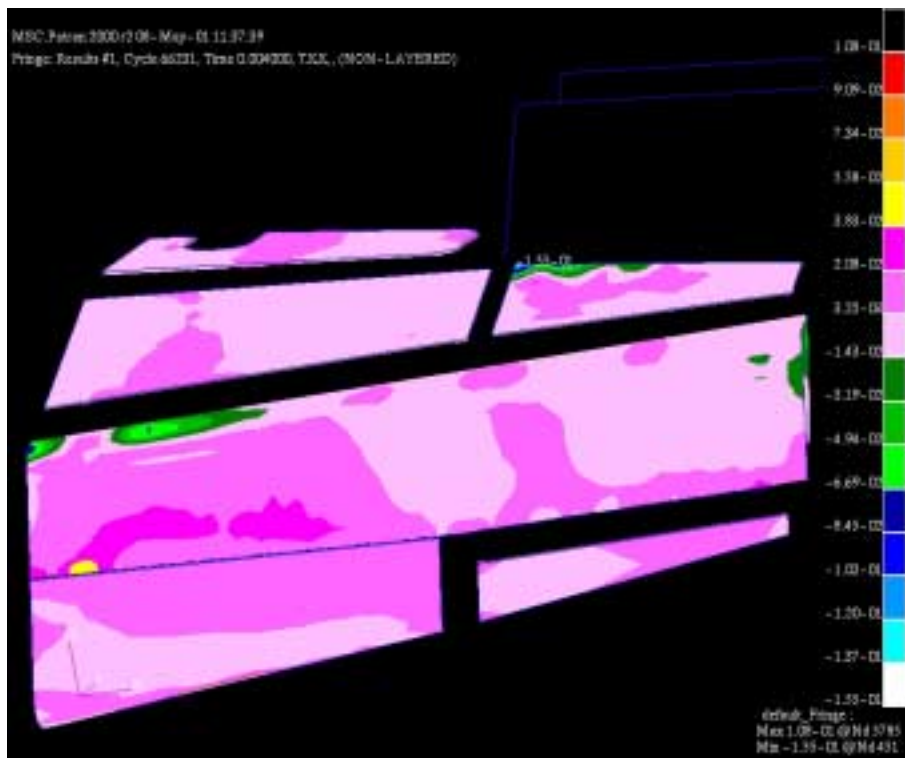


Figure 45: Solid Element Stress in XX Direction at Time = 4.0 milliseconds

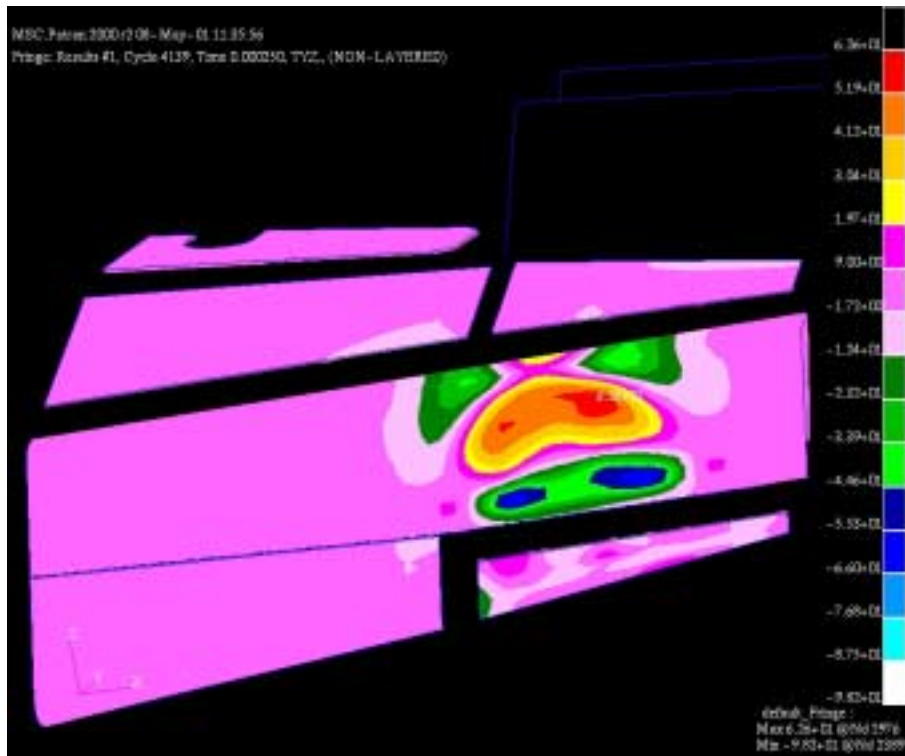


Figure 46: Solid Element Stress in YZ Direction at Time = 0.25 milliseconds

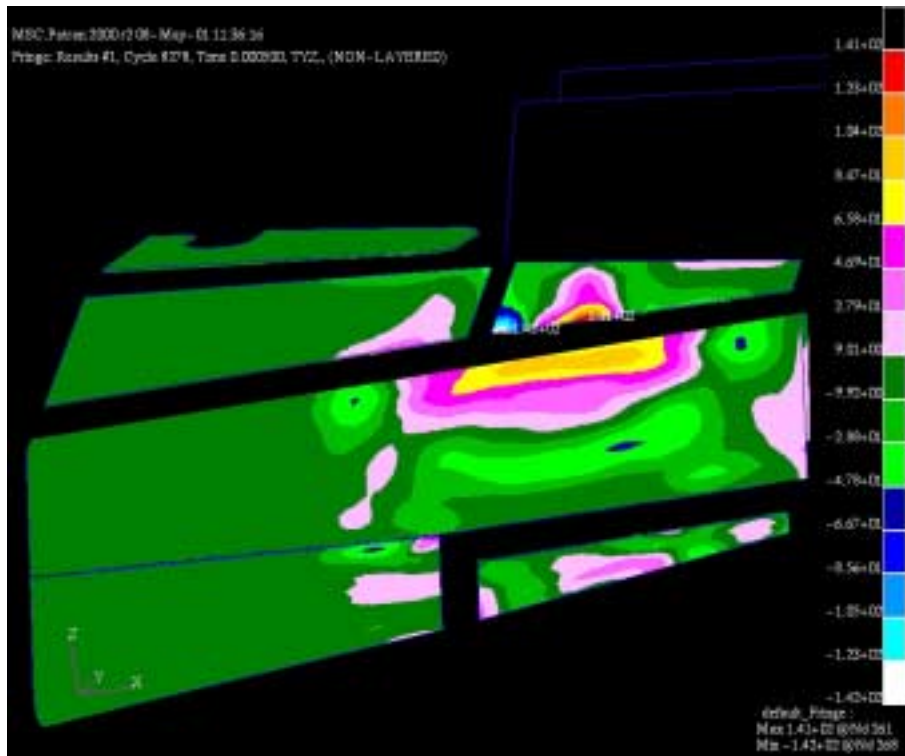


Figure 47: Solid Element Stress in YZ Direction at Time = 0.5 milliseconds

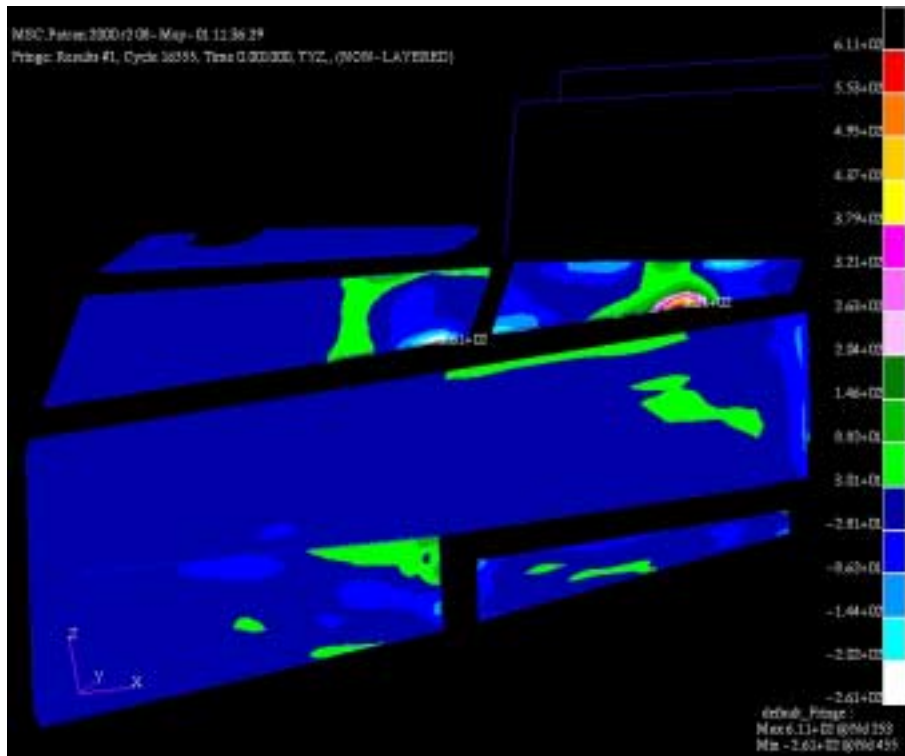


Figure 48: Solid Element Stress in YZ Direction at Time = 1.0 milliseconds

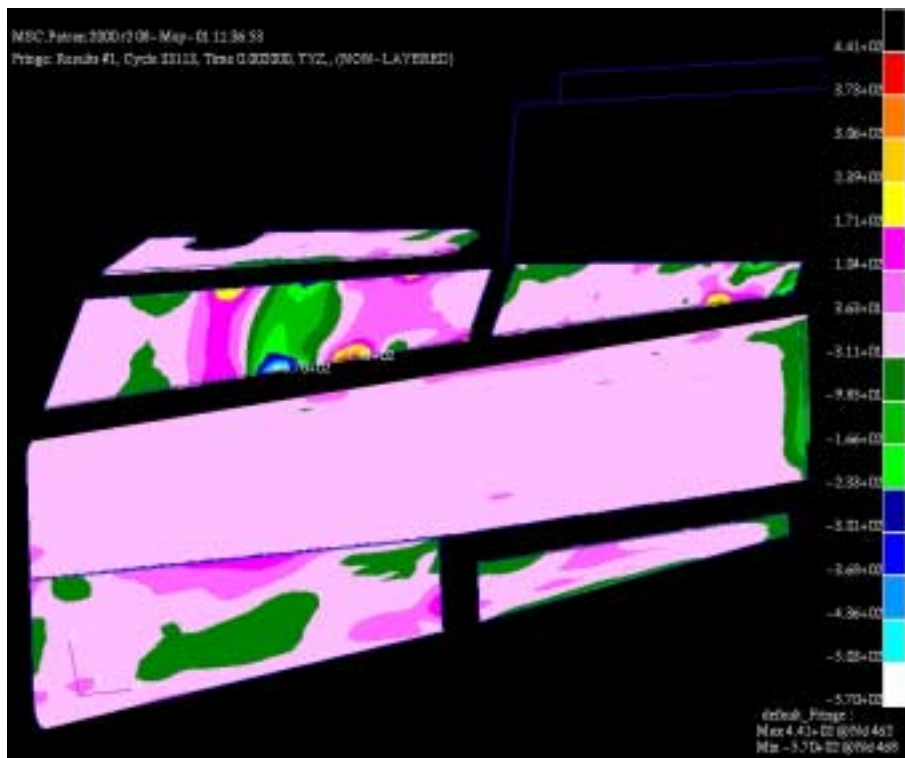


Figure 49: Solid Element Stress in YZ Direction at Time = 2.0 milliseconds

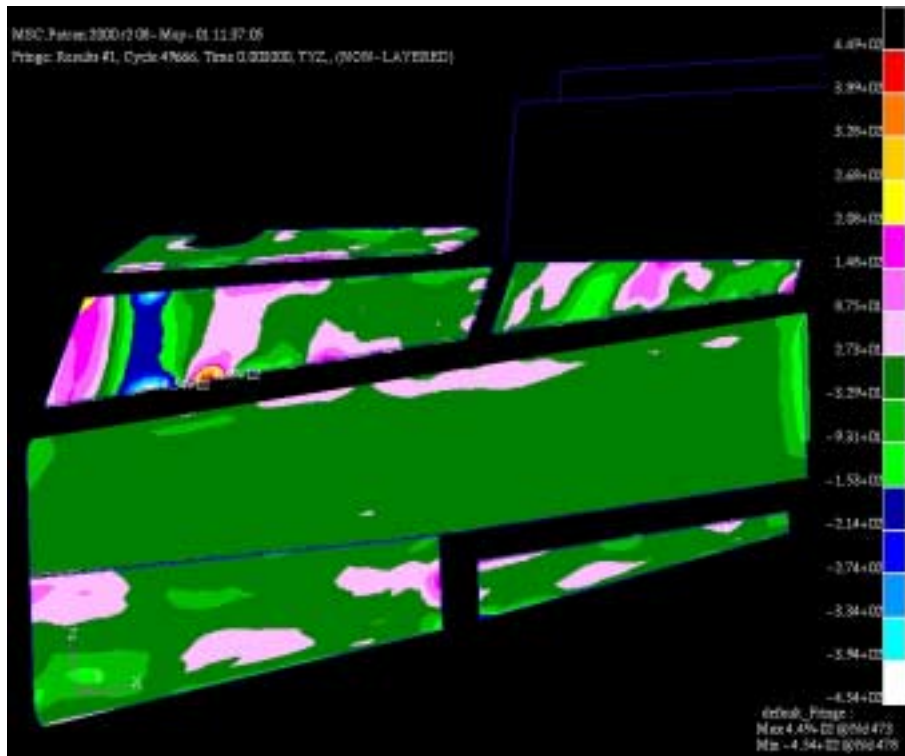


Figure 50: Solid Element Stress in YZ Direction at Time =3.0 milliseconds

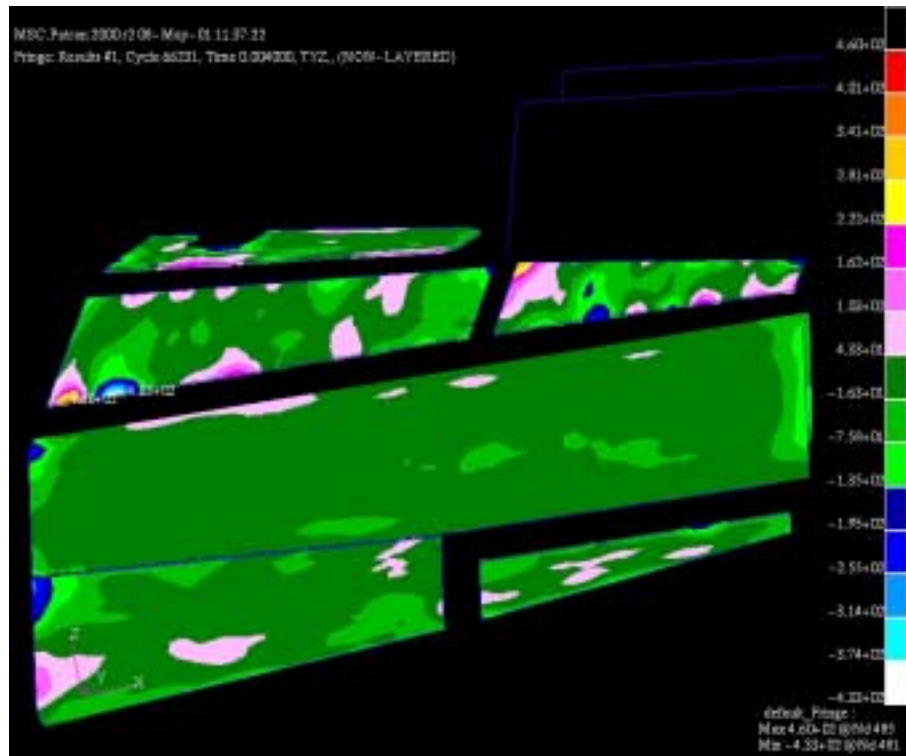


Figure 51: Solid Element Stress in YZ Direction at Time = 4.0 milliseconds

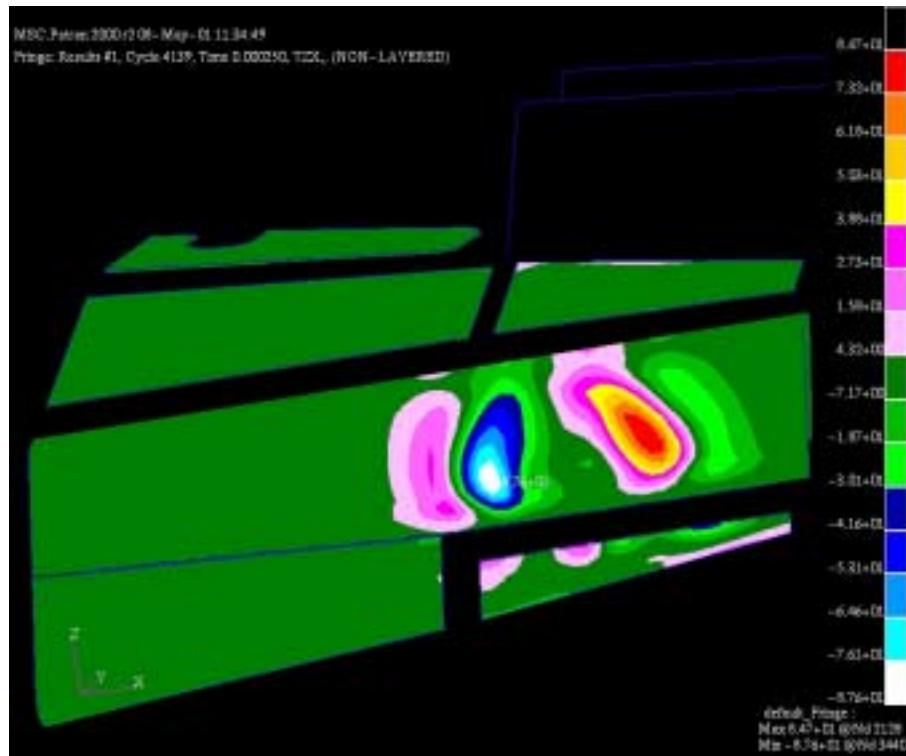


Figure 52: Solid Element Stress in ZX Direction at Time = 0.25 milliseconds

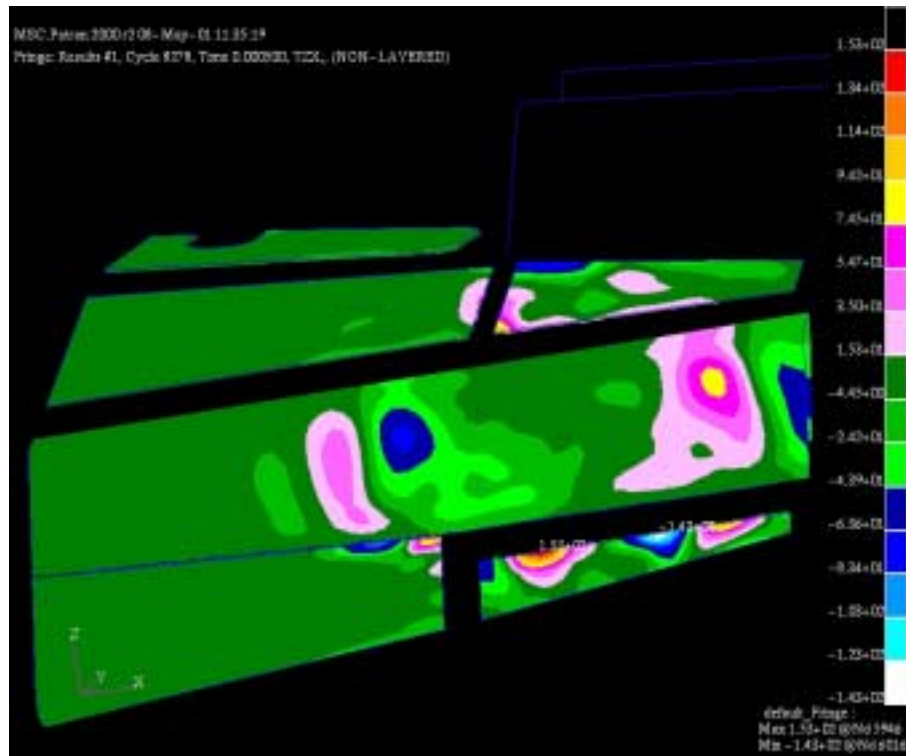


Figure 53: Solid Element Stress in ZX Direction at Time = 0.5 milliseconds

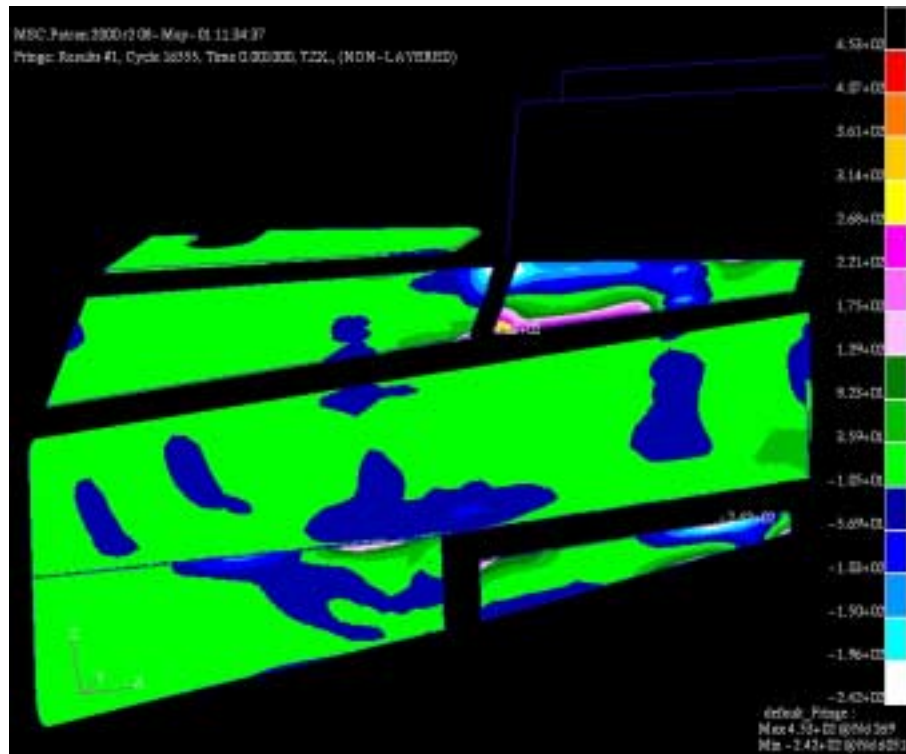


Figure 54: Solid Element Stress in ZX Direction at Time = 1.0 milliseconds

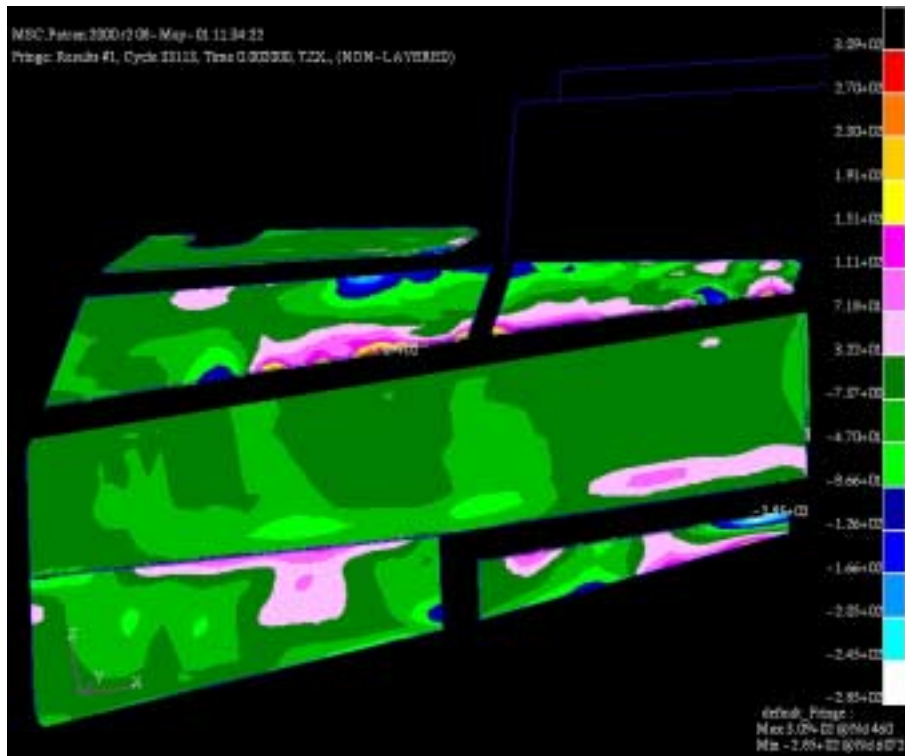


Figure 55: Solid Element Stress in ZX Direction at Time = 2.0 milliseconds

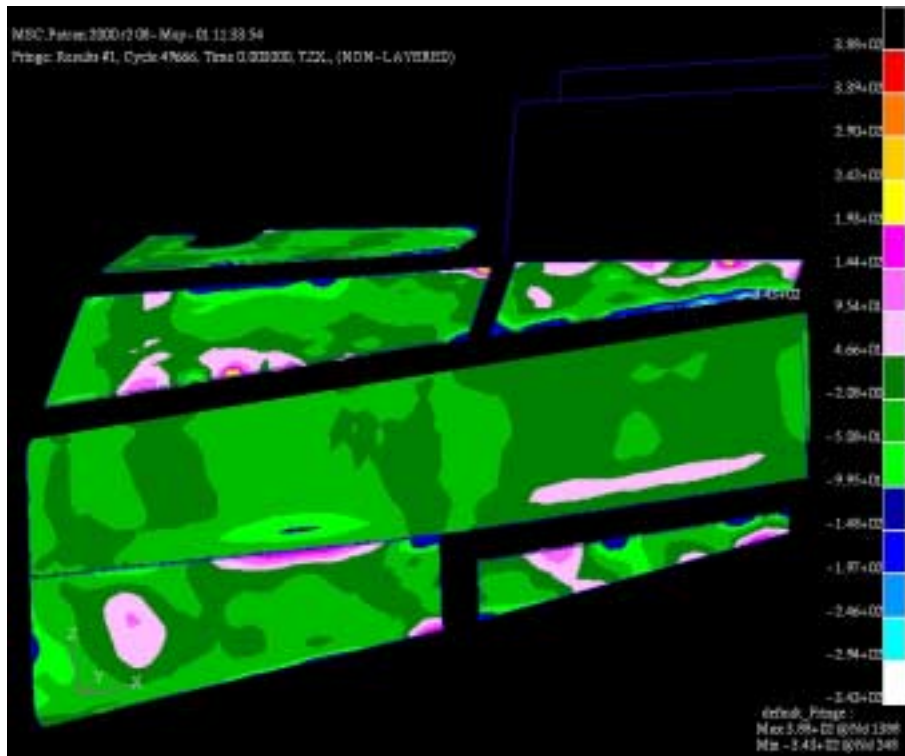


Figure 56: Solid Element Stress in ZX Direction at Time = 3.0 milliseconds

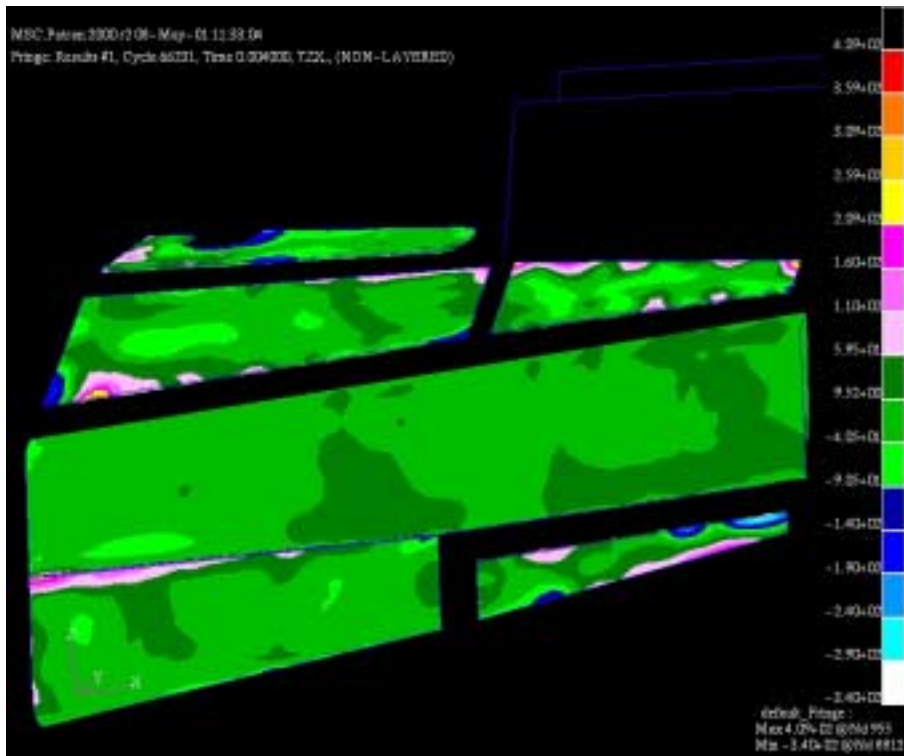


Figure 57: Solid Element Stress in ZX Direction at Time = 4.0 milliseconds

The following figures are a sample of the dimensionless strain output results. The results are for the outside surface in the XX, XY, and YY directions of the model varying by time:

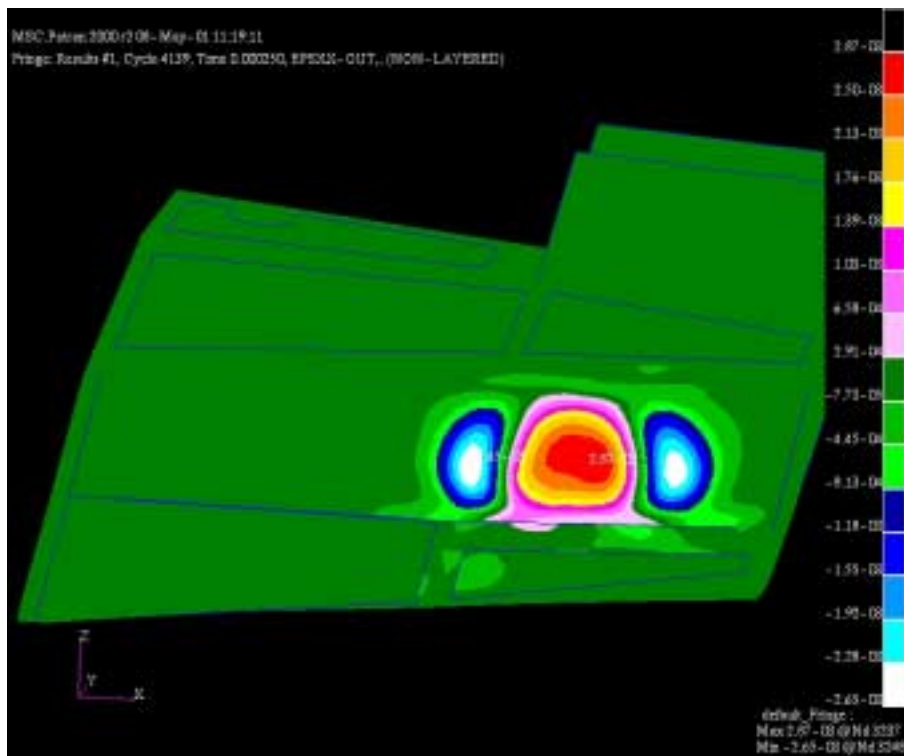


Figure 58: Shell Element Strain in XX Direction at Time = 0.25 milliseconds

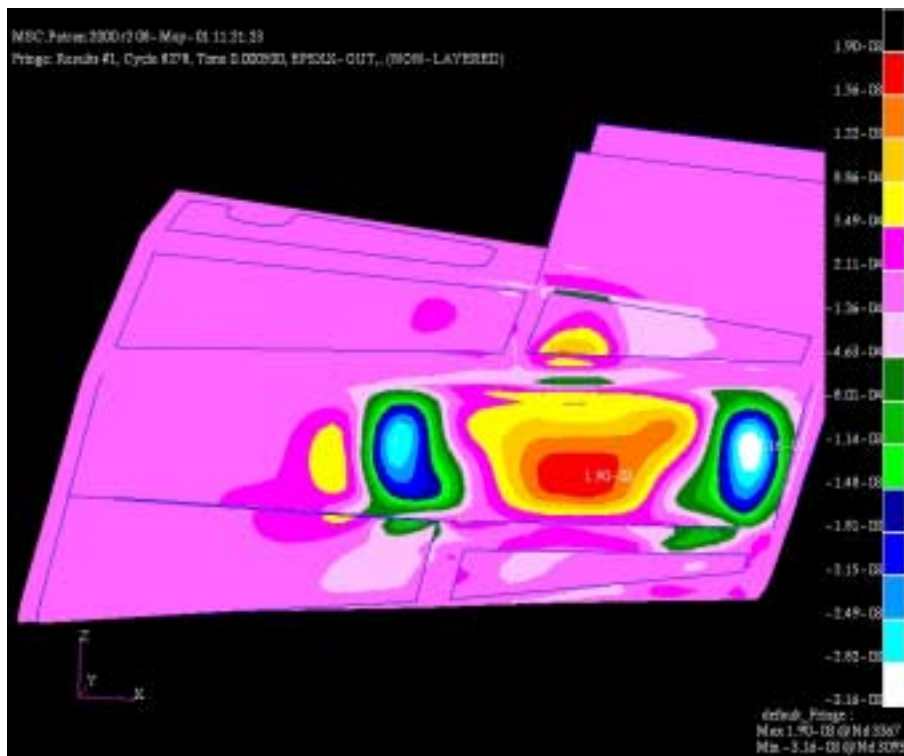


Figure 59: Shell Element Strain in XX Direction at Time = 0.5 milliseconds

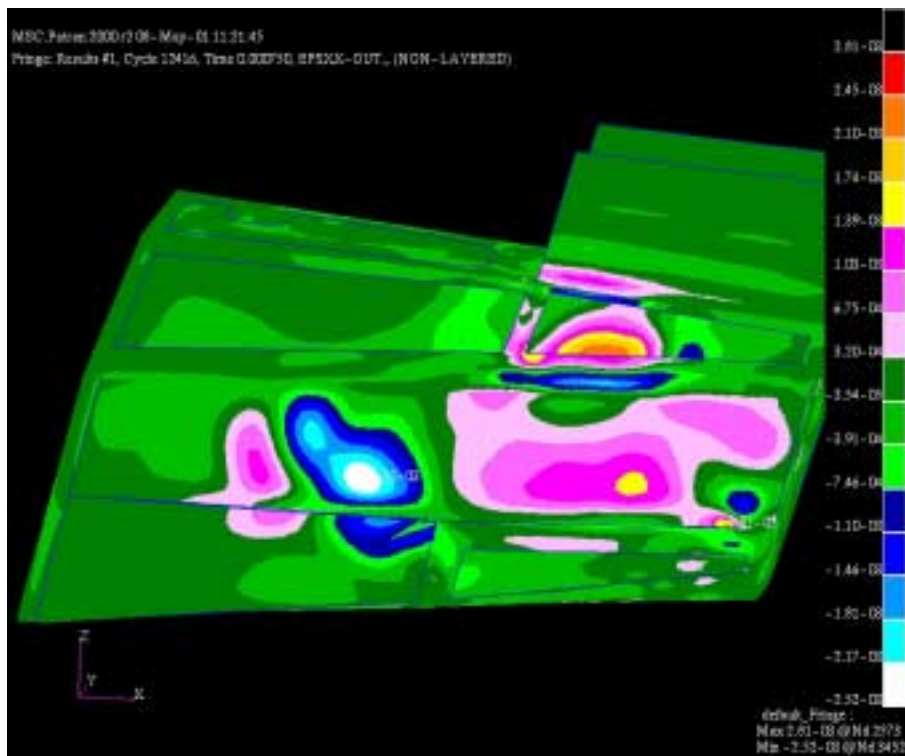


Figure 60: Shell Element Strain in XX Direction at Time = 0.75 milliseconds

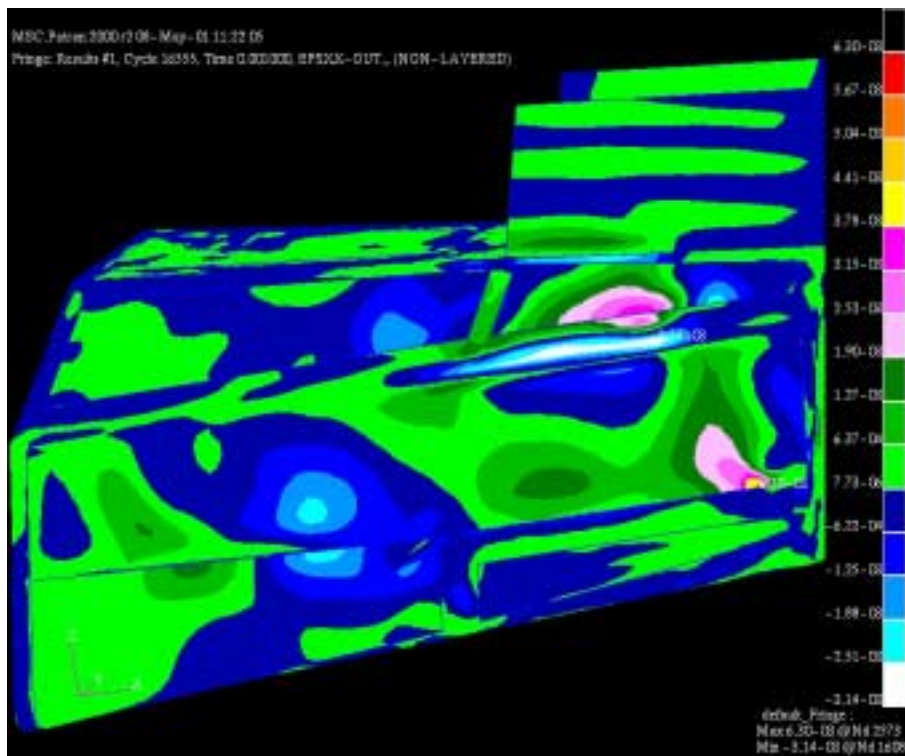
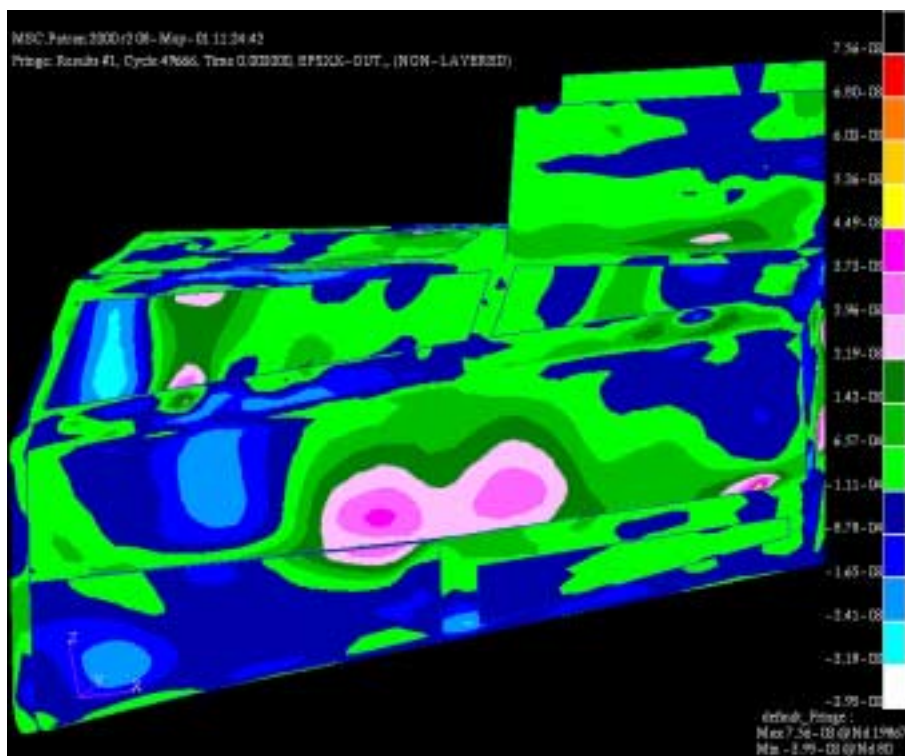
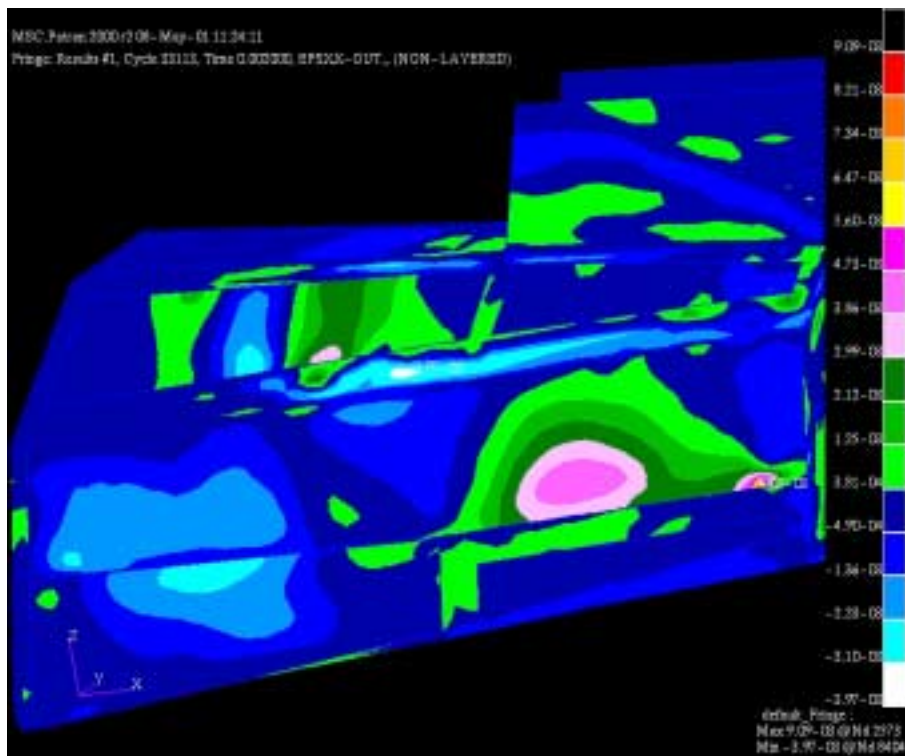


Figure 61: Shell Element Strain in XX Direction at Time = 1.0 milliseconds



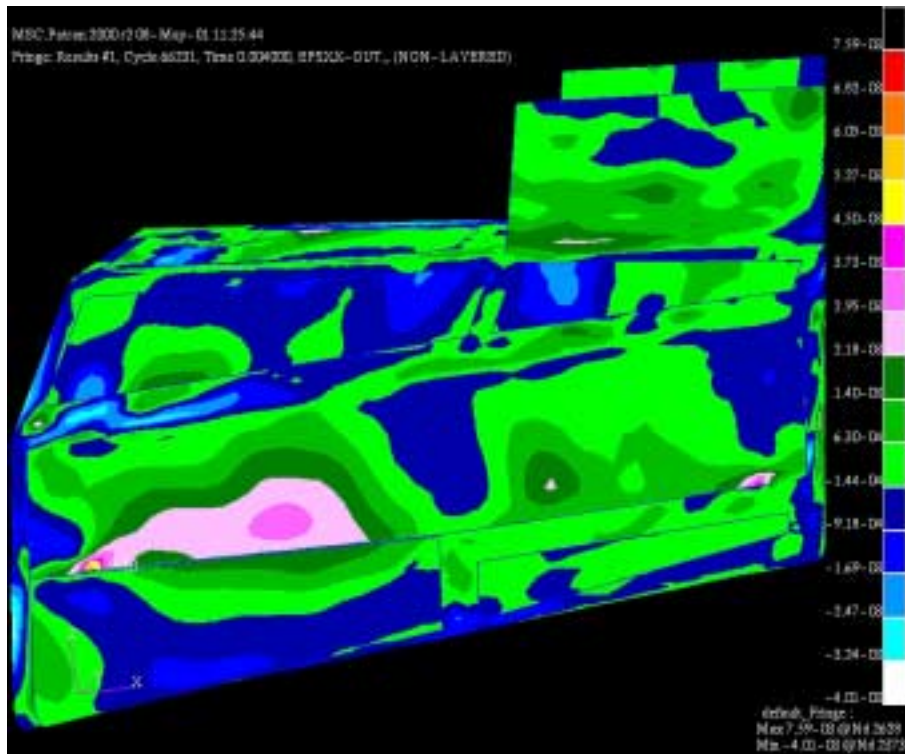


Figure 64: Shell Element Strain in XX Direction at Time = 4.0 milliseconds

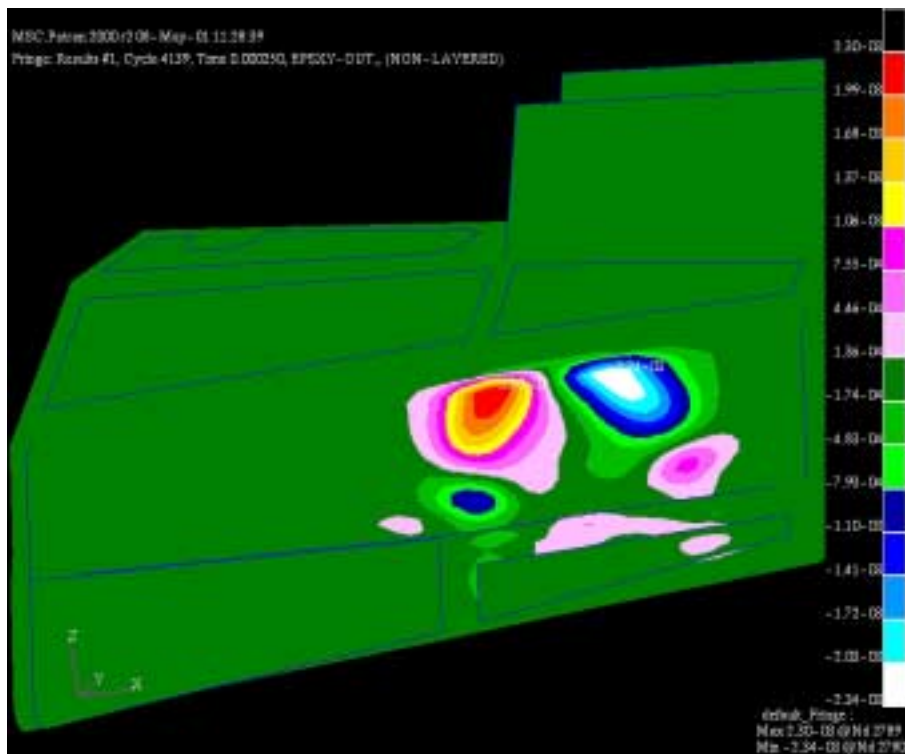


Figure 65: Shell Element Strain in XY Direction at Time = 0.25 milliseconds

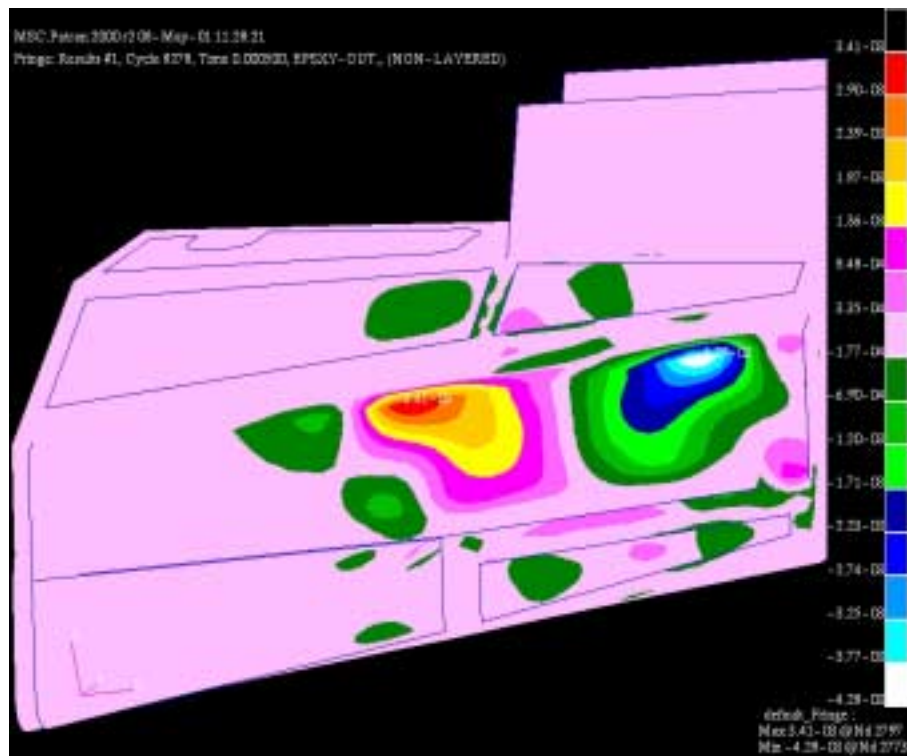


Figure 66: Shell Element Strain in XY Direction at Time = 0.5 milliseconds

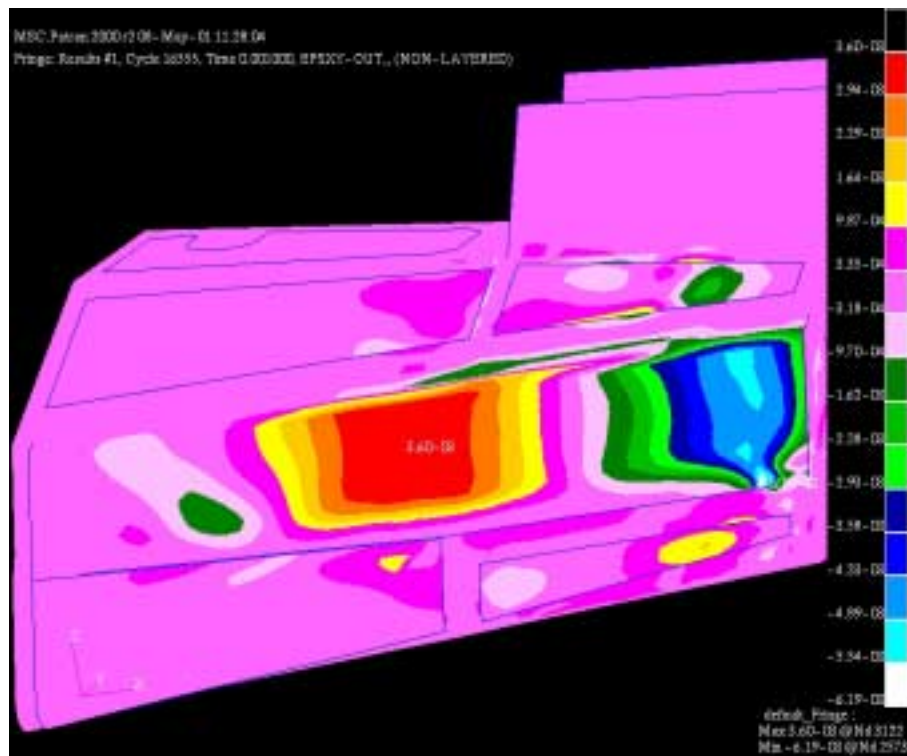


Figure 67: Shell Element Strain in XY Direction at Time = 1.0 milliseconds

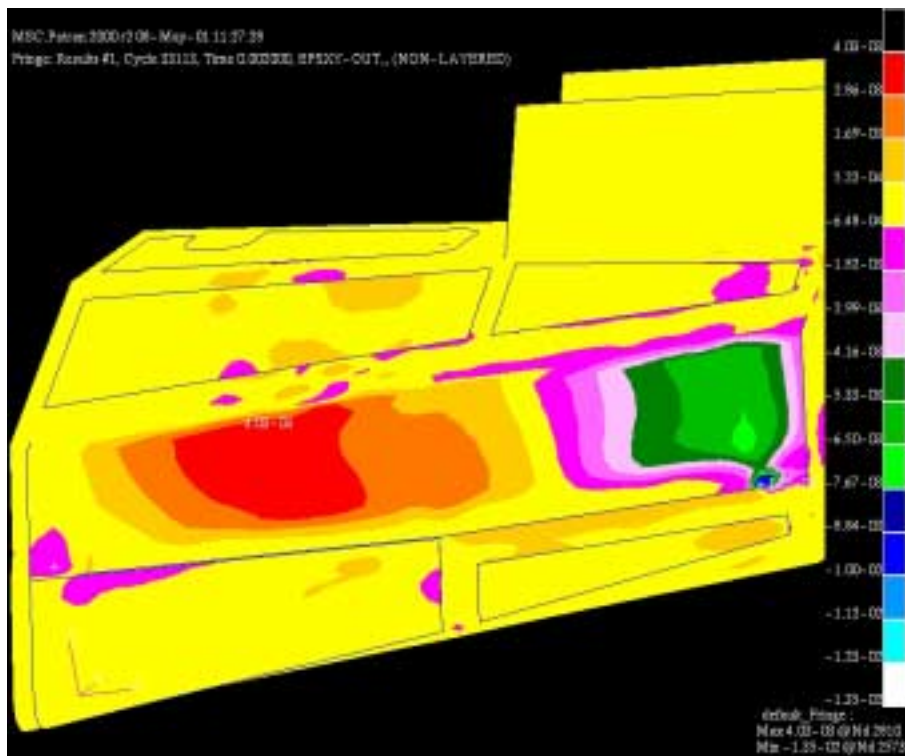


Figure 68: Shell Element Strain in XY Direction at Time = 2.0 milliseconds

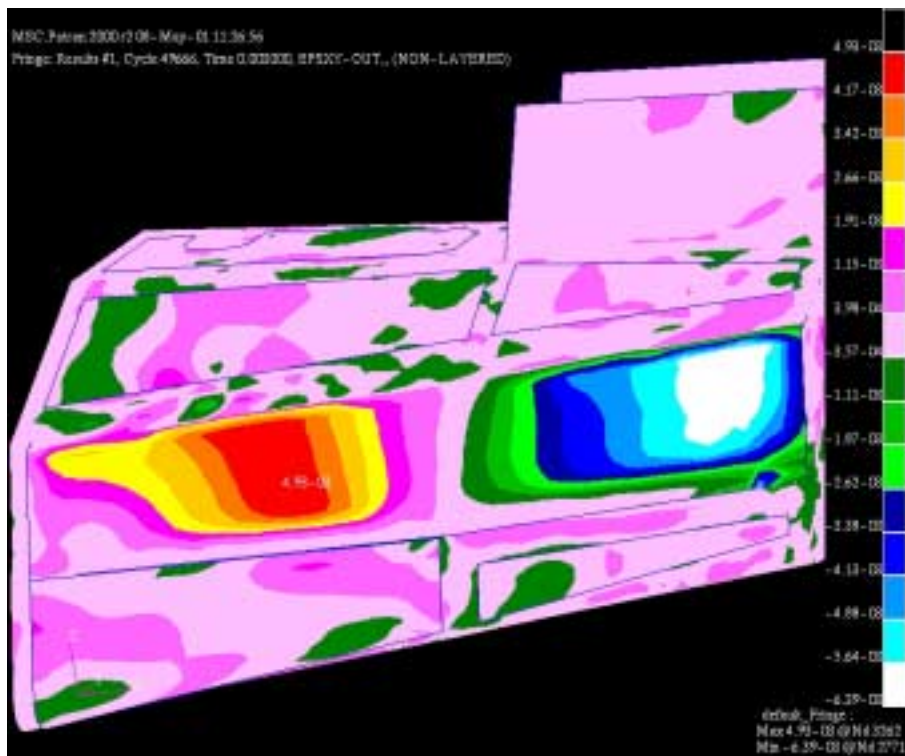


Figure 69: Shell Element Strain in XY Direction at Time = 3.0 milliseconds

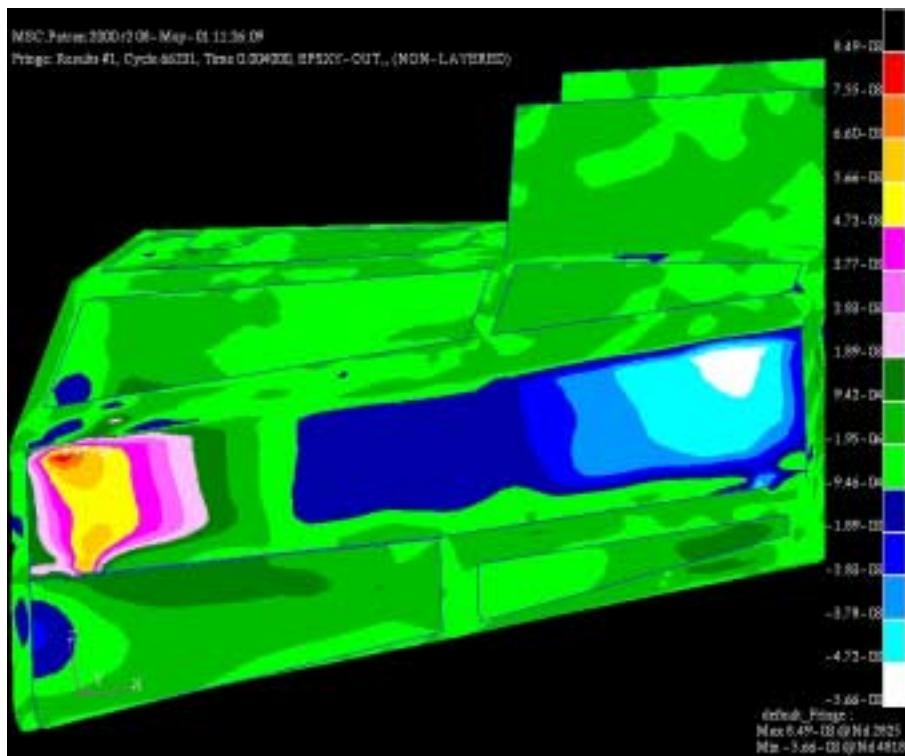


Figure 70: Shell Element Strain in XY Direction at Time = 4.0 milliseconds

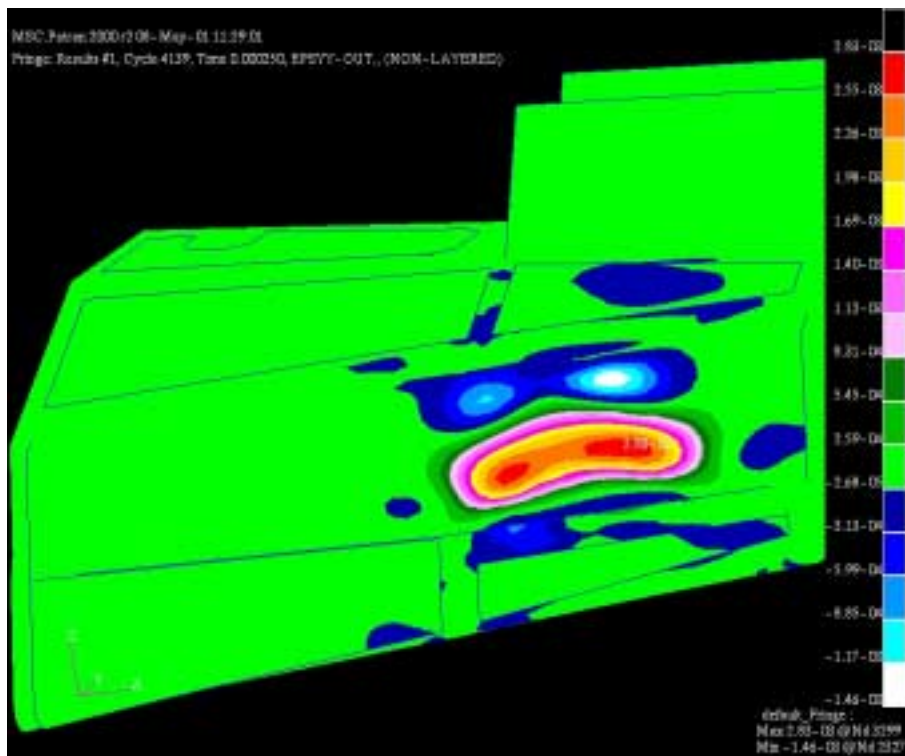


Figure 71: Shell Element Strain in YY Direction at Time = 0.25 milliseconds

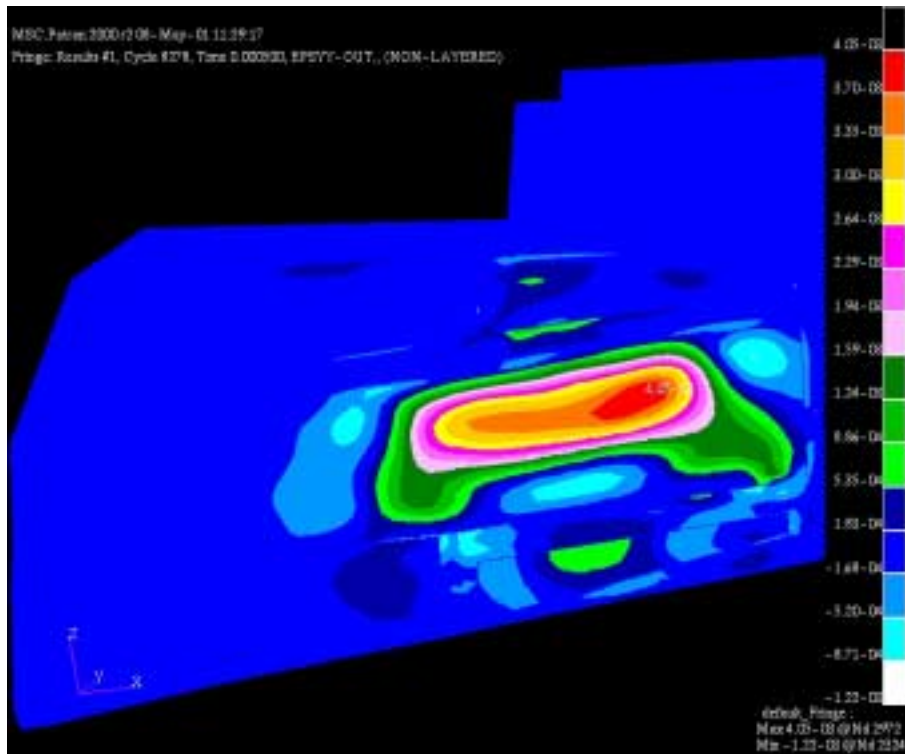


Figure 72: Shell Element Strain in YY Direction at Time = 0.5 milliseconds

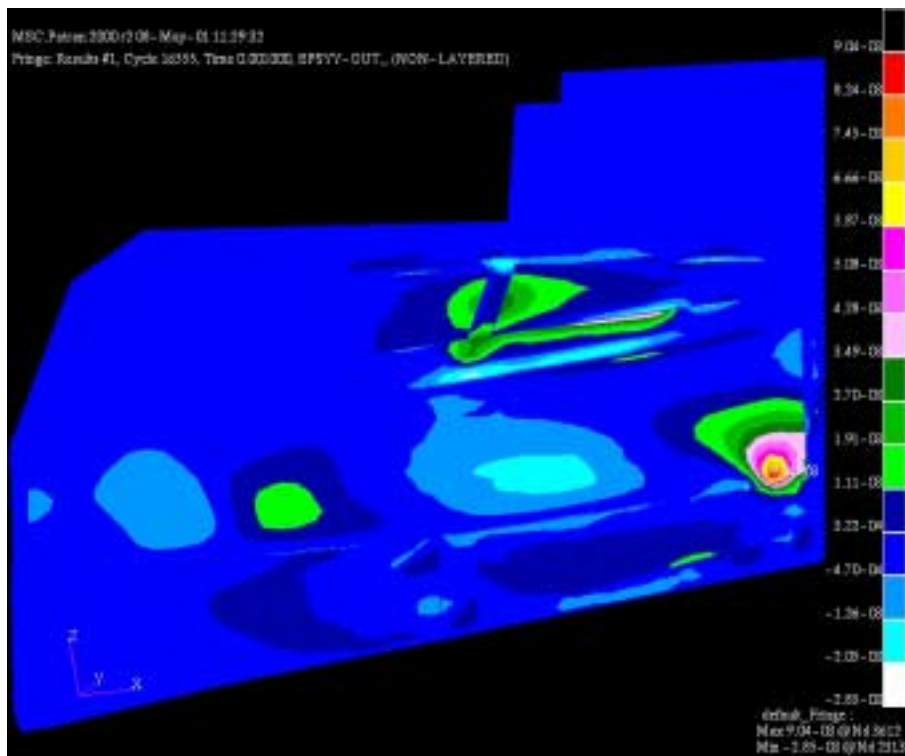


Figure 73: Shell Element Strain in YY Direction at Time = 1.0 milliseconds

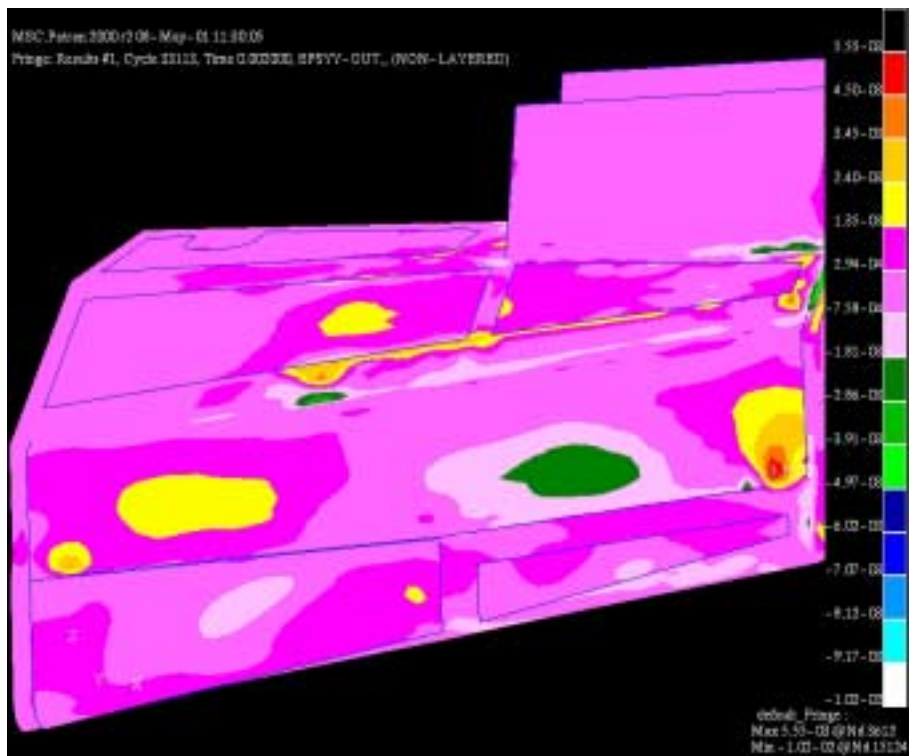


Figure 74: Shell Element Strain in YY Direction at Time = 2.0 milliseconds

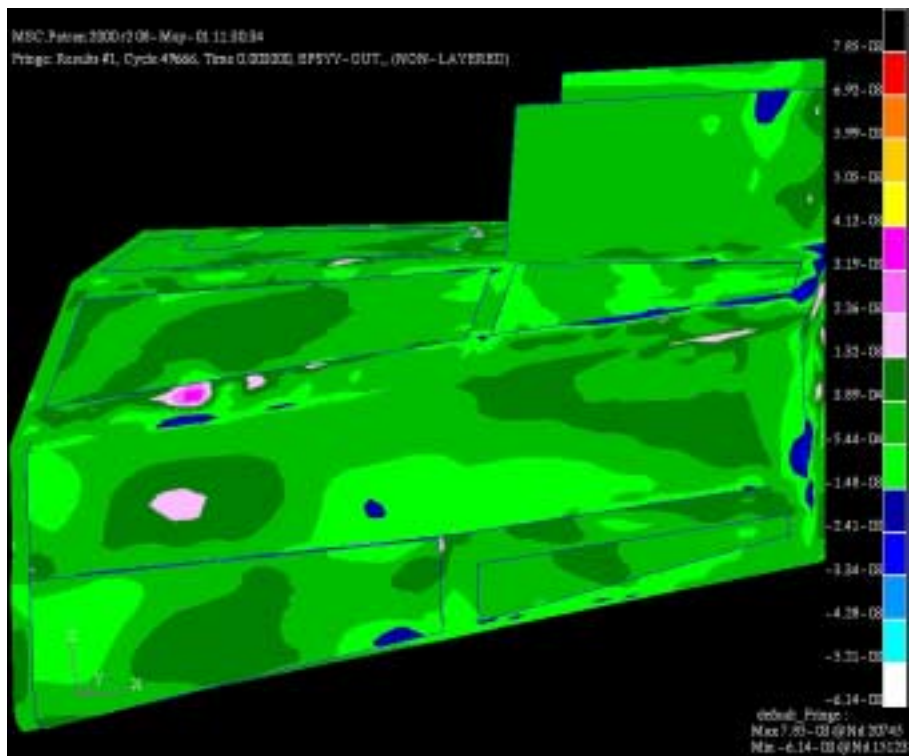


Figure 75: Shell Element Strain in YY Direction at Time = 3.0 milliseconds

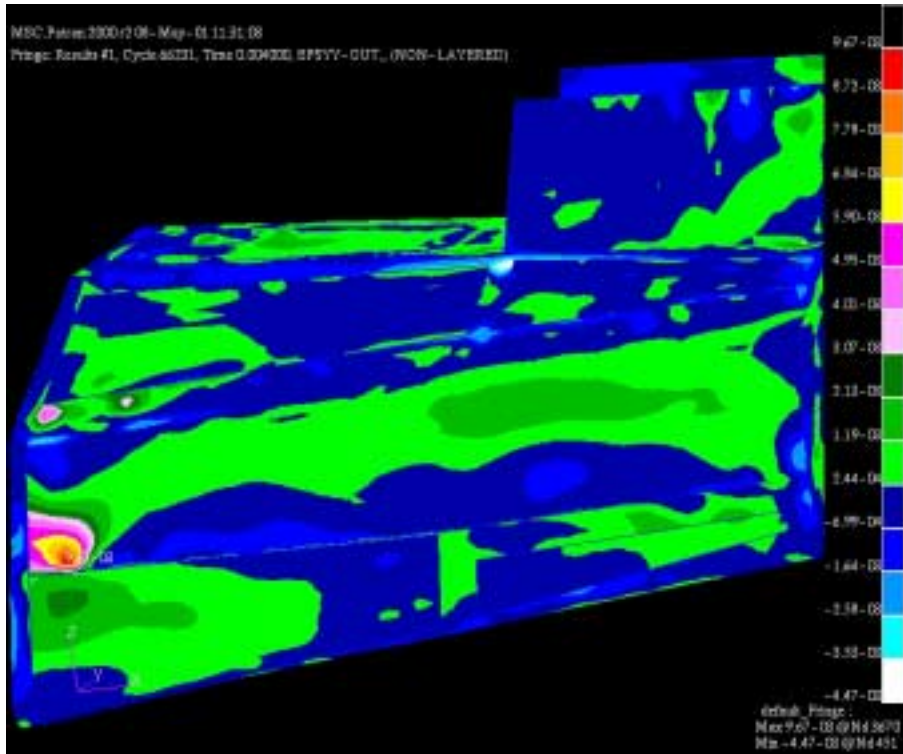


Figure 76: Shell Element Strain in YY Direction at Time = 4.0 milliseconds

E. FAILURE

The following figures depict elements that failed during the analysis of DYTRAN. The failing elements shown in the figures are associated with the vents. Prior to the analysis in DYTRAN, the modeler predicted that the analysis would show the failure of these elements because the vents consisted of a weak material. The remaining elements in the model did not fail. The color depicts the time of failure; thus, after element failure the color does not change with the model run time.

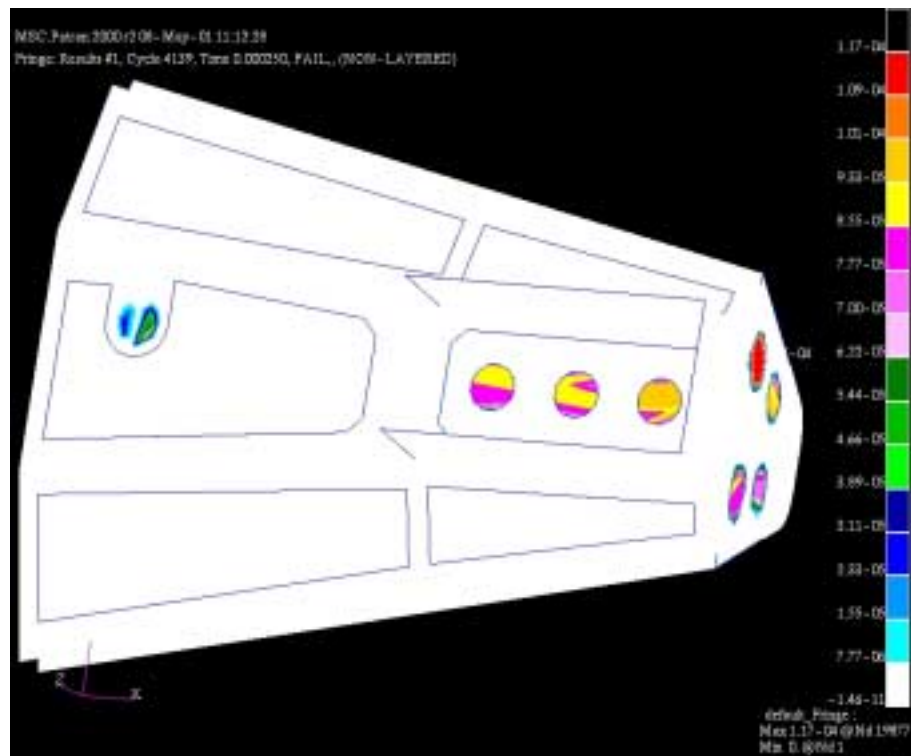


Figure 77: Failure of Shell Element Vents at Time = 0.25 milliseconds

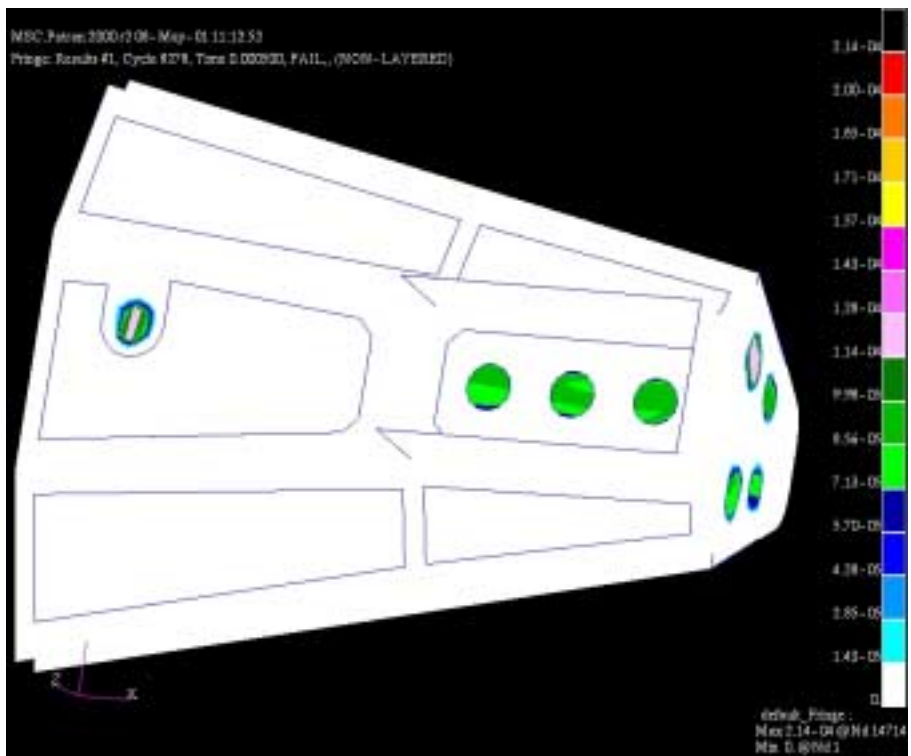


Figure 78: Failure of Shell Element Vents at Time = 0.5 milliseconds

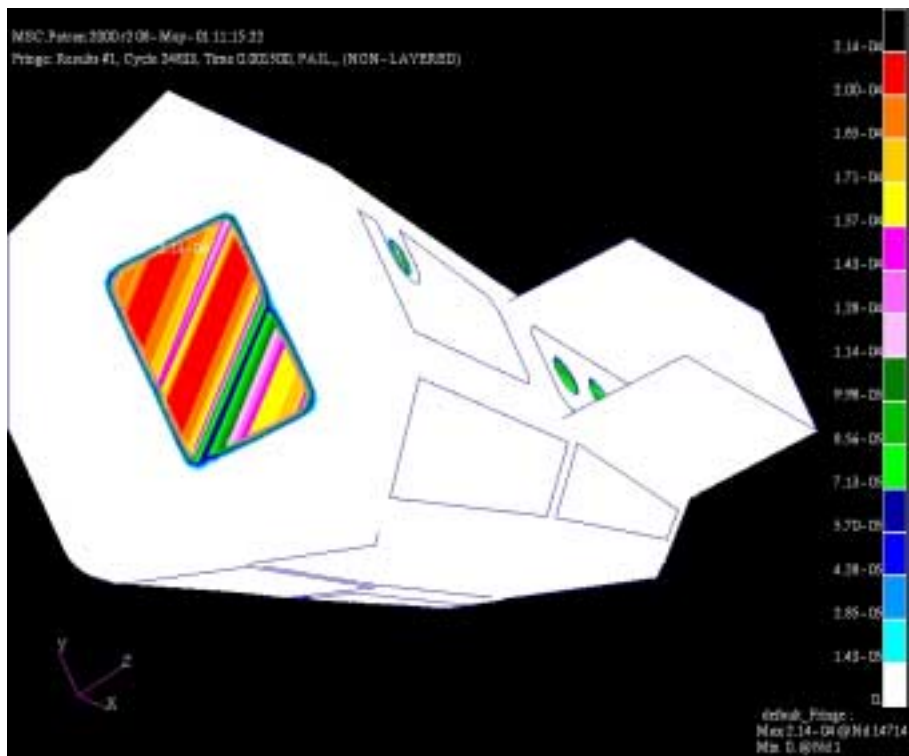


Figure 79: Failure of Front Shell Element at Time = 1.5 milliseconds

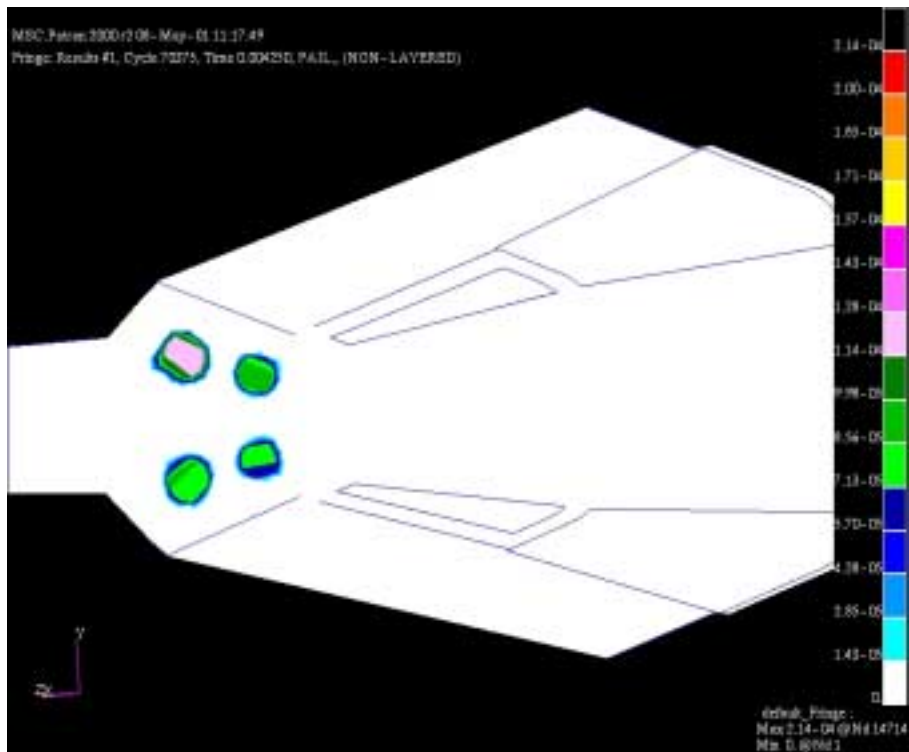


Figure 80: Failure of Shell Element Vents at Time = 4.25 milliseconds

V. CONCLUSIONS AND RECOMMENDATIONS

A. CONCLUSIONS

This thesis displays the numerous capabilities of MSC Software's PATRAN and DYTRAN. PATRAN allows the modeler to create and modify a model for any technological component without regard to the complexity of the system. DYTRAN provides the modeler with the ability to simulate and analyze extreme short duration events involving the interaction of fluids, and to select specific outputs in order to compare with any known data. The model results compared well with intuition; however, due to the classification of the specific 23mm HE SIE and live fire pressure-history results, a direct comparison of the data could not be made. The model was sent to Boeing in March 2001 to complete a classified DYTRAN run.

PATRAN and DYTRAN allows the modeler to change aspects of the project with ease. For example, after analyzing the results the modeler may find that a specific component has failed. Engineers can utilize this information to determine if additional plies of material or stronger materials need to be used for the failed component. The modeler can quickly incorporate these changes in the PATRAN model and modify the input decks for DYTRAN in order to run another analysis on the model. Furthermore, the modeler can simulate explosions at different locations and with different Specific Internal Energies (SIE) by simply changing one line of code in the input deck file. This allows the modeler to simulate the effects of varying explosive rounds and to model the effect of an explosion at any location within the model.

When validated, DYTRAN analysis will allow an extensive reduction in time and cost in determining the ballistic survivability of the Comanche helicopter or any new technological system. Also, engineers may come up with a better design, due to ease with which changes to model can be tested. The time and funds presently spent on conducting live fire tests and incorporating the necessary changes in design can be allocated to the development and production of more sophisticated systems to increase the lethality, mobility, and survivability of these systems. Furthermore, the production to fielding time can be greatly reduced and allow the ultimate users to incorporate the system into their inventories faster than standard methods presently used.

B. RECOMMENDATIONS

Extensive testing of DYTRAN explosion analysis against real life explosions needs to be conducted in order to validate the DYTRAN output. The classified specific internal energy of the explosive round used in the live fire test of the tailcone section needs to be incorporated into the input deck of this model. This would allow the modeler to correlate the time-pressure results of the model to the time-pressure results of the live fire test and make a determination on the validity of the computer-based simulation for this model. If validated, this DYTRAN modeling process could serve as the foundation for the elimination of future live fire tests for the Comanche helicopter.

In order to validate, comprehensive testing of the DYTRAN results is required. The Department of Defense should conduct similar computer based simulations for components used in live fire tests. If correlation efforts appear promising, the

Department of Defense, as the ultimate beneficiary of this testing procedure, should conduct a comprehensive evaluation of the capabilities of this type of analysis for application towards project standards. If this computer modeling technique can be shown to provide accurate results, the project test community could save the Department of Defense enormous amounts of money by utilizing simulation models to model explosions rather than conducting live fire tests. Ultimately, a successful computer based ballistic modeling program will lead to better products because the money and time saved over conventional ballistic testing methods could be applied to improve other areas of the program.

THIS PAGE INTENTIONALLY LEFT BLANK

LIST OF REFERENCES

1. <http://www.boeing.com/rotorcraft/military/rah66/rah66photos.htm>
2. Stephen, Allen, *Computerized Ballistic Modeling of the Comanche Tailfan Shroud*, Master's Thesis, Naval Postgraduate School, Monterey, California, December 2000.
3. Tobin, Vincent M., *Analysis of Potential Structural Design Modifications for the Tail Section of the RAH-66 Comanche*, Master's Thesis, Naval Postgraduate School, Monterey, California, June 1997.
4. Brauer, John R., *What Every Engineer Should Know about Finite Element Analysis*, Marcel Dekker, Inc., New York, New York, 1988.
5. O'Neil, Peter V., *Advanced Engineering Mathematics*, Wadsworth Publishing Company, Belmont, California, 1991.
6. Hahn, Harley, *The Unix Companion*, Osborne McGraw-Hill, Berkeley, California, 1995.
7. Mui, Linda, *When you can't find your UNIX system administrator*, O'Reilly and Associates, INC., Sebastopol, California, 1995.
8. MSC Software Corporation, *MSC.DYTRAN User's Manual*, Version 2000.
9. MSC Software Corporation, *MSC.Patran User's Manual*, Version 2000 (r2).
10. MSC Software Corporation, *MSC.Dytran User's Manual*, Version 4.7, 1997.
11. MSC Software Corporation, *MSC/PATRAN MSC/DYTRAN Preference Guide*, Version 7, 1997.

THIS PAGE INTENTIONALLY LEFT BLANK

INITIAL DISTRIBUTION LIST

1. Defense Technical Information Center 2
8725 John J. Kingman Road, Suite 0944
Ft. Belvoir, VA 22060-6218
2. Dudley Knox Library 2
Naval Postgraduate School
411 Dyer Road
Monterey, CA 93943-5101
3. Professor Donald A. Danielson, Code MA/DD 2
Department of Mathematics
Naval Postgraduate School
Monterey, CA 93943-5101
4. Professor Roberts Wood, Code AA/WD..... 1
Department of Aeronautics and Astronautics
Naval Postgraduate School
Monterey, CA 93943-5101
5. MAJ (P) Vincent M. Tobin, APM, Test and Evaluation..... 1
Building 5681 Wood Road
Redstone Arsenal
Huntsville, AL 35898
6. MAJ Brian Shoop..... 1
Comanche Program Managers Office
Building 5681 Wood Road
Redstone Arsenal
Huntsville, AL 35898
7. Mr. Robert Tomaine..... 1
Comanche Program Managers Office
SFAE-AV-RAH-TV (Tomaine)
Building 5681 Wood Road
Redstone Arsenal
Huntsville, AL 35898
8. Mel Niederer, Boeing Helicopter Structural Engineer..... 1
Building 325, Gate 6 (Stewart Avenue and Industrial Avenue)
Mail Stop P10-74
Ridley Park, PA 19078

| | | |
|-----|---------------------------|---|
| 9. | CPT Mark S. Gorak..... | 2 |
| | 12131 West Bel Mar Drive | |
| | Franklin, WI 53132 | |
| 10. | CPT Jeffrey A. Libby..... | 2 |
| | 68 White Oak Hill Rd | |
| | Poland, ME 04274 | |